Master's thesis

NTNU
Norwegian University of Science and Technology
Faculty of Natural Sciences
Department of Chemistry

Astrid Ellinor Schick

Using Hylocomium splendens as a Bioindicator for the Long Range Transport of Pollutants to Arctic Environments

Master's thesis in Environmental Toxicology and Chemistry
Supervisor: Øyvind Mikkelsen
Co-supervisor: Eiliv Steinnes
July 2021

Astrid Schick

NTNU
Norwegian University of
Science and Technology

Astrid Ellinor Schick

Using Hylocomium splendens as a Bioindicator for the Long Range Transport of Pollutants to Arctic Environments

Master's thesis in Environmental Toxicology and Chemistry
Supervisor: Øyvind Mikkelsen
Co-supervisor: Eiliv Steinnes
July 2021

Norwegian University of Science and Technology
Faculty of Natural Sciences
Department of Chemistry

NTNU
Norwegian University of
Science and Technology

Foreword

This thesis was conducted over the course of two years from fall 2019 to spring 2021 with the *Environmental Toxicology and Chemistry* program at NTNU. Moss was sampled in Svalbard near Ny-Ålesund in August 2020 and in southern Norway and Trondheim in September and October of 2020.

Trondheim, 2021-07-20

Signature

Astrid Ellinor Schick

Acknowledgements

The completion of this master thesis would not have been possible without the help and support of these people:

- Øyvind Mikkelsen, my main thesis advisor, for support and guidance throughout the entirety of the thesis project and my secondary advisor Eliv Steinnes for help during the planning and editing processes of the thesis.
- Anica Simic, Susana Villa Gonzalez, Per Ole M. Gundersen, Ingrid Naterstad Haugen, and Julie Asmussen for the processing of samples and help during analysis.
- Sylvia Weging for inclusion in experimental dual PAH and PCB extraction procedure.
- Kristian Hassel for the identification of moss and answering of moss related questions.
- To my research group for support during the master project.
- To my friends and family for emotional and physical support.

Abstract

Monitoring the effects of global pollutant transportation mechanisms in high Arctic areas has until recently, been neglected. These vulnerable ecosystems contain features that may amplify the accumulation of certain contaminates and provide insight into the state of human emissions when compared to other regions. The usage of biomonitors in long range transportation (LRT) studies is an established methodology and moss, specifically the species *Hylocomium splendens*, due to its widespread usage and unique accumulation properties was chosen for this thesis. Polyaromatic hydrocarbons (PAHs), polychlorinated biphenyls (PCBs) and various elements in the high Arctic area of Ny-Ålesund as well in Trondheim and Southern Norway areas, were targeted over ten separate locations and 48 samples. Analysis of PAHs was performed by both high-performance liquid chromatography with a fluorescence indicator detection and a diode-array detector (HPLC FID-DAD) and through an experimental tandem PAH and PCB analysis method with gas chromatography mass spectrometry (GC-MS). Elemental analysis was carried out using high resolution inductively coupled plasma mass spectrometry (HR ICP-MS). Of the organic pollutants, PAHs such as phenanthrene and pyrene were detected in the samples, but overall recovery was low and did not seem correlated to Arctic accumulation and no PCBs were detected in the samples. The elemental analysis revealed that Pb showed evidence of Arctic concentration when compared to other sampled areas and V, Cr, As, Cd, and Sn showed possible LRT accumulation when compared to Norwegian national moss survey data. Further study of metal, metalloid and PAH pollutant accumulation in Arctic areas is recommended for future studies.

List of Abbreviations

AAS	Atomic Absorption Spectroscopy
ANOVA	Analysis of Variance
AO	Arctic Oscillation
AMDEs	Atmospheric Mercury Depletion Events
ASE	Accelerated Solvent Extractor
CFC	Chlorofluorocarbon
DAD	Diode-Array Detection
DOM	Dissolved Organic Matter
FID	Fluorescence Detection
GC-MS	Gas chromatography -Mass Spectrometry
GEM	Gaseous Elemental Mercury
HPLC	High pressure Liquid Chromatography
HR ICP- MS	High Resolution Inductively Coupled Plasma Mass Spectrometry
ICP Vegetation	International Cooperative Program on Effects of Air Pollution on Natural Vegetation and Crops
INAA	Instrumental Neutron Activation Analysis
ISTD	Internal Standard
ITCZ	Inter-Tropical Conversion Zone
LRT	Long Range Transport
ME	Microwave Extraction
NDIR	Non-dispersive Infrared Spectrometry
NIST	National Institute of Standards and Technology
NTNU	Norges Teknisk Naturvitenskapelige Universitet
OC	Organic Carbon
PBT	Persistent, Bioaccumulate and Toxic
PAHs	Polycyclic Aromatic Hydrocarbons
PC	Principal Component
PCBs	Polychlorinated Biphenyls
PCA	Principal Component analysis
POPs	Persistent Organic Pollutants
PTFE	Polytetrafluoro Ethylene
SFE	Super Critical Fluid Extraction
SIM	Selected Ion Monitoring
SVOCs	Semi Volatile Organic Compounds
TCD	Thermal Conductivity Detection
RGM	Reactive Gaseous Mercury

Table of Figures

Figure 1. Atmospheric airflow patterns. 4
Figure 2. Illustration of the effect of the Arctic vortex transportation patterns. 5
Figure 3. A simple model for the probability of interactions in air and soil concerning the grasshopper effect. 7
Figure 4. The Adsorption of copper into moss by differing chemical groups varied by pH. 9
Figure 5. A theoretical diagram of mercury cycling in the Arctic. 11
Figure 6. Image of *Hylocomium splendens*. 17
Figure 7. Illustration of humic substances. 20
Figure 8. Diagram of a typical accelerated solvent extraction (ASE) design. 26
Figure 9. Simple figure of an Inductively Coupled Plasma (ICP) configuration. 29
Figure 10. Diagram of the inside of an idealized chromatography column. 31
Figure 11. A map of the sampled areas across Norway and Svalbard. 36
Figure 12. A close up of Ny- Ålesund sampling locations. 37
Figure 13. A map of the Southern Norway sampling locations. 38
Figure 14. A map of the Trondheim sample locations. 39
Figure 15. Box plots of V, Cr, Mn, Fe, Zn, As, Mo and Ag. 60
Figure 16. Boxplots of Cd, Sn, Sb, W, Tl, Pb and Bi. 61
Figure 17. PCA 1 & 2 for elements. 62
Figure 18. PCA 3 & 4 for elements 65
Figure 19. Image of the Zeppelin Mountain sampling location. iv
Figure 20. Image of the Storhylla sampling location. v
Figure 21. Image of the Stai sampling location. v
Figure 22. Image of the Spjotevannet sampling location. vi
Figure 23. Image of the V. Grimevannet sampling location. vi
Figure 24. Image of the moss found near Jonsvannet Area 11. vii
Figure 25. Image of the moss found near Jonsvannet Area 12. viii
Figure 26. Image of Jonsvannet Area 13. viii
Figure 27. Image of Espåa sampling area. ix
Figure 28. Image of Granåsen sampling area. x
Figure 29. Image of Baklidammen x

Table of Tables

Table 1 15
Table 2 42
Table 3 43
Table 4 44
Table 5 46
Table 6 47
Table 7 49
Table 8 51
Table 9 51
Table 10 54
Table 11 58
Table 12 68
Table 13 71
Table 14 75
Table 15 i
Table 16 ii
Table 17 vii
Table 18 viii
Table 19 ix
Table 20 x
Table 21 xi
Table 22 i
Table 23 i
Table 24 ii
Table 25 iii

Table of Contents

Foreword ... i

Acknowledgements ... ii

Abstract ... iii

List of Abbreviations ... iv

Table of Figures ... v

Table of Tables ... vi

1 Introduction ... 1

2 Background ... 3

2.1 Atmospheric interactions ... 3

2.1.1 Circulatory air patterns ... 3

2.1.2 Long range transport ... 4

2.1.3 Metals and metalloids ... 7

2.1.4 PAHs and PCBs ... 12

2.1.5 Specific PAHs and PCBs of interest ... 13

2.2 Sampling and pretreatment ... 16

2.2.1 Moss ... 16

2.2.2 Soil ... 19

2.2.3 Milling ... 22

2.3 Digestion Techniques ... 22

2.3.1 Dry ashing ... 22

2.3.2 Partial digestion ... 22

2.3.3 Total digestion ... 24

2.4 Sample extraction methods ... 24

2.4.1 Selective extraction ... 24

2.4.2 Liquid-liquid phase extractions and partitioning ... 24

2.4.3 Solid-liquid phase extraction ... 25

2.4.4 Accelerated Solid Phase extraction ... 25

2.5 Chemical Analysis Techniques 26
2.5.1...Total Organic Carbon and Total Inorganic Carbon determination........ 27
2.5.2...Inductively Coupled Plasma 28
2.5.3...Chromatography 30
2.5.4...Detectors 33
2.6 Quality assurance 34

3 Materials and Methods 36

3.1 Sampling 36
3.1.1...Study areas 36
3.1.2...Sampling methods 40
3.2 Sample preparation 40
3.2.1...Drying 40
3.2.2...Separation 41
3.2.3...Milling 41
3.2.4...Microwave Digestion 41
3.2.5...Accelerated Solvent Extractor (ASE) 42
3.3 Chemical Analysis 45
3.3.1...Total Organic Carbon, Residual Oxidizable Carbon and Total Inorganic Carbon 45
3.3.2...HR ICP-MS 45
3.3.3...GC-MS 45
3.3.4...HPLC FID-DAD 46
3.4 Statistical Analysis 47

4 Results 49

4.1 Total organic carbon 49
4.2 POPs data 50
4.3 HR ICP-MS 52

5 Discussion 67

5.1 PAHs in sampled areas 67
5.2 Elemental analysis 69

5.2.1...Principal component analysis 73
5.2.2...Variation between sampling sites 74
5.3 Experimental limitations 76

6 Conclusion 79

7 Future Work Recommendations 80

8 Citations 82

1 Appendix A i

1.1 Percent TOC, TIC and ROC data i

2 Appendix B ii

2.1 HR ICP-MS ii
2.2 Detection limits vii
2.3 Statistics viii

Appendix C i

2.4 PAH i
2.5 Detection limits ii

3 Appendix D iii

3.1 Sample locations iii
3.1.1...Pictures iv

1 Introduction

Monitoring the extent of pollution by long range transport (LRT), is an important part of the global effort to prevent and reduce environmental harm. To do so in a widespread thorough manner requires methodology that is applicable to a variety of different research scenarios, budgets and laboratory set-ups. The use of a bioindicator such as *Hylocomium splendens*, a moss species that concentrates air pollution, is an ideal solution to many of the issues encountered in this type of monitoring. *H. splendens* has a worldwide presence, low sampling costs and can accommodate various methods for analysis depending on the compounds studied[1].

Although large scale moss sampling surveys have been carried out fairly regularly in Norway[2], in high Arctic areas like Svalbard, studies have been limited. This may possibly be due to the harsh conditions, high travel costs, or overgrazing by reindeer of local moss species[3]. Despite these potential drawbacks, it is vital that more information be collected in this vulnerable area[4] as the Arctic is the northern hemisphere's release point for the pollutants that undergo LRT[5]. Ny-Ålesund's remote location on Svalbard as a research station has the potential for utilization in the study of LRT pollutants. There are few local air pollution sources in Ny-Ålesund compared to the town of Longyearbyen, which has pollution from the airport, traffic and a coal power plant[6], and therefore it may be possible to establish background LRT levels in Ny-Ålesund. There have been some studies in Longyearbyen, Spitsbergen and at the research center in Ny-Ålesund regarding long range atmospheric pollution[4, 6-11] and pollution monitoring in the Antarctic[12], but the use of *Hylocomium splendens* for LRT activities in such a pristine Arctic location is fairly novel.

This master thesis analyzes the metals, metalloids and persistent organic pollutants (POPs), specifically polyaromatic hydrocarbons (PAHs) and polychlorinated bisphenols (PCBs), associated with LRT by using moss as a bioindicator. The moss species *Hylocomium splendens* was sampled from locations around Ny-Ålesund, Svalbard to gather data in order to evaluate if LRT could be a source of pollution when compared to local sources[8]. Sampling was also done in Trondheim and the South of Norway to link this study to previous survey studies[2, 13-15] and to compare to the Ny-Ålesund concentrations. After the continual reduction of certain metals and legacy POPs in larger surveys of lower Arctic areas[16], this study seeks to elucidate if this trend is also present in high Arctic areas where the global distillation effect is theorized to be more evident[15].

2 Background

2.1 Atmospheric interactions

The physics and chemistry of the atmosphere are comprised of complex intertwining processes. The air circulation patterns created weave webs of seen and unseen substances globally. The gasses and molecules that make up the atmosphere ensure conditions that nurture life, but also contain the potential to harm it. Continually humanity has created chemicals that end up in the atmosphere and result in catastrophes far from their original sources, like the unintentional creation of ozone holes by chlorofluorocarbon's (CFC)[17]. This makes it vital that these atmospheric processes are understood in order to the reduce the pollution effects of new contaminants by modelling their behavior in the atmosphere before release[18] and manage current pollution problems.

2.1.1 Circulatory air patterns

In general, air circulation patterns are dependent on temperature and pressure differences and are bound by the rotation and tilt of the planet[19]. Winds form to equilibrize these heat and pressure differentials to result in three global air cells, the Hadley, Ferrel and Polar cell, over each hemisphere, that are centered at the equator and divided by the tropics and polar circles[19, 20]. Along the Equator and Polar circles air rises and sinks at the tropics and at the poles [21]. This results in a strong circular motion within the Hadley and Polar cells, but only a weak circular movement in the Ferrel cell as it moves mainly by the consequence of the pressure differentials of the other cells.

Within these cells, due to the earth's rotation, the mass of air particles in the atmosphere develops an east to west velocity, which is directed perpendicularly to the horizontal velocity vector causing air to flow to the right in the northern hemisphere and to the left in the southern hemisphere[19-21]. These horizontal and vertical motions comprise the various trade winds and westerlies that originate from the tropics and terminate at the intertropical conversion zone (ITCZ) and polar circles respectively in each hemisphere[20]. The ITCZ, located around equator, is defined by large parcels of rising hot air and significant quantities of rainfall[19]. Figure 1 shows the combination of these wind patterns as they theoretically should appear as well as a rendition that more accurately reflects reality.

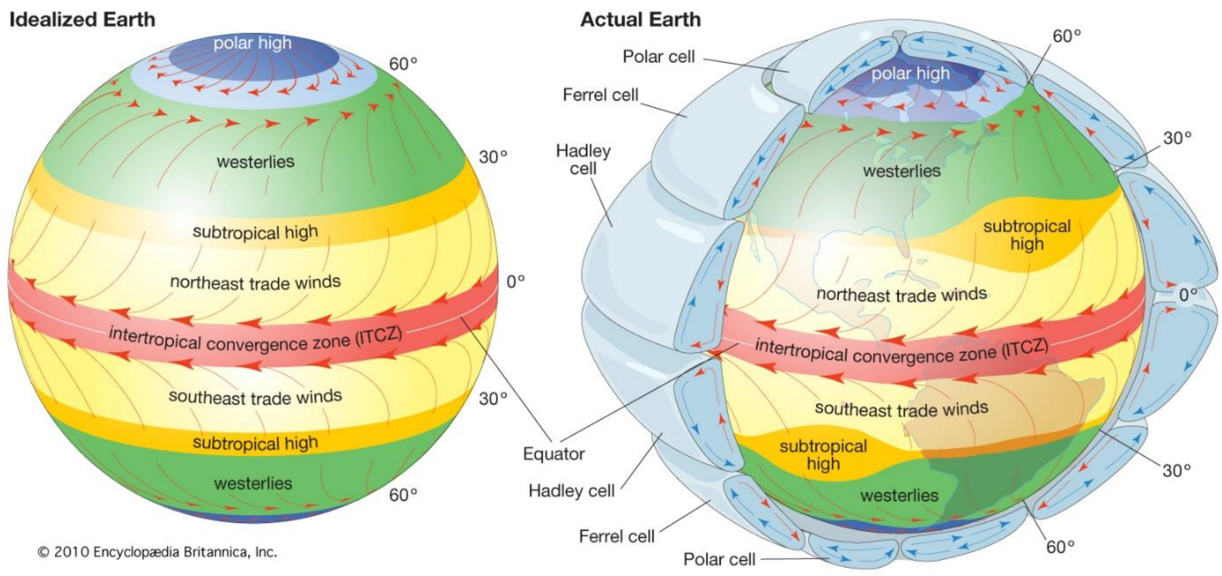

Figure 1. Atmospheric airflow patterns.

This figure illustrates the major wind cells and patterns surrounding the earth in an idealized fashion as well as in a realistic manner. By courtesy of Encyclopædia Britannica, Inc., copyright 2014; used with permission[20].

2.1.2 Long range transport

LRT refers to the travel of chemical species and other substances over large distances due to air circulation patterns[19]. The LRT of the substances of interest in this study travel mainly in the first and second layer, troposphere and stratosphere, of the five main atmospheric layers. The tropospheric layer contains the most matter and extends 8 to 14.5 km from the ground and the stratospheric layer extends from the troposphere to 50 km above the earth's surface[22] with the tropopause defining the space in between them[19]. In the bottom 0.5- 2 km of the atmosphere, otherwise known as the boundary layer, air motions are driven by kinetic imbalances that take place on the order of minutes while seasonal patterns that occur on the order of months and days happen in the "free" troposphere[19]. Chemical species and oxidated products of the original compounds that travel through boundary layer reactions which promote deposition, tend to be stable, non-reactive species[19, 23, 24] and may enter the free troposphere. In the free troposphere, air parcels travel long distances in longitudinal and latitudinal directions with the former being significantly hindered and the latter taking days to months[19].

It is possible for some chemicals to transfer across the troposphere into the stratosphere in tropopause area through the tropopause folding process[19].This often occurs in middle to high altitude areas and consists of wave driven pumping between high pressure rises and low pressure troughs that result in the uptake of air around the tropics and deposition around the poles[19, 21]. Certain air flow patterns, like the Arctic polar vortex shown in Figure 2, result from this and can transport pollutants from lower latitudes to the Arctic in a few days [5].

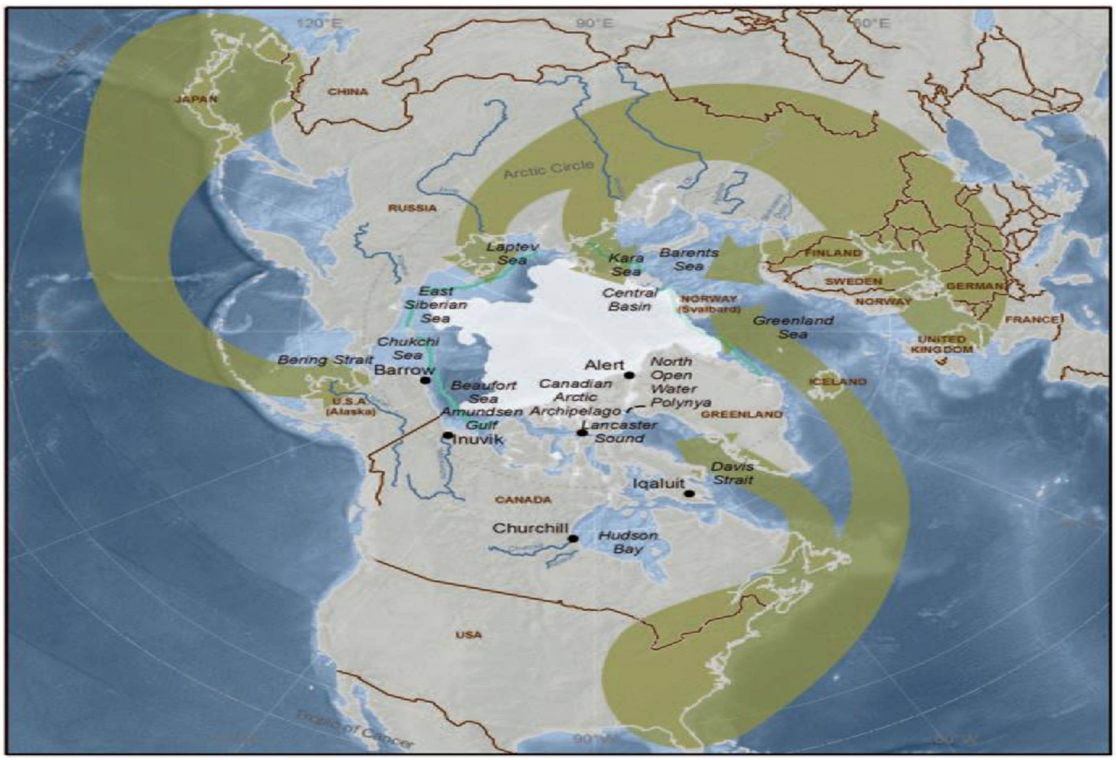

Figure 2. Illustration of the effect of the Arctic vortex transportation patterns.

The illustration shows how the westerlies in the North hemisphere act to pull air into the Arctic. This creates a vortex effect. The strength of the vortex is dependent on the pressure states of the beginning and ending areas. Figure reproduced with permission[5].

The strength of the Arctic polar vortex is often represented using an index referred to as the Arctic oscillation index (AO). A high AO score corresponds to a low pressure in the Arctic compared to the North Atlantic Ocean; this has been linked to increased pollution transportation[5].

The effect of climate change on global circulation patterns has the potential to disrupt current LRT patterns[5]. It is theorized that climate change may create conditions that mimic an increased AO number in addition to shifting air steam paths[5]. Moving forward, these changes need to be studied and evaluated for future research.

2.1.2.1 Atmospheric deposition

Particles of dust that are small enough to aerosolize may be bound to contaminates or interact with them through intermolecular attractions[5, 25]. Once airborne, these complexes can be transported both locally and over long distances[25]. This atmospheric transport eventually results in the deposition of the particles through both wet and dry processes[26]. The wet processes include all forms precipitation and the dry processes include the sedimentation of particles and gases[26].

In regards to the transport of pollutants, atmospheric deposition accounts for a majority of the LRT of metals and metalliods[26]. Wet processes dominate the bulk of these depositions, although dry deposition is significant as well[26]. POPs may also be transported through atmospheric deposition; this occurs if an extremely stable POP attaches to a particle, or through deposition of the stable byproducts of atmospheric reactions[5].

2.1.2.2 Global distillation and the grasshopper effect

Global distillation and the grasshopper effect both refer to the movement of substances over a distance through the air. Distillation describes the temperature dependent volatilization of substances into the atmosphere and their subsequent removal by condensation as heat decreases across distances and seasons[5,18]. The grasshopper effect explains how a substances' interactions with stationary and mobile mediums results in the continuation of a portion of the original substance, and the burial or degradation of the other portion[18].

POPs are the main pollutant that travels this way and species with properties that increase volatility, hydrophobicity and persistency travel the furthest[5, 18], but other persistent bioaccumulate and toxic (PBT) compounds like mercury may travel this way as well. The group of compounds with these properties are referred to as semi-volatile organic compounds (SVOCs), and include PAHs, PCBs, PCBEs, OC pesticides, dioxins and furans[18]. Fractionation of these compounds through LRT allows lighter congers to travel further than larger, heavier molecules[18]. The amount of POPs in the air increases during the winter with colder temperatures and decreases with warmer summer temperatures[5, 27], possibly due to heightened degradation and photochemical reactions with free radicals in the troposphere [18, 27] in warmer temperatures.

Colder climates accumulate pollutants due to slowed decomposition reactions, increased adsorption of volatiles on particles which allows for deposition, and decreased volatilization from soil and water bodies[23].

2.1.2.2.1 Modeling the grasshopper effect

Modeling programs can be used as tools to estimate the LRT potential of new compounds[18], addressing questions such as the potential emission rate, travel distance, or chemical fate a compound. In models, "k" is often used as a constant for the rate of a process. The capital "K" refers the equilibrium constant of a process. The subscript designates the specific process; the interactions important to LRT, are air to soil (AS), soil to air (SA), degradation in air (A), and degradation in soil (S) [18]. Figure 3 shows a simple example of a model that predicts the probability (P) of basic air and soil removal and can help explain substance loss due to the grasshopper effect.

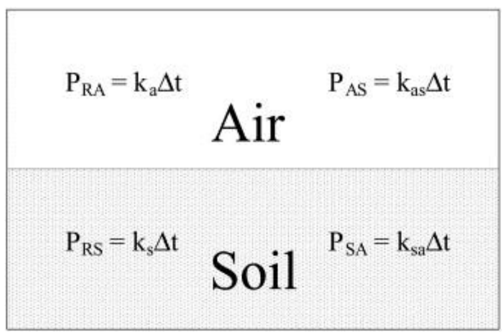

Figure 3. A simple model for the probability of interactions in air and soil concerning the grasshopper effect.

This is a simple "Monte Carlo" model that displays basic probability (P) equations for air and soil interactions. Such equations could be used to create a theoretical model of the amount of hops a substance might take with a set velocity and variation of time and the rate constants for degradation in air (k_a), soil (k_s), and air to soil and soil to air movements respectively (k_{as}, k_{sa}).[18]. Figure reproduced with permission[18].

2.1.3 Metals and metalloids

Metals and metalloids are present throughout the earth's crust[25] and compile most of the periodic table. They have many functions in biological processes and are vital to life on Earth when present at the correct concentrations[28, 29], but in excessively high concentrations the organ and cellular systems that use them may acquire serious harm[25, 28]. Natural emissions of these elements through processes such as volcanic activity, soil particle deposition, sea salt aerosol deposition[9], and lithogenic inputs like bedrock leaching, may create toxic conditions[25], but anthropogenic interferences have caused far more environmental problems. Agricultural practices including the use of fertilizers, sludges, pesticides, fungicides, and herbicides, add elements like arsenic, cadmium and lead to the soil in concentrations that have the potential to bioaccumulate in crop plants and livestock to levels that may harm humans if consumed[25]. Industrial processes like fossil fuel consumption, mining, smelting, and manufacturing non-ferrous metals[9, 25] and improper waste management, like unfiltered waste incineration plant emissions, leaching from mines and military waste [9, 25], may lead to local and atmospheric pollution of the environment by various metals and metalloids that have the potential to cause harm to life[25]. It is therefore important to monitor these elements near pollution occurrences[30] as well as globally for world-wide safety[25].

As described in section 2.1.2.1, most metals and metalloids travel and are deposited through atmospheric deposition[31], excluding mercury which has a specialized method of transport[5]. Both wet and dry deposition of metals occur, but wet deposition is assumed to be the most significant contributor[26].

After deposition, metals may accumulate in the environment. As soil and moss often are used to track metal and metalloid concentrations, it is advantageous to understand how metals and metalloids accumulate in them. Specific soil uptake mechanisms are detailed in Section 2.2.2 as their function is intrinsic to the composition of the soil. In moss, metal accumulation can occur chemically and physically on the surface of the organism. To determine an universal adsorption model for the transfer of metals into mosses[32], the factors that affect adsorption should be considered. One study suggests that exposure time and pH dominate the adsorption mechanisms in moss[32], which could be due to their lack of root systems[26] which would in an ordinary plant influence the surrounding conditions and bioavailability of metals[25]. Five minutes was determined to be the exposure time necessary for complete adsorption of the selected metals in the González 2014[32] study. The pH influences metal adsorption by changing the bonding sites of the functional groups on the outer layer of moss[32] by altering the protons associated with the potential bonding sites on the moss[32]. As the pH increases, potential bonding sites release their protons and become available for metal and metalloid interactions. The highest absorption rates for a variety of metals are achieved when the pH is above five[32]. The functional groups that are theorized to be available for bonding in different pH environments are; carboxyl and phosphoester at low pHs, phosphoryl and amine groups at middling pHs and the polyphenol groups at high pHs[32]. Figure 4 shows an illustration of the pH uptake effect on four different moss species *Hypnum sp.*, *Sphagnum denticulatum, Pseudoscleropodium purum* and *Brachytecium rutabulum* for specifically cooper[33], although other metals have been shown to undergo similar bonding changes[32]. The overall adsorption capacity of a moss can be calculated using Equation 1, which is a form of the Langumuirian adsorption equation that tracks absorption well for high organic material substances[25, 34]like moss and sludge.

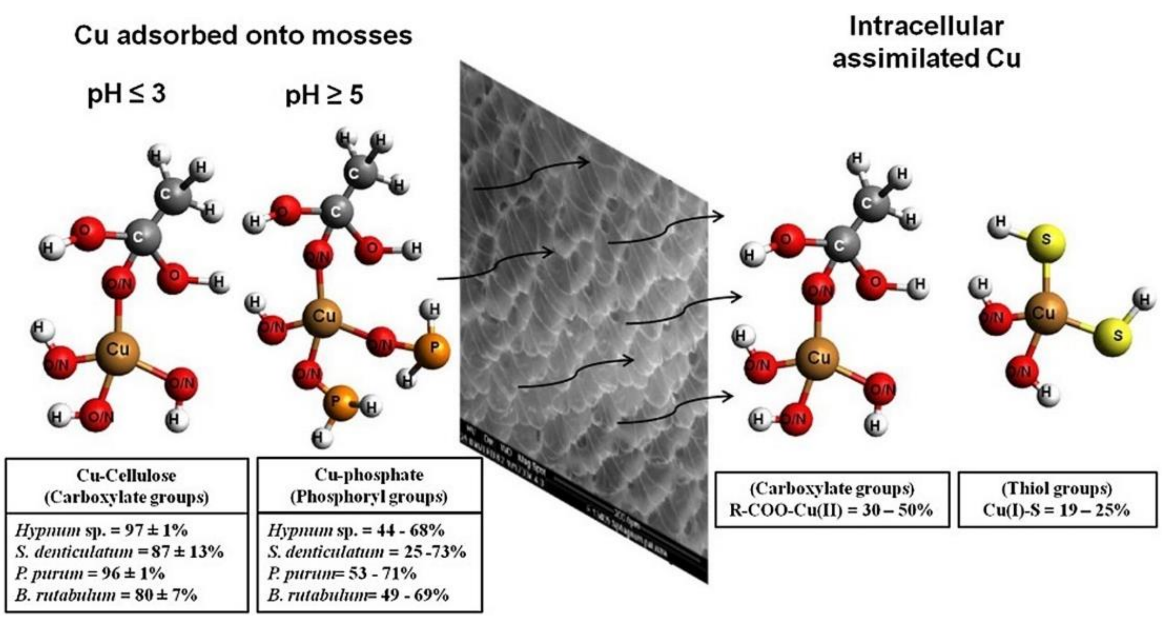

Figure 4. The Adsorption of copper into moss by differing chemical groups varied by pH.

This image illustrates the effect that pH has on surface bonding mechanisms that copper uses in different moss species. Figure reproduced with permission[33]

$$\frac{[Me^{2+}]_{aq}}{[Me^{2+}]_{ads}} = \frac{1}{K_L q_{max}} + \frac{[Me^{2+}]_{aq}}{q_{max}}$$

Equation 1. Linear form of Langmuirian adsorption isotherm for bisorbants. [32]

This is a modified form of the Langmuirian equation. The brackets signify concentration of a metal in the aqueous solution (aq) and the adsorbed concentration (ads)[32]. The other constants refer to the Langmuirian equilibrium (K_L) and the maximum adsorption capacity (q_{max})[32].

When one monitors the LRT of metals and metalloids, it is important to consider the purpose of the study, as general screening, total element determination and bioavailability monitoring schemes each require different approaches. The exact details of sample preparation for the different approaches will be continued in sections 2.2 and 2.3, but for general monitoring purposes the use of soil and biomonitors for the sample matrix is common and accumulation in the different matrixes can be compared with the appropriate positive matrix factorization[35]. Due to the significant contribution of metals and metalloids from natural[9] and anthropogenic sources, it is important to factor these into the data before determination of atmospheric deposition contributions[29]. This may be accomplished by taking sediment[29] or peat cores to establish the time and concentration scales of the target analytes at the sample site[36, 37].

This study focuses on metals and metalloids that previously have been prominent in Norway, or are of global concern for LRT, Ag, As, Bi, Cd, Fe, Mn, Mo, Pb, Sb, Sn, Tl, V, W, and Zn[28, 38]. These metals have potential sources in North America, Europe and Asia[38]. Metals like Cu, Cr, Co and Ni are interesting to include due to their concentration from closer transportation incidences, most probably arising from industries in and around Norway[39, 40]. Non-metal and metalloid elements that can link deposition patterns to natural influences, like bedrock composition, or ocean spray may also be useful to explain certain distribution patterns that occur[41].

2.1.3.1 Mercury

Mercury is commonly emitted through fossil fuel production, coal and precious metal mining, waste incineration, cement production, volcanic eruption, and rock weathering[25, 42] although the metal's prevalence is mostly due to the anthropogenic sources[9]. Mercury is toxic and can bioaccumulate in aquatic organisms in its methylated form to cause deadly neurological effects[28]. The most infamous occurrence of this happened in Minamata, Japan due to the mismanagement of industrial processes and pollution of the adjacent bay[28]. Further study of the chemical and biotic interaction of mercury in soil is needed as there is some evidence that mercury in soil is responsible for terrestrial exposure[9].

Mercury travels by global distillation after vaporization to gaseous elemental mercury (GEM), or Hg(0)[5, 9, 25]. This metal is able to travel extended distances due to its long atmospheric residence time of 6-12 months[5, 9, 25] and only usually deposits as reactive gaseous mercury

(RGM), or Hg(II) after oxidation[5, 9]. The deposited Hg(II) can be stored in the sea ice, snow and soil and undergo freshwater and marine emission later during melting and weathering processes[9], or re-enter the atmosphere[9] after photoreduction to Hg(0) and resume transport[5]. In the Arctic, atmospheric depletion events (AMDEs) may increase mercury deposition. AMDEs are triggered by polar sunrises[9] through UV aided mercury oxidation by bromine atoms[5] and other halogens[9, 37, 43]. Bromine ions may accumulate in the atmosphere around Arctic areas through the debromination of sea ice and anthropogenic emissions[5]. This process is partially illustrated in Figure 5.

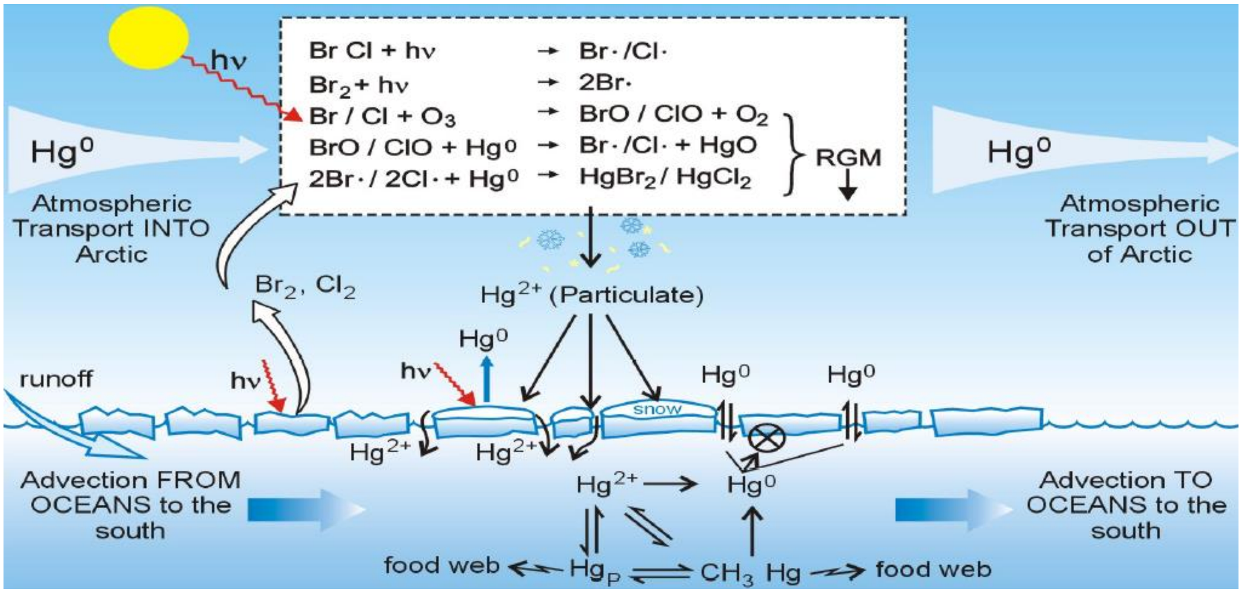

Figure 5. A theoretical diagram of mercury cycling in the Arctic.

This figure shows some of the proposed mechanisms that occur during Arctic mercury depletion events. Figure used from *A synthesis of atmospheric mercury depletion event chemistry in the atmosphere and snow* under creative commons license 3.0[43]

Monitoring mercury can be difficult due to its propensity towards vaporization, and often requires specialized equipment set ups[25]. The speciation of mercury is particularly important to analyze due to the different properties of the chemical species[25]. As the climate changes, currently known transportation pathways will be affected. These can be modeled to forecast future patterns, but only a few factors, pathways, sources, and sinks at a time can be selected[5]. Depending on which features are prioritized, some models investigate the effect of temperature on the reduction of Hg(II) to forecast increases due to warmer temperatures, while others seek to understand the possible effects of decreased sea ice and snow formation on free bromine release and the effects of Hg(II) encountering DOM, which it has a higher affinity for than ice[5].

2.1.4 PAHs and PCBs

Polycyclic Aromatic Hydrocarbons (PAHs) and Polychlorinated biphenyls (PCBs) are large classes of chemicals under the larger classification of persistent organic pollutants (POPs). To be a POP, a chemical must be persistent, bioaccumulate, toxic (PBT) and undergo LRT[15]. PAHs are fused aromatic rings[29] whose production stems from both natural and anthropogenic sources[19, 28] through incomplete combustion activities[19, 29], although human activities may account for the majority of their prevalence[19, 44]. This class of chemicals has been documented to interfere with biological systems, causing cancer[29, 44], endocrine disruption, and asthmatic and allergy conditions[15, 28]. PCBs are predominantly anthropogenic in origin and are produced as fire retardants, in electronics, as oil and plastic additives, and for other extraneous purposes[29, 45] and is primarily known for its immune system toxicity[28]. The classification of POPs' and their propensity for LTR, makes them important to monitor, although PAHs may degrade through photo oxidation[19], scavenging and microorganism decomposition[29].

Unlike LTR of metals which depends on wet deposition[26], the spread of POPs is determined by their volatilization from the soil along with dry particle bound deposition[27]. Wet deposition of POPs can be limited due to their hydrophobic nature[27]. To predict the concentration of POPs and other chemical substances in environmental science, partition coefficients are often used[46]. These coefficients serve to compare the concentration of a solute as it approaches or undergoes equilibrium across two phases[46]. For moss and soil deposition, the octanol to air (OA), or octanol to water (OW) partition coefficients, can be determined[10, 25]. These physiochemical properties of a compound and the sub-cooled liquid vapor pressure of a compound (p_L°), may be used to describe and predict the distribution of different PAHs and PBDEs in moss and soil[10, 11, 23] which is useful as the exact mechanisms behind POP accumulation in mosses are still under research[11] and PAHs levels in soil may be less than the amount deposited due to the biologically induced degradation[29] The higher the p_L° of a compound, the greater propensity it has to exist as a vapor, where the lower the p_L°value, the more likely it is to bind with particles[11, 23]. High log K_{OA} or lower log p_L° values correspond to heavier compounds, which favor soil accumulation through wet deposition, where mosses tend to accumulate from vapor phase chemicals with the opposite physiochemical properties[10, 11]. In general, K_{OA} values between 10^6 and 10^8 correlate to high volatility and p_L° values between 1 and 0.01 pascals results in deposition of compounds at temperatures of -30 °C, both traits which propel compounds to polar areas[23]. Using these generalizations, the mobility of certain POPs can be grouped for more general predictions based on the properties that correspond to these classifications, such as the amount of carbon rings or Cl and halogen groups on the molecule[23].

To measure POPs that undergo LRT, there are several different options. Air monitoring of POPs with electronic monitors, or filter collection units[47] can be used, but often they are placed for only short periods of time, or in limited areas[29] and they may have difficulty detecting POP concentrations at the levels in which they are present in the air[27]. Soil is generally considered a sink for POPs[27] making it a possible source for sampling, but as mentioned previously, microorganisms in the soil can degrade various PAHs[29] which may be less desirable for monitoring purposes.

Biomonitoring using animals, or plants is also an option[10, 11], but they have been shown to present different concentration patterns of POPs than soil samples, which is important to consider in any analysis comparisons[27]. In addition, the concentration of POPs in the air varies throughout the year, with a peak in the winter and low during the hotter summer months resulting in different accumulation levels in vegetation[27, 29]. As POPs are mostly hydrophobic, they rarely transfer into plants via root systems, leaving plants that lack proper root systems and rather draw nutrients exclusively from the air, concentrating pollutants along the way, optimal options[27]. Moss and lichen draw nutrients from the air and are both decent bioindicators for POPs due to their cost effectiveness and widespread distribution[27], but lichen accumulates less elements when compared to mosses[48]. Climate change too plays a part in the monitoring of POPs, by alteration of deposition rates as volatilization and scavenging processes change to release previously trapped pollutants, like those in ice formations or permafrost areas, and predicted residence times of compounds change[5].

2.1.5 Specific PAHs and PCBs of interest in analysis

As PAHs degrade over time in biological matter[29], compounds that are relatively stable and can undergo extraction and detection techniques are preferred for use. Compounds also can be selected based on their ability to undergo transformation in the atmosphere, which can be used to judge the distance that a pollutant has traveled from a potential pollution source by tracking the ratio between the pollutant precursors and byproducts of a reaction [18]. Reactive alkylated PAHs, like benz[a]anthracene and benz[a]pyrene and their more stable forms benz[e]anthracene and benz[e]pyrene are perfect for this purpose[18]. The PCB, endosulfan also can be tracked similarly for local pollution events, but after LRT it is found only as endosulfan sulfate[18]. Other compounds can be selected to monitor due their response to global conditions, like that of ɣ-hexachlorocyclohexane (ɣ-HCH) which correlates to LRT processes and changing temperatures[5].

As PCBs and PAHs are both groups that contain an ever-increasing number of compounds, only a few that were available as standards were selected to monitor in this study. Most of the selected PAHs and PCBs initially scanned for in this study were based on standards used by previous mixed PCB and PAH detection studies[49] or PAH studies[50]. Table 1 shows the POPs scanned for in this study along with some of the properties that correlate to their mobility, such as rings, Cl groups, p_L° and K_{OA}.

Table 1

A list of the PCBs and PAHs selected for detection. This table lists the PAH and PCBs specifically screened for in this study. The fluorinated PCB internal standards are designated with a "a" and PAH internal standards designated with a "b".

Compound name	Rings	Cl groups	Molecular weight	Log p_L° (Pa) at 25 °C	Log K_{OA}	Retention time (min)
Naphthalene[b]	2	0	128.17	1.6	5.1	7.76
4-Fluorobiphenyl[a]	2	0	172.20	-	-	8.871
Acenaphthylene[b]	3*	0	152.19	-	-	9.381
Acenaphthene[b]	3*	0	154.21	-	-	9.568
Fluorene[b]	3*	0	166.22	-	-	10.077
3-Fluorophenanthrene[a]	3	0	196.22	-	-	11.063
Phenanthrene[b]	3	0	178.23	-	-	11.222
Anthracene[b]	3	0	178.23	-1.1	7.3	11.286
3'-F-PCB 28[a]	2	3	275.54	-	-	11.624
PCB 28	2	3	257.54	-1.5	7.8	11.686
PCB 52[5]	2	4	291.99	-1.8	7.9	12.141
Fluoranthene[b]	4*	0	202.25	-2.1	8.6	13.363
PCB 101	2	5	326.43	-	-	13.624
Pyrene[b]	4	0	202.25	-1.9	8.6	13.917
5'-F-PCB118[a]	2	5	344.43	-	-	14.492
PCB 118	2	5	326.4	-	-	15.001
PCB 138	2	6	360.88	-	-	15.527
PCB 153[5]	2	6	360.9	-3.2	8.5	16.306
3-Fluorochrysene[a]	4	0	246.3	-	-	17.473
Benzo[a]anthracene[b] [18]	4	0	228.29	-3.2	9.5	17.819
Chrysene[b]	4	0	228.29	-4.0	10.4	17.988
PCB 180	2	6	395.32	-	-	18.323
Benzo[b]fluoranthene[b]	5*	0	252.31	-	-	22.744
Benzo[k]fluoranthene[b]	5*	0	252.31	-	-	22.857
Benzo[a]pyrene[b]	6	0	252.31	-4.7	10.8	24.374
Indeno[1, 2,3-cd]pyrene[b]	6*	0	288.4	-	-	30.131
Dibenzo[a,h]anthracene[b]	5	0	278.35	-	-	30.27
Benzo[ghi]perylene[b]	6	0	276.33	-	-	31.332

* These compounds have a 5-sided ring in addition to six sided rings
Molecular weights taken from Sigma Aldrich, the national center for biotechnology information (NCBI) and Chiron. Log p_L° and Log K_{OA} data from *Tracing the distribution of persistent organic pollutants* 1998 by Frank Wania.[23]

2.2 Sampling and pretreatment

The sampling and storage of samples should be carefully undertaken to prevent unnecessary errors. When taking samples, the background information about the location should be evaluated through previous reports of the area, maps, photos[51], geological records, weather patterns, topography, and plant density[52]. This information can help when there are multiple sample areas of mixed contamination levels, or when a study needs a distinctly different control location[52], but also in other applications. If an area has unknown qualities, a preliminary pilot study may be warranted to gather information about the area[52].For large all-encompassing studies, one site per 1000 km on a grid sampling is recommended and one type of sample material or species should be used to prevent the introduction of inter-calibration factors that for biomonitors like moss tend to vary depending on environmental conditions and location[26]. There are a few main types of sampling; probability sampling, which incorporates the randomness within the sample location in a way that allows for various statistical analyses on variability to be calculated and is useful in initial studies of an area[51, 52], judgment or hypothetical sampling, which is done by the use of prior knowledge held by the researcher to select locations[52] and its accuracy depends on the accuracy of the researcher[51], continuous sampling, which is often used in waste discharge situations[52], and haphazard sampling, which is when decisions regarding the sample locations were made due to convenience and no attempts to ensure the equal distribution amongst the sampled population was made[51]. The quality of scientific results can be severely affected by contamination and decomposition during the sampling and storage time periods[25], and should also be accounted for by any sampling scheme.

2.2.1 Moss

Since 1960's, moss began was used as a medium for atmospheric anayslsis[53 26]. Moss is an excellent candidate for research into atmospheric deposition and LRT due to its biological and physical characteristics[39, 54]. Biologically, moss absorbs nutrients from the air through the use of its entire structure as moss lacks root systems and cuticle layers[39, 40, 54 55]. The lack of a standard cuticle layer and single-cell leaf layers, allows for the easy movement of ions through the cell walls,[53] which makes moss sensitive to the air around it and provides a high surface area to volume ratio for adsorption processes[15]. Mosses also have higher adsorption capacities in general when compared to other plants, funguses and bacteria[32]. Physically, moss can be identified with practice from the naked eye and is prevalent across the globe. In addition, moss can be harvested at low costs[48] as it does not require any specialized equipment[26]. In regards to metal levels, the concentrations observed can be assumed to be proportional to the concentrations in the air at the time of growth[39], which is useful for analysis of specific years with moss species that grow in steps, like *Hylocomium splendens*[26] as shown in Figure 6.

Figure 6. Image of *Hylocomium splendens*.

This image of *Hylocomium splendens* showcases its tiered yearly step-like growth pattern. This image was accessed under the creative commons license 3.0[56].

Although soil sampling has many benefits, biomonitors like moss have some advantages over soil samples for air monitoring purposes as there is less potential for mobile elements to leach from the sampling area. Other positives of moss over more traditional deposition collectors include lower costs[57, 58] , reduced contamination from ground water and parent soil[40], easy sample collection across many different landscapes[40, 48, 59], simple chemical analysis as the moss concentrates substances[40, 48], small pollution event detection[1, 60], industrial output observation[13], and the potential to create maps of temporal and spatial contamination patterns across areas[1, 59], especially in comparison to mechanical collectors that are often placed close to factories and need to be maintained continually[61]. Moss monitoring is not ideal in every situation, for example seasonal deposition measurements that require time period measurements of less than a year are best done by continuous monitoring stations[26 40, 62, 63]. In addition, when multiple species of moss are used to expand the sampling range of a study, the intercalibration factors needed to compare the data may prove to be too extensive to evaluate as they are not universal and can vary depending on environmental conditions and location[26] but as there is some evidence that intercalibration factors may vary more with location than species[64], the positives of multiple species sampling may outweigh the negatives.

When evaluating pollutants from moss samples, there are natural distribution, redistribution[40] and adsorption effects to be accounted for. As not all metals and metalloids that have been shown to correlate between wet depositions and moss concentrations[26], it is important to design a study that can accommodate this. As, Cd, Ce, Co, Cu, Er, Mo, Pb, Sb, Sm, Tl, V, Y and Zn levels in moss significantly correlate to wet deposition levels[40], but Ba, La, Mn, Na, and Rb do not[3, 26, 40, 54] although dry deposition processes may account for some of the differences in studies that compare moss uptake abilities to precipitation collectors[26]. The reliability of Cr, Fe, Ni, and Sr concentrations in moss is conflicted and so these elements should be considered with background location information[3, 40, 54]. Metal concentrations in mosses can be influenced by outside factors such as minerals from living and dead plant material, which primarily affects elements Ba, Ca, Cu, Cs, Mg, Mn, Rb, Sr, Zn[40]. Interactions from sea-salt cations, acid rain precipitation, contact with soil compounds during snowmelt, or other events that increase soil water contact can also change the elements inside moss[40]. Calibration factors for metals accumulated from soil should be used in areas where this is a concern[65].

Although the exact mechanisms behind POPs accumulation in mosses are still under research[11], higher molecular weight compounds take longer to diffuse through plant surfaces[27]. Wet deposition, like rain fall, can disrupt this process and initially decrease the incidence of PCDD/Fs detected[27]. Atmospheric conditions also play a role in the uptake of POPs, with uptake increased by high concentrations in the air and strong winds due to the disruption of the laminar boundary layer around the plants surface[27]. In addition, the concentration of POPs in the air is variant throughout the year, with a peak in the winter and low during summer months, which may result in different accumulation levels in vegetation sampled at different time periods during the year[27, 29].

This study uses *Hylocomium splendens* to monitor the impact of LRT as there is extensive precedent to do so,[26, 65] due to its distinct shape and widespread availability. Another commonly used moss species, *Pleurozium schreberi* , has similar benefits, but has been shown to accumulate less elements and seasonal uptake variations are more evident[40]. The use of moss bags, moss samples grown, or treated in a laboratory area then taken to sample sites for a period to accumulate pollutants, is a well-documented alternative that reduces many of the errors and difficulties with traditional moss sampling[15, 48, 66, 67].

2.2.2 Soil

Soil serves as a sink for many trace elements and pollutants of note[52], although this reservoir can be transient and release substances with changes in temperatures into nearby waterways[29].The composition of soil determines its metal and metalloid adsorption capacity and is highly dependent on the area, but in general it contains inorganic materials such as sand, clay, oxides, and hydroxides and organic materials, which decrease in a gradient from the surface[25, 52]. Sand is the least active in soil concerning metal and metalloid retention, but clay does retain some. The diameter of an average clay particle is less than 0.002 mm and is primarily composed of silicate, aluminosilicate, hydroxyl groups, and small levels of other groups[25, 52]. The substitution of Al and Si in the lattice structure of the phyllosilicate’s planar clay structure, and the zeolite’s 3-D tetrahertdal clay structure, creates a positive charge void that cations, like some of the trace metals, are drawn into and bound by if the space allows[25]. Although phyllosilicates have lower cation exchange properties than zeolites, they do irreversibly bind elements like Ni, Co and Zn easier than the high size exclusion properties of zeolites allow for, which only irreversibly bind minimally to dehydrated Zn and Cd ions[25]. Oxides and hydroxides, specifically those of Fe and Mn, are also important to soil chemistry as they effectively absorb and fix many trace elements in a wide range of pH and redox conditions through inner sphere mono and bidentate surface complexes[25]. The organic matter content (OMC) in soil makes up 2-5% of the total soil and strongly effects its pollutant retention capabilities[29, 52]. This usually results in increased absorption of organic halogen compounds, but exact retention effects vary from component to component[29]. OMC is made up of humic matter, that is divided into humic acid, fulvic acid and humin[25]. These are chemically active through surface groups that contain O, S and N and may adsorb pollutants, although retention is often reversible with Cu and Hg as exceptions[25]. A summary illustration of these groups is presented in Figure 7. Smaller ligands like dissolved organic carbon (DOC) and inorganic groups such as phosphates, sulfates and chlorides also effect soil chemistry[25, 52], with DOC often mobilizing Cu and chlorides increasing the mobility Cd[25].

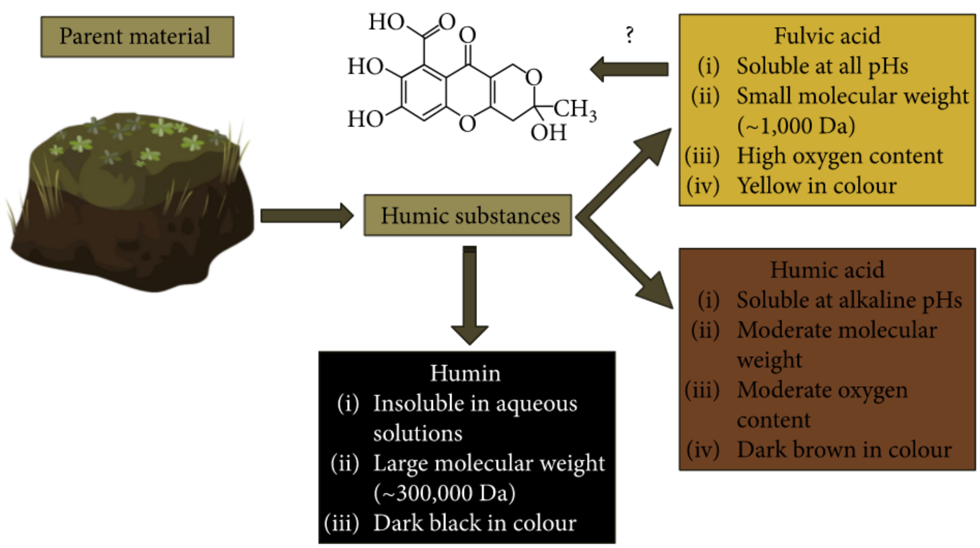

Figure 7. Illustration of humic substances.

The figure displays the three major subgroups within Humic substances. Their defining properties are described and a generalized chemical structure for fulvic acid is included. Content is accessed through the creative commons license 4.0[68].

Soil sampling and monitoring can be done in a variety of ways. A mechanism for creating a representative survey of an area beforehand is essential and is dependent on what type of statical significance one is trying to achieve. Sampling soil can be complicated depending on the goal. In non-aqueous locations, surface level sampling can be accomplished with a trowel and disposable polyethylene gloves[52]. It is preferred that the trowel is nonmetal, but stainless steel can be employed if precautions are made[52]. For deeper sampling, an auger or corer can be used and in aqueous sediments, a grab instrument or corer can be used as long as the analyzed sample material did not touch the sampling instrument[52]. Some methods of soil sampling do not require any soil to be taken, such as with a diffusive gradient thin film (DGT) device. These devices contain a filter membrane around 45 μm thick that is in contact with the sample material and allows small particles past to a diffusive membrane layer that is more selective and guides target analytes to accumulate on the ion exchange resin behind it, which can later be chemically modified to release the analytes in the lab[69].

Recommended extraction methods for metal and metalloid analysis is dependent on the desired outcome of the analysis. A 80µm M Ca Cl_2/$CaSO_4$ solution after washing with deionized water or using a 0.001 M $CaCl_2$ solution can be useful for evaluating metals that would be bioavailable or mobile under field conditions[52]. The use of a chelating agent, which can be employed in DGT devices, also has been shown to demonstrate a relationship to the bioavailable metal and metalloid soil fractions and concentrations can be easily calculated after extraction with Fick's first law of diffusion in Equation 2 [69] .

$$C = \frac{M\Delta g}{DAt}$$

Equation 2

This is Fick's first law of diffusion where M is the mass of the analyte deposited on the resin interface, Δg is the thickness of the diffusive layer, D is the diffusion coefficient of a particular metal, A is the area of the diffusive layer and t is the time that the DGT was employed.

Microwave extraction and hot-acid extraction are the most complete of the bioavailable extraction methods and details the use of a weak acids, pressure and heat[25]. This procedure can be dangerous and the process is usually preformed by a machine specially designed for the purpose[51]. The most common technique for environmental analysis uses HNO_3 [51]. Total metal extraction requires HF and HCl acids and is extremely dangerous[25].

Due to soil's ubiquity, higher concentrations of trace metals than water samples[52] and potential low cost, its use as a sampling source is ideal, but it is important to do so properly for the analyte one wishes to measure. Challenges with soil sampling often arise from its active nature. Compounds that enter the soil are influenced by the chemical makeup of the matrix, pH and redox conditions[25]and by the biota[29]. The extensions of two most popular soil modeling attempts, the Windermere humic acid model (WHAM) and the non-ideal competitive adsorption model (NICA), are only able to predict metal and metalloid concentrations within 0.5 to 1 $\log_{10}$ units as many soil processes are still not understood[29].

Although soil was not used as a sampling matrix in this study, it is important to understand its interactions for contamination purposes.

2.2.3 Milling

Milling is a generally recognized as an acceptable way to homogenize samples[1]. There are many different sizes and designs of mills and selection of the correct one depends on the sample amount, consistency desired and target analyte. Mills work by rotating or shaking an object to break it down into smaller pieces. This study used an Oscillating Mill MM400 that operates by shaking two canisters at a certain frequency for a specified duration. The machinery can be equipped with, tungsten carbide, agate, zirconium oxide, Teflon, stainless steel, or hardened steel to accommodate a variety of different target analytes[70]. An important safety consideration when operating a mill is noise pollution. This should be addressed by wearing the proper safety gear and operating the mill in a location where the disturbance is minimal.[70]

2.3 Digestion Techniques

Many analytical techniques require the sample to be processed beforehand to remove non-target analytes and other materials that may cause physical, spectral, or chemical interferences to the delicate and expensive equipment[52]. Sample digestion often either heats and exposes a sample to a solution in order to recrystallize and precipitate the target analytes in a way that removes impurities, or decomposes the matrix to release the target analytes[71]. These processes are often destructive and best suited for elemental analysis[72].

2.3.1 Dry ashing

This method is detailed in section 2.5.1 as it is a digestion and analysis procedure.

2.3.2 Partial digestion

The use of nitric acid, hydrochloric acid, or hydrogen peroxide to digest a sample is referred to as “pseudo” extraction since, silicate bound metals will not be brought into solution[25]. If done without any equipment, the sample is weighed and allowed to stand overnight in a mixture of 3:1 HCL and HNO_3 and then heated to reflux for two hours before it is cooled, filtered and diluted with water or dilute HNO_3[25]. It is more common now to use one of the various machines that automize and supplement different parts of this method such as block and bomb digesters. Block digestors control the digestion temperature and can be automated to run cheaply with pre-calibrated non-reusable sampling equipment[25]. Bomb digestors create a controlled sealed environment for analysis that reduces the loss of volatile species and is heated on a hotplate, or in an oven, but if the pressure exceeds the container's maximum rating, ther could be safety concerns[25].

2.3.2.1 Microwave Digestion

This is the most modernized pseudo extraction technique and is often employed to measure the biologically available, or mobilizable metals and metalloids in an sample[25]. Microwave extraction may result in heat degradation of compounds and does not perform as well with nonpolar and volatile components, but it is a cheap and energy efficient option that reduces time and solvent use[73].

The practice of microwave extraction (ME) varies significantly from other methods that extract compounds from their matrixes. Instead of heat, this technique uses electromagnetic waves to alter the cell structure of the sample through concurrent heat and mass gradients, which produces high yield extractions[73]. Energy transfer occurs through dipole rotation and the effects of dipole reversal on ionic conduction[73]. The temperature increase produced aids solvation as the viscosity and surface tension of the solvent decreases, which allows for better matrix penetration and solubility of the solutes[73]. For this reason, solvents with sufficient polarity to be effected by microwaves must be used, unless the user is purposely attempting to maintain a lower temperature in the sample vial to prevent the loss of volatile components[73]. Pure hexane or hexane mixed with other solvents often produces favorable results for lower temperature applications[73]. To increase the efficacy of this technique, the surface area of the sample should be high so that solvent contact is optimized and recommended particle sizes are between 100 µm and 2 mm[73]. High water content in the sample aids in the rupture of the cells, lowers oxide formation and can improve extraction efficiency[73]. The time and the number of microwave cycles can be increased to produce greater extraction yields, but this may decompose some target analytes further than intended[73].

2.3.3 Total digestion

Acid digestion is used for the total digestion of a sample[25, 51]. As briefly mentioned in section 2.2.2, HF acid can be used to do this[51]. This extremely corrosive acid will dissolve silicates, which are otherwise undisovled[25]. Special equipment, including non-glass containers, fume hoods for corrosive vapors and personal protective gear are required for use[25]. Generally this method is for geochemical surveying studies and if acid digestion techniques do not suffice for the toughest refractory minerals, the sample may be heated to the point of fusion and then dissolved in nitric acid[25].

2.4 Sample extraction methods

Extraction processes separate the target analytes from the matrix [52] while avoiding destruction of the compound[52]. This can be done physically through size exclusion methods for speciation studies[25], or chemically through processes that isolate compounds based on their chemical properties. Chemical separation techniques are often effective, but they do not necessarily correlate to in-situ conditions[25].

2.4.1 Selective extraction

Physical treatment procedures such as filtration, dialysis, centrifuging, and displacement may be done for the analysis of the most kinetically mobile species in soil, but as the concentrations of target metals and metalloids may be low, they often require more specialized extraction and concentration techniques[25]. Sonification of a sample through ultrasound waves may be used in combination with other extraction techniques to speed up solvent extraction processes[72]. A more advanced physical extraction technique is molecular exclusion chromatography, or size exclusion chromatography. This method separates molecules through the use of pores in the stationary phase that slow smaller compounds while allowing larger compound to pass[71]. This technique may be used in organic matter (OM) speciation studies[25].

2.4.2 Liquid-liquid phase extractions and partitioning

Liquid-liquid extractions use the chemical properties of solvents to solvate target analytes and remove them from the original liquid[52]. This is done with a separatory funnel to gently mix and separate the two immiscible solvents[52]. Partitioning, or the transfer of analytes between different solvents, also relies on the interactions of immiscible solvents and uses the interface between the solvents to exchange analytes[52]. This type of method may be useful for the extraction of organic analytes that are non-volatile or semi-volatile[72], but has limitations when the sample contains several compounds and may be best suited to general screening studies[74].

2.4.3 Solid-liquid phase extraction

The extraction of analytes from a solid matrix has traditional been done with a Soxhlet apparatus. This method depends on the constant exposure of fresh solvent to the sample so that dissolution of the analytes from the sample is continually promoted[73] within the extraction compartment[72]. This process is suitable for organics that are nonvolatile and semi-volatile[72]. Super critical Fluid (SCF) extraction is another solid matrix extraction method. This process can collect solutes, including nonpolar solutes and volatile ones, effectivley[73], but the specialized equipment required dissuades its usage[72]. SCF uses a three step sample treatment process where supercritical low temperature carbon dioxide, a mixture of supercritical carbon dioxide and methanol modifier and a system purge using carbon dioxide is applied[72].

2.4.4 Accelerated Solid Phase extraction

Also referred to as pressurized liquid extraction or pressurized solvent extraction[73], accelerated solid phase (ASE) extraction is used to clean the sample material and extract relevant analytes before analysis and detection. By using temperature, pressure and solvent manipulation, ASE is able to extract analytes from a sample in faster time periods and with less solvent than previous methods, like Soxhlet extration[75]. Temperature serves to disrupt the surface equilibrium in the sample[75, 76]. The high heat and pressure environment increases the solubility and diffusion rates of the analyetes[75]. The addition of fresh solvent throughout the process creates a continual differential concentration gradient that encourages analyte extraction[75]. Together these changes affect the cohesive and adhesive interactions of the solute to itself and the matrix, which reduces the activation energy of desorption from various chemical interactions and decreases the viscosity of the solvent to allow for deeper reach and extraction from the sample matrix[75, 76]. The high pressure also effects the surface chemistry by extending the liquid state of the solvents to force complete penetration of the sample matrix and decreases the time required for the extraction process[75, 76]. A schematic of a typical ASE layout is presented in Figure 8.

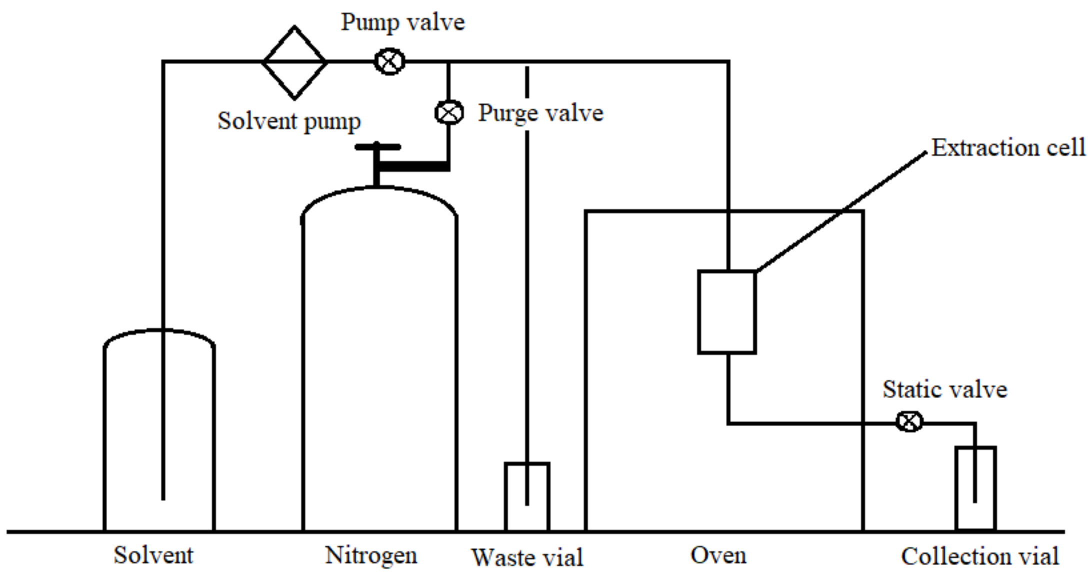

Figure 8. Diagram of a typical accelerated solvent extraction (ASE) design.

The figure above shows a line rendition of a simple accelerated solvent extraction set-up.

This method is designed for solid, or semi-solid samples to be loaded into a canister, or cell[75, 76]. Within the extraction cell, filters, alumina, and other chemicals depending on the procedure, server to filter and clean the sample which reduces the need for separate clean-up procedures[76]. By altering the contents of the cell, the extraction of specific analytes can be targeted[76]. Potential downsides to ASE include the high initial purchase cost and difficulties in selective extraction[76].

2.5 Chemical Analysis Techniques

Depending on the goal of a study and kinetics of the target analytes, there are different analytical detection techniques that can be employed. Total metal content, biologically available metal content, POP content, on-site analysis, off-site analysis, accuracy, and precision are just a few of the factors that determine what the correct instrumentation for the experiment is. Kinetic considerations are important to consider especially for species that may reach equilibrium faster than an analytical technique can separate them from their matrix as the measured distribution will be different from the true distribution in the sample[25].

Metals and metalloids can be monitored in many ways. X-ray spectroscopy techniques, for example, can determine the total metal content, or speciation of a compound with minimal sample preparation and the possibility of on-site analysis[25], but if the goal of the study is the determination of biologically accessible carbon at lower detection limits, a chemical extraction method combined with detection instrumentation is better[25]. Instrumental neutron activation analysis (INAA) can be used for metal analysis[59] without sample destruction in small quantities with smaller detection limits[25], although its low availability and highly trained technician requirements have led to the popularization of other more accessible methods[25]. For the analysis of specific metal fractions, such as bioavailable ones, digestion and filtration processes are used first to separate the analyte from the matrix before analysis[25]. Atomic absorption spectroscopy (AAS) is an older type of technique that encompasses many others and is still used for limited applications despite newer techniques, especially with the improvements in atomization methods from flame to electrothermal[31, 59]. More advanced techniques like inductively coupled plasma mass spectrometry (ICP- MS) and inductively coupled plasma atomic emission spectrometry (ICP- AES) are used more commonly now due to lower detection limits and the possibility of multiple element analysis[25].

To detect POPs, various types of chromatography and detectors are employed. Gas chromatography (GC) has been around since the 1950's and its usage along with high-performance liquid chromatography (HPLC) in the separation of organics has been instrumental in the field[72]. Different detectors have targeted applications like, electron capture for halogenated and phosphorus compounds[72] or fluorescence detectors combined with diode array detectors (FID-DAD) for method development and PAH identifcation[77]. Mass spectrometry can also be employed and are particularly effective with both GC and HPLC for lower detection limits and identification of compounds through chemical structure databases[72].

2.5.1 Total Organic Carbon and Total Inorganic Carbon determination

Carbon content analysis has a variety of applications. It can be used to monitor the carbon cycles in an area, the water treatment processes, and for chemical characterization[78]. The carbon content of a substance can be determined several different ways. Oxidation either by combustion or chemical means remains the most commonly used method, but inductively coupled plasma, as well as near infrared spectroscopy can be employed as well[78]. Generally, CO_2 formation is induced so that it can be quantitatively measured. Depending on if the analysis is for both organic carbon (OC) and inorganic carbon (IC), or only one of them, the methods vary[78]. For specifically OC analysis, IC can be removed either by treating the sample with an acid like HCl, H_2SO_3, H_3PO_4, or H_2SO_4 and $FeSO_4$ for wet combustion applications if it is assumed that all inorganic carbon is bound by carbonate[78]. Ashing and loss-on-ignition are other methods of separating carbon that, with modifications, allow for the analysis of both OC and IC. The weight of the respective carbon groups can be determined through the measurement of the weight loss of a sample after exposure under pure oxygen conditions to a temperature that correlates with OC transformation to CO_2 and then a temperature that corresponds to IC conversion[78]. Traditional ashing techniques that solely depend on weight require calibrations for different material types and must either expect water loss errors or employ accommodations for the mass lost due to water content[78]. The use of CO_2 detection systems greatly decreases mass loss errors and include most notably non-dispersive infrared spectrometry (NDIR), which has high sensitivity and a low detection limit, gravimetry, titration, thermal conductivity detection (TCD), and chromatography[78]. Elemental analysis through the separation of total organic and total inorganic carbon at different temperatures is a method with high accuracy, no preparation or extra chemical use and speed[78].

There are a few difficulties with carbon analysis. Volatile organic compounds can be notoriously difficult to analyze, and are usually considered negligible compared to the non-purgeable organic carbon concentrations[78]. The leaching of OC and IC together during combustion is another issue that cannot be completely discounted[78].

2.5.2 Inductively Coupled Plasma

This method of analysis uses inductively coupled plasma (ICP) to atomize a sample[52]. It is destructive and primarily used for element analysis.

The sample is drawn into a chamber by the rapid flow of a gas and aspirated when leaving the tip of the nebulizer to hit a glass bead[71]. The sample is further diluted by direction onto a 1 MHz oscillating quartz crystal that creates a fine aerosol, which is then carried by the gas to a the heating chamber[71]. This chamber evaporates and collects the solvent and then sends the dry particles to the plasma. The plasma is created through a set of radio induction coils wrapped around a quartz torch, otherwise known as a tesla coil[25, 71]. Argon gas that is passed through the flame, is energized to the point of ionization and the free electrons influenced by the radio field created heat the gas to temperatures between 6,000 and 10,000 K[71]. This extreme heat increases the residence time of the analyte, reduces the formation of analyte oxides and hydroxides to negligibility, creates a background free of radiation, and is consistent throughout the chamber, which increases the accuracy of calibration curves, but also requires an outer cooling gas to control[25, 71]. When the sample enters this chamber its chemical bonds are dissolved in a process referred to as atomization[71]. The atoms are then funneled into a mass spectrometer intake inlet, which is described further in another section[71]. A graphic of a simple ICP is shown in Figure 9

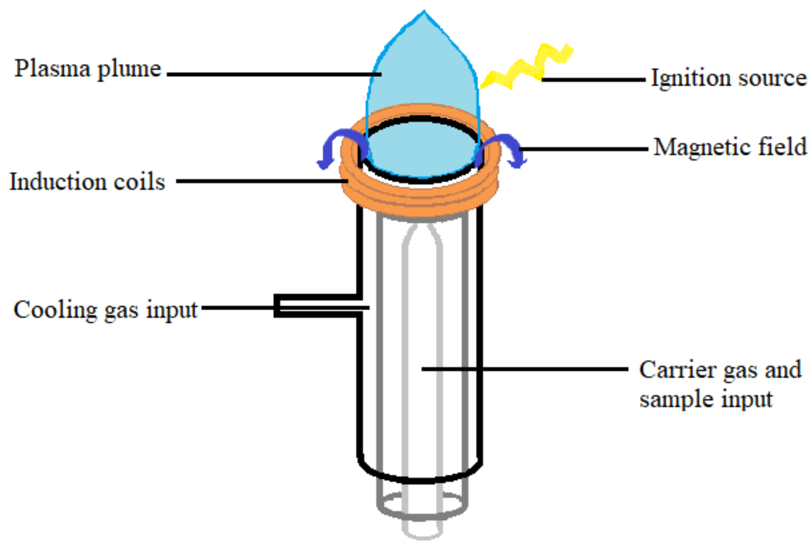

Figure 9. Simple figure of an Inductively Coupled Plasma (ICP) configuration.

In this figure, the basic components of an inductively coupled plasma torch are displayed.

The disadvantages of ICP include the difficulty of operation[71] as it requires a specialized technician. The machinery is also expensive to operate and purchase and is very sensitive to blockages produced by charred samples and requires organics to be loaded with O_2 for oxidation[71]. To ensure proper loading of a sample, it is important to guarantee that the metal concentration in within the machine's capabilities to handle. The recommended equation for the calculation of metal concentration from the US EPA 1994 method shown in Equation 3[51].

$$M\ (\mu g\ g^{-1}) = C\ (\mu g\ L^{-1}) \times DF \times 0.100L / (wt.\ soil\ g \times (1 - mc))$$

Equation 3

The above equation details the calculation of total metal content in a sample where M is the overall content of a metal in a sample, C is the concentration measured, DF is the dilution factor employed before a sample is run, and mc is the moisture content of the sample[51].

2.5.3 Chromatography

Chromatography is a process that separate components by pushing a sample through a column coated, or filled with substances that retain compounds at different rates[71]. There are several phases; the mobile phase, which refers to the gas or liquid solvent, and the stationary phase, which refers to a solid or liquid usually covalently bonded to the inside of the column, or to other solid particles inside the column[71]. After separation, the extracts can be analyzed by a detector.

There are five main types of chromatography: adsorption, partition, ion exchange, molecular exclusion, and affinity[71]. Adsorption chromatography depends on the adsorption of the solute onto the surface of a solid stationary phase[71]. Partition refers to the equilibrium of a solute between a liquid stationary phase and the mobile phase[71]. Ion exchange chromatography uses covalently bonded ionic groups to attract solutes with a liquid mobile phase[71]. Molecular exclusion uses only size distribution to separate components by passing the solutes through a stationary phase with pores that temporarily trap smaller components to allow larger ones to pass[71]. Affinity chromatography also uses a covalently bonded stationary phase, but is more specific at targeting compounds and may require a chemical change to release the solute, like a pH change[71].

These types of chromatography may be employed on different types of columns. Traditionally, a column was packed with particles coated in the stationary phase, but now some columns are not packed and instead line the inside of the column with the stationary phase[71]. This allows for greater column lengths and better resolution of the analytes, but these columns cannot handle as much solute[71]. Equation 4 shows the method for the calculation of theoretical plates, a measure of column resolution. Plates originally referred to the sections where equilibrium between volatized gases and liquids occurred in initial chromatography expiriments[71]. The height of a plate, calculated by dividing the length of a column by the number of plates, reflects the quality of a separation, where a large number represent a poor separation[71]. Figure 10 attempts to display the effects of a column on separation and resolution.

$$N = \frac{5.55\ t_r^2}{w_{1/2}^2}$$

Equation 4

This equation details the method for the calculation of theoretical plates where N is the number of plates, t_r^2 refers to the retention time of the compound on the column and $w_{1/2}$ is the width of the peak at its halfway height.

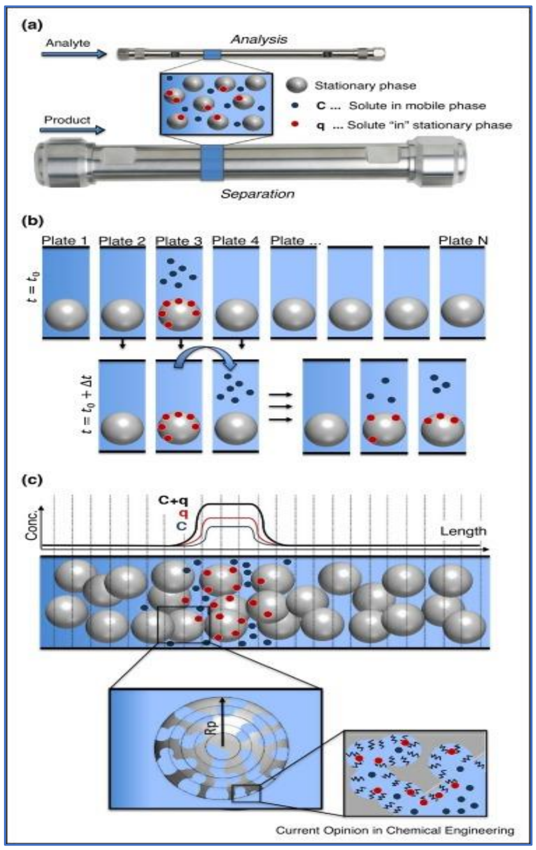

Figure 10. Diagram of the inside of an idealized chromatography column.

This image shows how column chromatography works. A) Shows the theoretical movement of a solute from an unbound state (C) to a bound state (q). B) Shows an idealized process of how solutes move from C to q and divides the solute over the theoretical number of plates. C) Shows how what is in the column is reflected by a sensor as well as possible idealized chemical structure level that holds some compounds and releases others. Figure used with permission from Recent advances in modelling and control of liquid chromatography[79]

Some of the issues with chromatography include band spreading or broadening, which widens the signal peak[71]. This usually effects the components that are retained longest as the equilibrium times between the mobile and stationary phase vary and the longitudinal diffusion effects increase with the length of time inside a column[71]. In a packed column the multiple flow paths through and around the material can increase the time spent in the column and may widen the peaks[71]. Through solvent, temperature and flow rate adjustments, or use of an open tubular column, smaller peak widths and clearer separations can be obtained[71].

2.5.3.1 Gas chromatography

Gas chromatography (GC) uses a carrier gas to convey the sample through a column lined with a solid or a bound liquid phase[71]. The gaseous sample is injected into the carrier gas, or heated to vaporization in the case of a liquid sample, before entering the heated column[72]. The varient column temperatures, controls the vapor pressure of the components and their respective retention times by the elution of low boiling components before higher boiling compents[71]. If polar compounds are retained on a column’s silica surface, tailing errors may occur[71]. Eventually this signifies the need to replace a column, but guard columns that are silanized and stationary phases that are covalently bonded can reduce tailing errors and extend the life of a column[71].

2.5.3.2 High performance liquid chromatography

High performance liquid chromatography (HPLC) uses high pressure to force the liquid eluent through a column packed with micrometer sized particles[71]. The size of the particles determines the resolution to a point; if the size decreases until the pressure required for use is too great for the system, the resolution decreases[71]. Altering the pressure and the solvent mixture to increase, or decrease polarity can control the elution of the elutes[72]. Due to the expensive columns required, a guard column with the same stationary phase theoretically binds any substances that may irreversible bind to the main column and may be replaced more frequently at a lower cost that the main column[71]. This method’s high resolution capabilities without possible damage to the sample through volatilization, makes it preferred for the detection of pharmaceuticals, hormones and endocrine disrupting species[72] such as PCBs.

2.5.4 *Detectors*

Detectors allow the scientist to "see" what they have separated. Many are specialized to specific applications, while others are adaptable to multiple situations at the expense of accuracy and precision. The most commonly employed detector is the mass spectrometer as it provides massive quantities of information about the structure of the molecules detected[71]. Luminescence, often measured as fluorescence or phosphorescence, is another commonly used detector, often due to its high sensitvity[52, 71]. The detectors employed in this study include Mass spectrometry and a Fluoresce detector (FLD) with a diode-array detection (DAD).

Inside a mass spectrometer after the eluents have been ionized by electrons or chemically, with the former resulting in more complete and fragmented ionization, they are accelerated before they enter a chamber that consists of metal rods in proportion to which type of mass spectrometer it is[71]. The most common is a quadrupole that has four rods[71]. These oscillate at a specific voltage to create an electric field that only allows a certain mass to ion charge ratio to pass[71]. Changing the magnetic field shifts which ion charge to mass ratio is detected and a complete spectrum can be run in under a second[71]. This method results in a detection range of 0.00000- 0.0001 ng/g and can detect multiple elements at once[71].The use of a magnetic sector technology in HR ICP-MS increases the mass resolution further, but can be considerably higher in price to operate[25].

Possible issues with a mass spectrometer include damaging the structural integrity of a compound and confusing compounds with similar mass to charge ratios. Mass spectroscopy data can have difficulties with isobaric interferences in the signals, which occurs when the mass to charge ratios from a signal are too similar to differentiate between[71]. If scan detection mode is run, it is possible to identify unknown components, although detection rates will be lower and isobaric interferences may lead to incorrect conclusions. Selected ion monitoring (SIM) mode uses known mass spectra data to only scans for masses of interest and leaves out compounds in favor of higher sensitivity[80].

At the most basic level, fluoresce detectors operate through excitation of the sample to a specific wavelength and then observation of the maximum emissions[71]. Either naturally occurring fluorescent molecules, or molecules modified by derivatization, can be used in a fluoresce detector (FLD), which uses a photon multiplier at an 90 degree angle from light source to detect the light emissions from the excited molecule[77]. To achieve a high energy light source, a xenon lamp is often used[77]. A diode- array detection (DAD) unit then serves to optimize the chromatographic separation of the molecules by the capture of the entire spectrum of a compound at once[71]. This occurs when the light beam is split into its component wavelengths with a polychromator that the DAD uses to direct the wavelengths to multiple individual diodes, semi-conductor detector elements, for detection[71].

The strengths of this method include simultaneous measurement at multiple wavelengths, repeatability and the ability to handle stray light errors[77]. Issues with a FLD- DAD detector set-up can include poor resolution of wavelengths between 1-3 nm[77].

2.6 Quality assurance

Equally important to the measurement of samples, are the steps undertaken to assure the quality of the data before analysis[52]. The precision, or the closeness of a data set, and accuracy, or the proximity to the true answer, are ways to measure this[25, 52]. Precision of a data set is often measured by using a modification of the standard deviation, usually the relative standard deviation as shown in Equation 5[25].

$$RSD = \frac{\sigma}{\bar{x}}\ x\ 100\%$$

Equation 5

The equation describes the relative proportion of the standard deviation for a sample set to the average value. Here the "σ" refers to the standard deviation of the samples and "$\bar{x}$" refers to the mean of the samples collected.

The precision of the instruments used is another important consideration and is often expressed using the detection limit (LOD), or smallest amount of analyte detected differently from a blank[25, 71] and the limit of quantification (LOQ), or the lowest reading that can be measured with accuracy[71]. Both are displayed in Equation 6. It is worth noting the LOD of an instrument may be different than the LOD of the method employed[25]. Precision can also be influenced by the limitations of the machine users. Periodic calibration checks during large sample sets and the insertion of blind sample tests, where analyte concentrations are known, but not by the individual preforming the analysis, may offset some of the user induced interferences[71].

$$LOD = \frac{3\sigma}{m} \qquad LOQ = \frac{10\sigma}{m}$$

Equation 6

The equations shown calculate the limit of detection and the limit of quantification. Here the "σ" refers to the standard deviation of ten replicate measurements of a blank, or low concentration of the analytes and "m" refers to the slope of the calibration curve.

The accuracy of a measurement must be considered during quality assurance procedures as well. Matrix effects may compromise the accuracy of measurements and are important to account for. This is often achieved with certified reference material, a substance of a similar matrix to the analyzed sample with verified concentrations of the target analytes guaranteed by an approved laboratory [25, 52]. In house reference material may be used due to the high cost and low variance of certified ones, but they should be calibrated against a certified reference material intermittently[25]. Additionally, matrix effects can be monitored with internal standards or "spiking". This is done by inserting a known amount of analyte into part of the sample and comparing the results with the un-spiked sample portion to create a calibration curve for the matrix effects of each component[71]. Other interferences that affect the accuracy of sample readings, such as the materials used and the laboratory conditions, can be accounted for using a variety of blanks, with reagent, method and field blanks being among the most common[71]. With these features in consideration prior to analysis, the quality of the data can be ensured for repeatability and verifiability purposes.

The use of certified sampling protocols, such as those constructed by the International Organization for Standardization (ISO), a worldwide organization that promotes standardization of intellectual, scientific technological and economic activity for the purpose of fluid trade exchanges[81], or by a governmental bodies like the US EPA, also can be used to ensure the overall quality of one's data. These types of organizations have determined techniques for all steps of the scientific process, from sampling to extraction and their referenceable methods serve as a foundation for many study methods. Deviations that arise are often due to the high cost of some of the methods configurations[1]. Developed methods may also be tested by several different laboratories, or sent to official laboratories that specialize in method verification to certify their validity or gauge the uncertainty present[25].

3 Materials and Methods

3.1 Sampling

3.1.1 Study areas

Moss sampling occurred in three main groups, Svalbard, Trondheim and southern Norway as shown in Figure 11. Sample areas were selected by using; previous sampling sites included in the Norwegian Environmental agency's atmospheric monitoring surveys, the suggestions of Eliv Steinnes, a prominent researcher in the field and through the Norsk institutt for naturforskning (NINA) database of plant species locations. Around five samples were taken from each location, although the southern Norway samples were taken in groups of two, or three due to time constraints. The coordinates for every sample were recorded (see Table 25 in Appendix D).

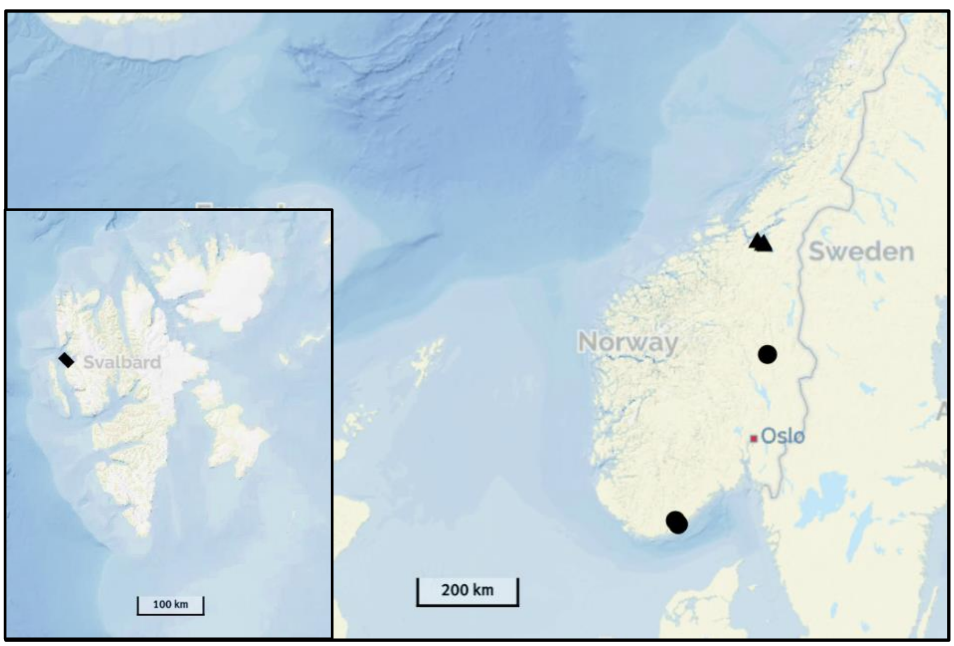

Figure 11. A map of the sampled areas across Norway and Svalbard.

This map shows the main sampling locations of the study. The different shapes distinguish Svalbard (diamonds), Trondheim (triangles) and southern Norway (circles). ©norgeskart.no

3.1.1.1 Svalbard locations

The sampling in Svalbard took place during late August of 2020 close to Ny-Ålesund. Ny-Ålesund is located approximately 78 ° North and 11 ° East and is currently used as a research station. Locations were accessed by hiking and are displayed in Figure 12. This sampling district composed 22.9 % of the samples.

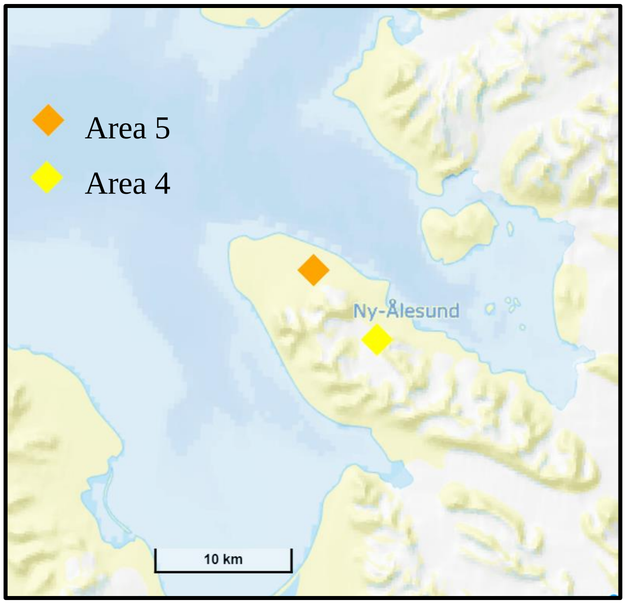

Figure 12. A close-up of Ny- Ålesund sampling locations.
This image shows sampling areas 4 and 5 in the Kongsfjorden area nearby Ny-Ålesund, Svalbard. ©norgeskart.no

Sampling Area 4 was a flat location, inland from the adjacent fjord, past a gravel field and the local water reservoir for Ny-Ålesund at the base of Zeppelin Mountain (see Figure 19 in Appendix D). The Zeppelin monitoring station for various air pollutants was located at the top of the mountain. The moss at this location was fairly dry and its growth was visibly stunted. Area 5, locally called Storhylla, was near the base of the cliff that is known to be visited by seabirds (see Figure 20 in Appendix D). The moss sampled was fairly wet and the vegetation was highly developed moss compared to other locations in the Ny-Ålesund area.

3.1.1.2 Southern Norway

The sampling in Southern Norway took place during late September of 2020. Area 10 is located approximately 61 ° North and 11 ° East and areas 6 and 8 are close to 58 ° North and 8 ° East. Locations were accessed by roads and hiking and displayed in Figure 13. This area composed 14.6 % of the samples taken.

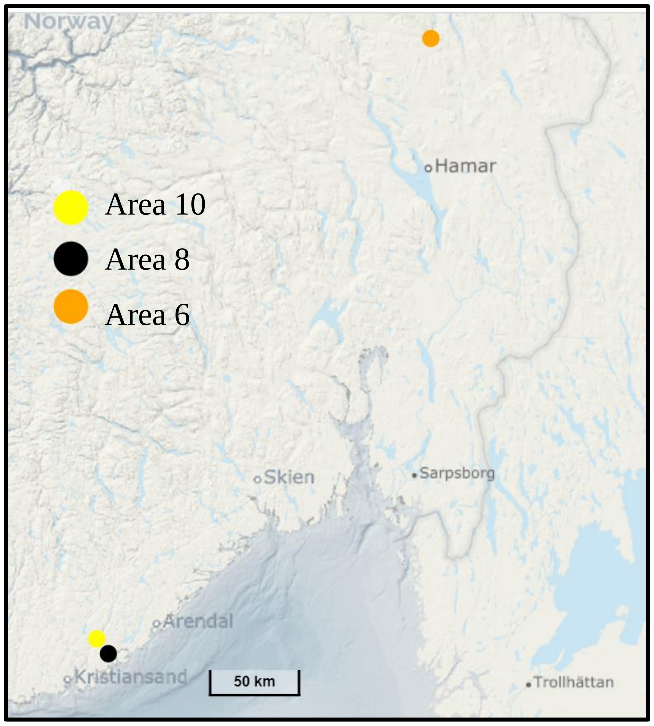

Figure 13. A map of the Southern Norway sampling locations.
The map depicts the sampling locations taken in Southern Norway. ©norgeskart.no

Area 6 was located close to the town of Stai and the sampled area was situated near highway number 3, and E6, the largest highway connecting Oslo and Trondheim. Samples were taken in a forested area that was high in moisture (see Figure 21 in Appendix D). Sampling Area 8 was close to Spjolevannet in a natural area. The moss sampled was highly mixed, developed and slightly wet (see Figure 22 in Appendix D). Grimevannet was nearby Area 10. The moss sampled here was also mixed and highly developed (see Figure 23 in Appendix D).

3.1.1.3 Trondheim

The sampling in Trondheim took place during October of 2020. The areas are located approximately 63 ° North and 10 °. Locations were accessed by roads and hiking as seen in Figure 14. The sampling district composed 62.5 % of the samples taken.

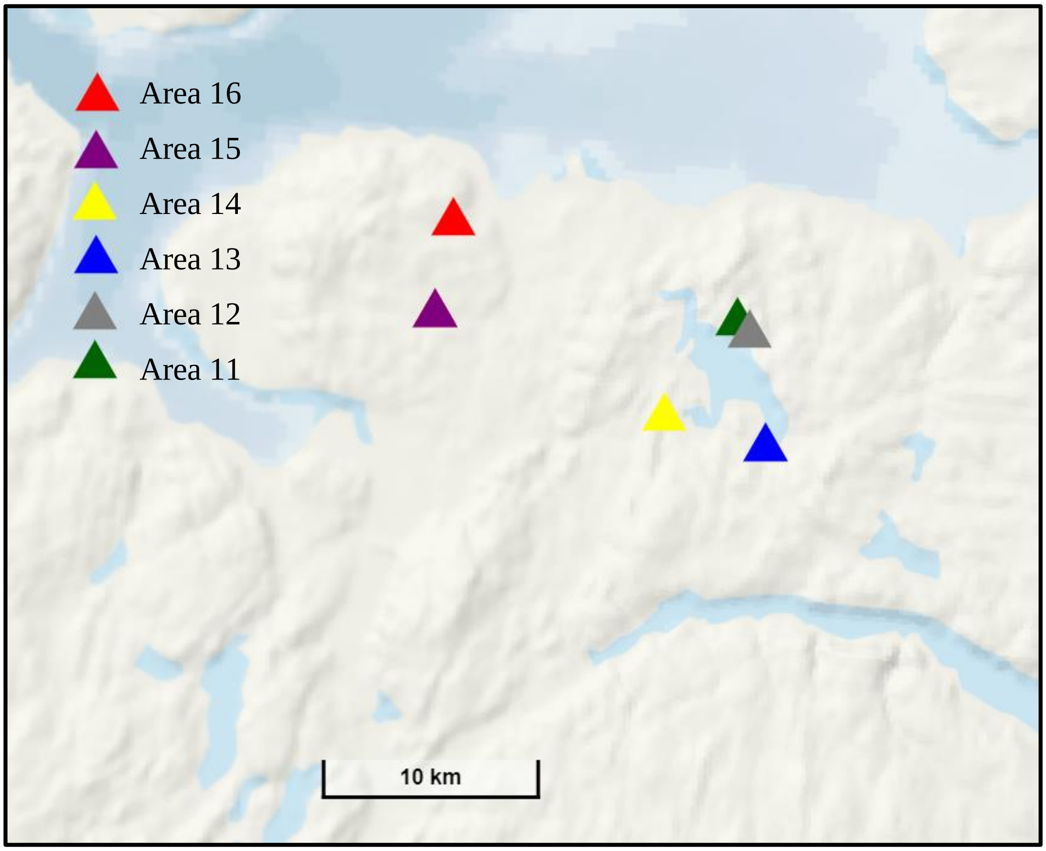

Figure 14. A map of the Trondheim sample locations.
This figure shows the sampling locations around Trondheim.

The samples in Area 11 were taken to the north of Jonsvatnet the Trondheim reservoir lake. The location was wooded with leaves and detritus mixed in the sample. The samples taken were dry (see Figure 24 in Appendix D). Area 12 was near the north side of Jonsvatnet nearby a second lake in the reservoir system. The place had heavy tree cover, but samples were taken in small open area by a stream. Elevation of the sampling area was below the road level. The moss sampled was wet and slightly underdeveloped (see Figure 25 in Appendix D). To the southeast of Jonsvatnet in Area 13 there was a significant moss population nearby a small waterfall on a plateau overlooking the lake and the road (see Figure 26 in Appendix D). There was mixed tree cover and wet moss at this location. Area 14 was to the west of the Trondheim reservoir close to Espåa. The sampled area had significant tree cover and a swamp-like lake (see Figure 27 in Appendix D). Nearby Granåsen in a wooded place, Area 15 was sampled in a clearing (see Figure 28 in Appendix D). There had been heavy frost several times before sampling. The last sampling location, Area 16, was nearby Baklidammen in Trondheim, although the lake was drained at the time of sampling (see Figure 29 in Appendix D). Heavy frost had occurred at several times before the moss was sampled. There was possible foot traffic contamination.

3.1.2 Sampling methods

The International Cooperative Program on Effects of Air Pollution on Natural Vegetation and Crops (ICP Vegetation) *Heavy Metals, Nitrogen and POPs in European Mosses: 2015 Survey*[82] monitoring manual and other current moss studies served as guides for moss sampling. Sub-samples of each area were done within a 50 by 50 meter area and an effort was made to avoid sampling areas with overhanging trees. When there was potential contamination from roadways, sampling areas were chosen at least 100 meters from local roads. To transport samples for metal analysis, paper bags and plastic latex and powder-free gloves were used. Samples taken for PAH and PCB analysis were stored in aluminum containers and taken with bare hands "cleaned" using the moss bath technique with moss from the site[83]. Plant species were confirmed with the help of Kristian Hassel who holds a Ph.D. in botany and plant biology and is an associate professor at NTNU.

3.2 Sample preparation

3.2.1 Drying

Metal free samples were left out to dry at room temperature (23 °C) in their collection bags for several weeks. Samples were weighed to track water loss and declared ready to process when the weight remained similar. PAH and PCB samples were frozen after collection at – 18 °C for 3 – 4 months inside collection tins. Samples were removed and allowed to dry at room temperature (23 °C) for around two weeks depending on the weight derived water loss.

3.2.2 Separation

Plastic tweezers were used for the separation of the target species from other species, soil, leaves and other large contaminates in the metal-free samples and stainless steel tweezers were used for the PAH and PCB moss samples[84]. All parts of the sample that were not visibly brown were used.

3.2.3 Milling

Samples for metal analysis were loaded into 35 ml Teflon canisters for the Retsch oscillating Mill MM 400 with Teflon milling balls. Samples for PAH and PCB analysis used stainless steel canisters with zirconium oxide linings and milling balls. They were ground at 25/s to 30/ s Hz, for 2 minutes to achieve particle size of <100 µm as specified by the manual[70, 85].

3.2.4 Microwave Digestion

Microwave digestion was done using a Milestone ultraCLAVE. Sample preparations were performed using 20 mL Teflon (TFM PTFE UC) vials that were internally tracked to avoid contamination across laboratory runs. The storage solution of ultrapure water and 65% ultrapure nitric acid produced at NTNU from 65% pro analysis quality nitric acid from AnalaR Normapur VWR using a sub-boiling distillation system by SubPur Milestone was cleaned off with three rises of ultrapure water. 50 mg of each sample or reference material M1 321 5 vvvv *pleurozium schreberi* from the muhos research station under Finnish Forest research institute moss, was added to the vial. Reference material was the same as recommended in the ICP Vegetation protocol[82]. The two blank vials were cleaned the same but left empty. Then 2 mL of 50% HNO_3 diluted from the 65% with ultrapure water was added to each vial. The microwave digestion operated with a base load of 300 mL ultrapure water, 30 mL of 30 % AnalaR Normapur H_2O_2 (VWR), and 2 mL of suprapur H_2SO_4 (Merk). The parameters were set to microwave pulse, load pressure 50 bars, release pressure 10 bars per minute, cooling temp 40°C, and ventilation time 1 hour and 15 minutes. The temperature program was set according to

Table 2. A 75-minute period was used to cool and reduce pressure after the program was run. The water cleaning system employed was Elga Purlab Option-Q DV 25.

Table 2

Details of time parameters of the microwave digestion program employed for metal analysis.

Step	Temperature (˚C)	Heating time (minutes)	Hold time (minutes)
1	50	5	10
2	100	10	0
3	110	10	0
4	240	25	57

Dilutions were performed in Teflon vessels of 50 mL and 100 mL by weight after emptying the reaction vial and using ultrapure water to dilute to the total weight of approximately 26.94 grams. Approximately 15 mL of the dilution was added to 15 mL metal free polypropylene centrifuge tubes (VWR) before further analysis.

3.2.5 Accelerated Solvent Extractor (ASE)

A Dionex ASE 150 by Thermo Scientific was used for the processing the sample set prepared for PAH analysis. The samples for the GCMS were prepared by the thesis student and the samples for the HPLC were prepared internally by NTNU.

3.2.5.1 ASE for GCMS

The ASE was equipped with HPLC grade dichloromethane and 25 mL stainless-steel cells. The cells were loaded with cellulose filters (Thermo Fisher Scientific), activated copper using < 425 μm 99.5% copper lot number MKCK0242 (Sigma-Aldrich), reagent grade hydrochloric acid 37% lot number 19J214014 (VWR) and HPLC grade acetone lot number 19C124018 (VWR) in accordance with U.S. EPA method 3660B and activated aluminum oxide lot number S38055-506 (Sigma-Aldrich) for in-cell clean-up purposed in the following order, two cellulose filters, 2 g of activated copper, 1 cellulose filter, 2 g of activated aluminum oxide, a cellulose filter, the sample mixture, and Ottawa sand lot # 1557961 (Fisher Scientific) purified with U.S. EPA method 3545A to fill any space left in the cell. The sample mixture was composed of 2 g of milled sample, 2 g of Diatomaceous earth lot number 165 (Thermo Scientific) purified by U.S. EPA method 3545A and 50 ppm of prepared standards in ethyl acetate stored at -20 °C. The standards added included, fluorinated standards 5’-Fluoro-

2,3’,4,4’,5-pentachlorobiphenyl / 5-F-PCB 118 10 ug/mL batch number 5864 in toluene (Chiron AS), 3’-Fluoro-2,4,4’trichlorobiphenyl /3-F-PCB 28 0.1 mg/mL batch number 4220 in toluene (Chiron AS) and F-PAHs all in one cocktail (naphthalene, acenaphthylene, acenaphthene, fluorene, anthracene, phenanthrene, pyrene, fluoranthene, benz[a]anthracene, chrysene, benzo[b]fluoranthene, benzo[k]fluoranthene, benzo[a]pyrene, dibenz[a,h]anthracene, indeno[1,2,3-cd]pyrene, benzo[g,h,i]perylene), 200 µg/mL in toluene (Chiron AS). Extraction parameters are detailed in Table 3. A method blank was constructed in the same way, minus the 2 grams of sample. This methodology was experimental and adapted from articles detailing a method for simultaneous PAH and PCB testing[49, 86] and a masters thesis[87].

Table 3

ASE program settings for the extraction of PCBs and PAHs.

Internal controls	Value
Internal pressure (psi)	1500
Oven temperature (°C)	100
Static extraction time (min)	5
Static cyles (#)	3
Flush volume (%)	60
Nitrogen purge (s)	60
Extraction time (min)	24
Total solvent per sample (mL)	40

Further clean-up was preformed after drying samples to 2 mL under nitrogen at 35 °C using a Biotage TurboVap LV concentration Evaporator Workstation. Then 10 mL of HPLC grade ethyl acetate was added to change solvents and transfer to 15 mL metal free polypropylene centrifuge tubes (VWR) before filtration with 0.22 µm nylon syringe filters (VWR). After, the sample was concentrated to 1 mL at 35°C and transferred into amber vials.

3.2.5.2 ASE for HPLC

The ASE was prepared using 10 mL cells and HPLC grade solvents acetone and dichloromethane in a 1:1 mixture. Cellulose filters (Thermo Fisher Scientific), copper at <425 µm 99.5% lot number 06718AHV (Sigma-Aldrich) and activated alumina from 0.05-0.15 mm alumina (Sigma-Adrich) in accordance with EPA Method 3610B was used for in cell clean-up purposes. The cell was loaded with 1 cellulose filter, 1 g of copper, 2 g of activated alumina and the sample mixture. The sample mixture contained 2 mL of diatomaceous earth (Thermo Fisher Scientific), 2 g of sample, or 1 g of reference material 1941b Organic in Marine Sediment from the National Institute of Standards & Technology, and 200 ng of F-PAH internal standard from a PAH mix (1-fluoronaphtalene, 4-fluorobifenyl, 3-fluorophenanthrene, 1-fluoropyrene, and 3-fluorochrysene) with 200 μg/ mL in toluene from Chiron AS. Method blanks were also employed without sample material. ASE parameters were run according to Table 4. Method was based on the HPLC column manufacture recommendation[50] and a U. S. EPA 3545 verified method[88].

Table 4

Accelerated solvent internal controls for the PAH only method.

Internal controls	Value
Internal pressure (psi)	1500
Oven temperature (°C)	100
Sample size	5
Static extraction time (min)	5
Static cycles (#)	2
Rinse volume (mL)	6
Nitrogen purge (s)	90
Extraction time (min)	19

Samples were dried to 500 μL under nitrogen at 35 °C using a Biotage TurboVap LV concentration Evaporator Workstation, then 10 mL of HPLC grade acetonitrile lot number 20J121960 (VWR) was added to change solvents before filtration with a 0.45 μm nylon syringe filter (VWR). The sample was then concentrated to 1 mL at 45°C and acetonitrile from the same source was added until 1.5 mL was achieved before transfer into 1.5 mL amber vials. A solvent blank was added at this point. Samples were split into two sets and one was spiked with 200 ng / ml from a 100 ug/ mL 16 PAHs mix (Napthalene, Acenaphthene, Acenaphthlene, Fluorene, Phenanthrene, Anthracene, Fluoranthene, Pyrene, Benz[a]anthracene, Benzo[a]pyrene, Benzo[b]fluoranthene, Benzo[ghi]perylene, Benzo[k]fluoranthene, Chrysene, Dibenz[a,c]anthracene, Indeno[1,2,3-cd]pyrene) Batch number 16679 in toluene (Chiron AS) and one was left unaltered before analysis.

3.3 Chemical Analysis

3.3.1 Total Organic Carbon, Total Inorganic Carbon and Residual Oxidizable Carbon

Samples of 100 mg were loaded into ceramic crucibles (2SN100370) and heated according to the SKALAR Methods DIN19539 for TOC, TIC and ROC analysis in a SKALAR Primacs SNC 100-IC-E. Temperatures for analysis were 400°C, 600°C and 900°C with a ramping rate of 70°C/ minute with 200 ml per minute of oxygen for a total time of 480 minutes for each temperature. Ultrapure grade 99.995% purity oxygen was used for combustion. A seven-point calibration curve was used with black carbon.

3.3.2 HR ICP-MS

Samples were measured using HR ICP-MS with a Thermo Finnigan Element 2 (Thermo Finnigan, Bremen, Germany) at the St. Olaf Hospital laboratory. Plasma parameters were set to 1250 W power, 16 L/min cooling gas flow, 0.99 L/min auxiliary gas flow, 1.0 L/ min sample gas flow with individual sample optimization. Resolution for the elements was taken in low, medium and high settings when possible. Internal standards at 2 µg/ L were applied by using Re for elements Tb, Dy, Ho, Er, Tm, Yb, Lu, Hf, Ta, W, Eu, and Gd; Ir for elements Pb, Pt, Au, Hg, Tl, Bi, Th, and U; and Rh for all other elements. Spectral interferences were corrected for due to the interferences of the oxides species MoO, WO, HfO as follows, Cd using Mo content, Hg using W content and Pt using Hf.

3.3.3 GC-MS

A GC-SQ 7890A machine from Agilent with a 5970 inert mass selector device from Agilent Technologies and an autosampler from CTC analytics was used for the PAH and PCB analysis with a Thermo TG- 5MS column using 30 m x 250µm x 0.5 µm dimensions. The carrier gas selected was helium. The injection port maintained a temperature of 290 °C with an injection volume of 1 µm at a speed of 50 µl/s. The oven program started after holding 50°C for 2 minutes, then increased at the series of rates and intervals listed; 25°C per min until 250 °C holding for 1 minute, 3 °C until 286 °C holding for 3 minutes, 8°C per minute until 308 °C holding for 1 minute, and lastly 1 °C per minute until 310 °C holding for 3 minutes. The machine used a front SS inlet with direct introduction heated to 290°C. An electron ionization source was held at 230°C with 70 eV of energy. The MS was run with selected ion monitoring (SIM) as detailed in Table 5. A full scan from 50 m/z to 550 m/z was also completed in the same run. Identification of signal peaks was confirmed using internal standards and a full scan of EI mass spectra of identified compounds that were in agreement with the MS Library spectra from the NIST MS library.

Data was corrected using a standard calibration curve and fluorinated internal standards. This methodology was experimental and adapted from articles detailing a method for simultaneous PAH and PCB testing[49, 86] and a masters thesis[87].

Table 5

The scanning program for the mass spectrometer. Groupings refer to the order of elution from the column.

Group	Time (min)	Mass to Charge ratio (m/z)
1	6	128
2	8.25	172
3	9.25	152,154
4	9.8	166
5	10.8	178,196
6	11.5	255.90,273.90
7	11.9	289.9
8	13	202,325.80
9	14.2	343.90,345.90
10	14.8	325.9
11	15.4	359.8
12	17	246
13	17.7	228
14	18.2	393.8
15	19	252
16	26	276,278

3.3.4 HPLC FID-DAD

An Agilent HPLC 1260 Infinity II G7111B with an automatic liquid sampler G7120A and ZORBAX Eclipse PAH 600 bar 1.8µm diameter 4.6 x 100mm column installed was used. A calibration curve with the same external standards of 16 PAHs, naphthalene, Acenaphthylene, Acenaphthene, Fluorene, Phenanthrene, Pyrene, Benzo[a]anthracene, Chrysene, Benzo[b]fluoranthene, Benzo[k]fluoranthene, Fluoranthene, Anthracene, Benzo[a]pyrene, Dibenz[a,c]anthracene, Benzo[ghi]perylene and Indeno[1,2,3-cd]pyrene, and five internal standards of fluorinated PAHs, 1-Fluoronaphtalene, 4-Fluorobifenyl, 3-Fluorophenanthrene, 1-Fluoropyrene, 3-Fluorochrysene, as previously used was made. Quality assurance was maintained by spiking with external standards and the use of method blanks, reagent blanks and concentrated regent blanks. HPLC grade acetonitrile and water were the primary solvents for extraction with concentrations percentages and time applied listed in Table 3. Pressure was held at 590.00 bars and a temperature of 20 °C was maintained throughout the run. An injection volume of 5.00 uL per sample was used. The detectors used included a diode array detector (DAD) G4212B and a fluoresce detector (FLD) G1321C. The software used was OpenLAB CDS ChemsStation Edition for LC&LC/MS systems version C.01.07[27]. The procedure based off of recommendations from Agilent[50] and Dionex[88].

Data corrections were preformed using the standard calibration curves and the recovery factors were calculated from the reference material due to improperly applied internal standards.

Table 6

The HPLC parameters for a sample analysis run are listed below.

Time (min)	Water %	Acetonitrile %	Flow (mL/min)
0.50	60.0	40.0	1.800
8.00	20.0	80.0	1.800
11.00	20.0	80.0	1.800
13.00	0.0	100.0	1.800
18.00	0.0	100.0	1.800
18.10	60.0	40.0	2.000
20.50	60.0	40.0	2.000

3.4 Statistical Analysis

For the statistical analysis of the data IBM SPPS Statistics version 27.0 was used. Significance levels were set at $p < 0.05$ unless otherwise stated. For the non-pooled data sets the three requirements to run an ANOVA test concerning independence, normality and homogenous variance assumptions[89] were checked visually and calculated if needed. To the knowledge of the researcher, all the samples were independent. Due to the small numbers of samples per area, when testing for normality the Kolmogorov test could not be used, so the Shapiro-Wilk test was selected and check visually with Q- plots. A Levene's test to check the equality of the variances of the data was run as well, although it is common to assume equality of varience[89]. If the assumptions were all met, a single tailed ANOVA test was run with a Tukey Honest significant Difference (HSD) post hoc test for groups that were significantly different. If normality could be assumed but not variance, a Welch test was run to correct the ANOVA values[89, 90]. If the groups were significantly different this was followed by a Dunett's T3 test, which considers normal data with unequal variances and can accommodate small and similar but not equal sample sizes[91].

A two-tailed Spearman correlation chart to determine probably elemental connections was used for non-normal data. Principal component analysis (PCA) was employed with the Unscrambler 11 program to analyze the relationships among the variables to detect relationships to the parent soil composition, local sources, or potential LRT sources. Data was mean scaled and centered by the standard deviation. Excessively noisy values were removed or scaled down to a value < |1|.

4 Results

4.1 Total organic carbon

The descriptive statistics for the total organic carbon (TOC) levels in a selection of samples from the sampled areas are shown in Table 7. The data ranged between 34.48 % and 39.46% TOC. The overall mean of TOC values was 38.20 % with a standard deviation of 1.21 %. When an ANOVA test was preformed, not any of the areas were determined significantly different.

Table 7

This table displays descriptive statistics for the total organic carbon percent of the sampled areas and selected samples. The detection limit for the instrument was ± |0.002| mg. The complete dataset is available (see Table 15 in Appendix A).

Area	Amount	Mean	Median	Min	Max	STD	RSD %
4	3	35.79	35.38	34.48	37.52	1.56	4.36
5	3	37.26	37.75	35.63	38.39	1.44	3.88
6	2	37.69	37.69	37.62	37.76	0.10	0.26
8	2	38.81	38.81	38.16	39.46	0.92	2.37
10	2	38.56	38.56	38.00	39.11	0.78	2.04
11	3	38.38	38.69	37.71	38.73	0.58	1.51
12	3	39.44	39.53	38.92	39.88	0.49	1.23
13	3	38.50	38.73	37.94	38.84	0.49	1.28
14	3	38.90	38.96	38.53	39.21	0.34	0.88
15	3	38.76	38.74	38.63	38.91	0.14	0.36
16	3	38.27	38.71	37.36	38.74	0.79	2.06

4.2 POPs data

This section contains the results from the two different analytical procedures for the detection of PAHs and PCBs. Due to laboratory limitations, individual samples were pooled into one sample for each area.

For the HPLC FID-DAD method, due to errors with the original internal standards, the PAHs in the certified reference material (see Table 23 in Appendix C) were used to calibrate the sample readings along with a calibration curve. Of the nine PAHs in the certified reference material, six were detected in the samples after method blank subtraction and are displayed in Table 8

Phenanthrene and pyrene were detected in every sample, with the highest values occurring in Area 4 located in Ny-Ålesund. Without the Area 4 data, the average and standard deviations of the two components were 8.820 ± 3.565 and 5.920 ± 3.893 (ng/g) respectively. benzo[b]fluoranthene, benzo[k]fluoranthene, benzo[a]pyrene, and benzo[ghi]perylene were also detected and occurred mostly in the mainland Norway samples, although benzo[ghi]perylene was present in Area 4. LOQ and LOD values were not available.

In the experimental GC-MS procedure, PCBs were not detected, but PAHs were and are listed in Table 9. ASE extracts were diluted before analysis. No values were recorded for Area 6 after method blank subtraction. Internal standards and a calibration curve were used to calibrate the results. The PAHs present above the LOD (see Table 24 in Appendix C) included Naphthalene, Acenaphthylene, Fluorene, Phenanthrene, Fluoranthene, and Pyrene. Of these, Naphthalene and Acenaphthylene were detected most frequently with the highest occurrence in Area 13 and Area 12 respectively. There was a wide range of detected values for all PAHs and there were no obvious trends in the data.

Table 8

This table contains the readings from the pooled sample for the HPLC-FID- DAD an analysis. Data was corrected using a calibration curve, the reference material and the method blanks. Full data set in the supplementary material.

Area	Phenanthrene	Pyrene	Benzo[b]fluoranthene	Benzo[k]fluoranthene	Benzo[a]pyrene	Benzo[ghi]perylene
	ng/g	ng/g	ng/g	ng/g	ng/g	ng/g
4	25.99	20.37	-	-	-	10.84
5	6.356	10.71	-	-	-	-
6	8.858	5.669	5.925	0.4739	-	-
10	11.73	12.94	15.18	3.033	20.72	16.41
11	5.735	3.373	-	0.3531	-	-
12	5.505	2.476	-	0.4373	-	-
13	4.302	1.767	-	0.5278	-	-
14	11.56	7.704	-	-	-	-
15	10.53	2.730	10.65	-	-	-
16	14.80	5.914	9.179	-	-	-

Table 9

This Table shows the compounds detected from the GC-MS procedure with internal standard corrections using 4-fluorobiphenyl, 3-flurorphenathere, and 3-flurorchrysene. Method blank subtractions were also applied. The detection limits are listed (see Table 24 in Appendix C). Full data set in the supplementary material.

Area	Naphthalene	Acenaphthylene	Fluorene	Phenanthrene	Fluoranthene	Pyrene
	ng/g	ng/g	ng/g	ng/g	ng/g	ng/g
4	35.74	172.7		36.97		
4 [a]		30.11	8.85 [b]		16.49	11.85 [b]
5	138.8	197.4				
5 [a]		26.99			6.979 [b]	5.501 [b]
10					198.7	
11	307.4	359.4				
12	207.3	1226		37.88	26.17	
13	334.9					
14	196.6					
15	103.5	254.8				
16	75.84	221.6		5.365 [b]	15.17 [b]	

[a] These sample were concentrated at a stronger level than the other samples.

[b] Below the limit of quantification

4.3 HR ICP-MS

The results for the elements with a propensity towards LRT, or that are of other interest, V, Cr, Mn, Fe, Zn, As, Mo, Ag, Cd, Sn, Sb, W, Tl, Pb, and Bi, are listed in Table 10 and their areas averages are recorded in

Table 11. The results for all 60 elements detected in the samples are available in the supplementary information. Descriptive statistics for all tested element readings above LOQ values (see Table 17 in Appendix B) were calculated for the sampled regions, Svalbard, Trondheim and southern Norway (see Table 16 and Table 17 in Appendix B). V was present in the highest levels in areas 4 and 11 with means 6.599 ± 4.358 µg/g and 6.543 ± 1.997 µg/g respectively, and all other areas produced similar lower values. The maximum Cr level was in Area 4, mean of 5.558 ± 3.855 µg/g, although the variance within the sampled areas was large. The minimum for Cr was in Area 6 with a mean of 0.5076 ± 0.1978 µg/g. The Mn values were higher in Area 6 and Area 13 with means of 413.6 ± 192.7 µg/g and 394.281 ± 95.85 µg/g respectively, and the lowest values were in Area 5 with a mean of 15.76 ± 6.29 µg/g. Fe presented a broad range of readings with the greatest values from Area 4, mean of 2539 ± 1555 µg/g, and the smallest from Area 5 with a mean of 533.2 ± 212.0 µg/g. The highest Zn values were from areas 4 and 6 with means of 38.13 ± 16.73 µg/g and 36.09 ± 10.64 µg/g respectively, and the lowest values were from Area 5, mean of 11.22 ± 2.676 µg/g. As levels were greatest in Area 4, mean of 0.4366 ± 0.2310 µg/g, and minimum values occurred in Trondheim areas 12-16. Elevation of Mo concentrations occurred in areas 8 and 10 with means of 0.1916 ± 0.02941 µg/g and 0.1732 ± 0.07545 µg/g, followed by the Svalbard regions and the smallest values occurred in the Trondheim areas 12-14 and 16. Ag levels were highest in Area 4, mean of 0.3858 ± 0.1363 µg/g, and the other areas had similar lower values. The highest Cd values occurred in Area 4 and Area 5 with a means of 0.2564 ± 0.1251 µg/g and 0.1875 ± 0.02738 µg/g respectively, and the other areas had similar lower values. Sn levels were highest in Area 4, mean of 0.1257 ± 0.05632 µg/g, although areas 11 and 15 showed signs of elevation as well and the minimum was in Area 5 with a mean of 0.06515 ± 0.02848 µg/g. The Sb values were largest in areas 8 and 10 with means of 0.11859 ± 0.0251 µg/g and 0.1100 ± 0.01395 µg/g respectively, while the other areas maintained similar levels. The highest W values were in Area 11 with a mean of 0.3948 ± 0.02295 µg/g, but areas 8 and 10 showed similar elevation and greater means and the Svalbard areas 4 and 5 were the values with the lowest means of 0.008102 ± 0.005068 µg/g and 0.01647 ±

0.005279 µg/g respectively. Tl was highest in Area 8 with a mean of 0.1043 ± 0.02685 µg/g, but Area 4 showed elevation as well, and the lowest values were in Area 12 with a mean of 0.00628 ± 0.00151 µg/g. The values of Pb were highest in Area 4 with a mean of 3.212 ± 1.706 µg/g, although areas 5, 6, 8 and 10 appeared elevated, and the Trondheim areas 11-16 were similar lower values. The Bi levels were elevated in Area 10 with a mean of 0.1063 ± 0.1200 µg/g and all the other locations were similar lower values. Boxplots of the selected 15 elements in Figure 15 and Figure 16 shows the variation in concentrations the across the sampled areas.

Statistical analysis of values that were above the limit of quantification for the data was pursued through the Welch correction to the ANOVA test, which showed that all elements had significant differences for the area groupings (see Table 20 in Appendix B). The results of the Levene variance and Sharpiro Wilk normality tests are summarized (see Table 18 and Table 19 Appendix B). A Dunnett's T3 post hoc test elucidated which areas were significantly different from each other for each element (see Table 21 in Appendix B). A summary of the Spearman correlation chart for all 60 analyzed elements showed that most elements were positively correlated to each other with the exception of Ta (see Table 22 in Appendix B). The full Spearman's correlation rank matrix is listed in the supplementary material. Principal component analysis (PCA) of the data was employed, and the loadings and results charts are in Figure 17 and Figure 18. Principal component (PC) 1 and 2 correlate to 48% of the variance of the data and PC 3 and 4 correlate to 22 % of the data.

Table 10

This table contains the data for the samples taken of the elements with long range transport potential. Detection limits and the complete data set for all elements are available (see Table 17 in Appendix B). Reference material (Ref.) is included as a base value.

Sample number	Area	V51 (MR)[a]		Cr52 (MR)		Mn55 (MR)		Fe56 (MR)		Zn66 (MR)		As75 (HR)		Mo98 (MR)		Ag109 (MR)	
		μg/g	%RSD	μg/g	%RSD	μg/g	%RSD	μg/g	%RSD	μg/g	%RSD	μg/g	%RSD	μg/g	%RSD	μg/g	%RSD
19 a	4	2.204	4.9	1.8155	5.4	45.19	2.8	938.8	2.1	29.01	4.0	0.2217	28.6	0.05906	8.0	0.5023	1.9
20a	4	2.123	4.4	1.7318	0.8	198.2	2.8	854.6	0.9	66.54	1.3	0.1487	24.4	0.05469	14.1	0.3331	6.6
21a	4	7.732	5.5	6.0989	3.8	77.51	5.6	3173	3.6	25.57	2.1	0.6106	22.1	0.1360	7.3	0.5172	6.0
23a	4	12.11	1.5	10.7760	2.9	206.8	1.3	4291	1.6	39.73	1.9	0.5969	14.8	0.1154	6.9	0.3920	6.3
24a	4	8.829	1.9	7.3699	2.4	111.7	2.7	3439	0.6	29.81	3.6	0.6049	6.8	0.1047	7.6	0.1842	11.1
25a	5	0.4306	4.7	0.3577	6.2	5.781	2.9	167.6	3.1	8.439	4.1	0.1175	41.6	0.05890	0.4	0.03595	1.3
26a	5	1.483	0.8	1.0386	3.4	15.57	0.2	459.1	1.1	11.72	2.6	0.1833	22.0	0.07711	11.1	0.1108	10.8
27a	5	4.992	1.7	2.7295	1.7	24.53	2.3	753.0	1.5	15.66	4.3	0.3332	28.9	0.09351	5.7	0.2125	8.0
28a	5	1.367	3.4	1.0786	4.6	19.71	5.4	493.3	6.5	12.57	2.9	0.1830	47.5	0.06026	9.1	0.08206	12.0
29a	5	2.115	1.7	1.5803	3.3	13.37	0.6	694.2	2.4	9.311	3.0	0.3217	20.6	0.07048	9.5	0.07723	4.2
30a	5	1.953	4.9	1.4813	3.4	15.60	4.0	631.7	2.2	9.640	0.6	0.2516	11.4	0.09230	13.1	0.08050	14.7
31a	6	0.5145	2.8	0.3375	7.7	635.0	4.1	207.8	1.7	48.36	2.2	0.1048	5.9	0.08022	2.9	0.07433	9.7
32a	6	0.6856	2.6	0.4606	2.6	283.3	2.2	385.0	1.7	29.32	2.5	0.1565	47.0	0.09374	20.4	0.08369	20.7
33a	6	1.229	1.3	0.7246	3.4	322.6	1.6	768.7	2.8	30.59	0.9	0.1205	30.5	0.1328	13.4	0.1876	12.3
41	8	2.634	4.2	1.707	4.7	197.8	1.7	1304	0.5	52.63	3.4	0.1621	48.5	0.2124	6.3	0.1381	5.0
42	8	1.319	9.3	0.8919	8.4	81.07	9.7	401.1	9.1	45.57	4.8	0.1959	29.0	0.1708	16.1	0.09402	11.0
44	10	2.599	1.5	1.657	2.6	314.1	0.6	1516	0.4	32.38	4.0	0.2049	19.7	0.2266	7.3	0.08289	9.4
46	10	0.9612	2.1	0.7288	3.4	333.3	2.8	332.4	2.9	53.44	4.4	0.1480	42.9	0.1199	5.6	0.1125	5.4
47a	11	4.920	3.8	2.610	1.7	244.1	0.9	1470	1.3	24.20	2.7	0.1981	48.5	0.08094	14.2	0.09337	19.0
48a	11	4.963	2.7	2.705	3.4	243.7	0.9	1469	2.8	34.92	3.6	0.1961	29.6	0.09978	8.7	0.1073	2.6
49a	11	5.630	5.4	2.917	3.8	264.7	4.1	1665	3.4	21.01	2.6	0.1953	32.6	0.1607	5.7	0.1117	9.1
50a	11	9.475	1.8	4.709	2.5	213.7	2.3	2829	3.0	26.15	2.7	0.2604	21.4	0.07897	13.8	0.05798	21.2
51a	11	7.726	1.1	3.932	3	264.7	2.9	2293	0.7	33.57	1.7	0.2338	7.3	0.07839	13.9	0.08765	3.8
52a	12	2.458	5	1.396	5.9	252.5	4.2	715.2	3.5	22.48	2.6	0.09538	8.6	0.03631	10.9	0.02794	13.3
53a	12	2.510	2.7	1.356	2.5	332.1	2.2	733.8	2.9	23.62	3.9	0.1546	39.2	0.03838	16.3	0.04536	17.7
54a	12	1.933	2.1	1.078	3.3	329.1	0.9	568.9	1.2	20.14	1.1	0.1135	33.1	0.02434	12.3	0.03078	13.8
55a	12	1.423	6.8	0.8873	4.4	230.1	4.4	428.3	4	13.64	3.2	0.07814	8.6	0.01988	4.3	0.02928	11.4

Sample number	Area	V51 (MR)[a]		Cr52 (MR)		Mn55 (MR)		Fe56 (MR)		Zn66 (MR)		As75 (HR)		Mo98 (MR)		Ag109 (MR)	
		µg/g	%RSD	µg/g	%RSD	µg/g	%RSD	µg/g	%RSD	µg/g	%RSD	µg/g	%RSD	µg/g	%RSD	µg/g	%RSD
56a	12	1.528	5.2	0.8884	3.1	127.3	1.1	433.4	1.6	9.086	6.0	0.07861	33.7	0.03108	29.3	0.03643	12.3
57a	13	3.764	4.1	1.963	4.4	543.6	3.7	1123	5.2	27.77	3.2	0.08143	16.1	0.03948	22.3	0.02083	16.6
58a	13	5.245	1.4	2.523	0.5	424.6	3.1	1540	2.5	27.08	2.1	0.1018	54.8	0.04328	36.1	0.01747	19.3
59a	13	3.217	1.5	1.716	1.8	338.0	2.1	940.9	1	30.03	0.2	0.1093	10.8	0.05533	10.3	0.02335	12.6
60a	13	4.125	4.7	2.036	6.1	369.7	3.8	1195	3.1	24.65	5.5	0.1732	31.5	0.04610	15.8	0.02782	3.0
61a	13	3.060	2.6	1.498	4.8	295.5	2.2	917.2	0.7	28.76	3.5	0.1112	47.5	0.05638	13.6	0.02644	20.2
62a	14	3.139	3.8	1.702	3.5	349.1	2.8	840.2	3.3	31.84	2.6	0.09812	22.4	0.05346	4.1	0.05054	4.1
63a	14	1.397	9.6	0.8186	6.2	224.2	6.7	405.7	4.4	16.07	2.7	0.06486	49.5	0.01419	18.5	0.02725	11.7
64a	14	1.317	5.8	0.7488	6.3	192.1	6.1	359.3	6.6	18.83	7.6	0.04783	37.0	0.04802	13.8	0.02668	22.5
65a	14	1.146	7.1	0.7864	7.8	259.5	6.2	330.6	5.7	17.43	6.5	0.06886	14.6	0.04220	10.1	0.02902	12.5
66a	14	1.425	1.3	0.9353	3.3	222.9	1.5	413.4	1.7	18.40	1.5	0.1012	35.5	0.05884	7.2	0.02003	12.2
67a	15	4.823	2.5	4.671	4.1	270.4	2.9	1461	3.0	27.87	2.3	0.1982	28.6	0.05881	9.5	0.02588	6.1
68a	15	1.470	2.7	1.284	4.1	91.12	2.00	456.7	1.8	21.88	2.3	0.1149	34.6	0.09326	11.9	0.02198	9.2
69a	15	1.453	6.3	1.180	2.7	218.2	4.6	447.0	2.4	22.63	6.6	0.08808	27.5	0.06993	8.2	0.04159	6.3
70a	15	0.7528	4.4	0.8886	6.3	168.3	1.5	232.8	2.6	15.63	2.2	0.03738	87.1	0.09317	14.9	0.04095	20.6
71a	15	2.615	3.2	2.109	2.8	111.4	2.7	804.9	1.9	21.43	4.6	0.1724	13.7	0.1168	13.3	0.03527	11.6
72a	16	2.411	2.4	2.022	1.4	322.6	1.3	752.4	0.7	35.38	2.3	0.1757	12.9	0.1431	2.5	0.02464	15.7
73a	16	1.300	3.8	1.041	7.1	234.0	3.6	410.4	3.9	18.31	4.4	0.07916	32.3	0.07153	38.6	0.03895	17.8
74a	16	1.061	4.6	0.9308	4.8	169.7	2.00	332.1	4.1	21.21	0.1	0.07842	28.1	0.04925	17.3	0.02807	11.2
75a	16	1.416	4.1	1.191	5.2	208.3	3.5	444.0	1.5	19.96	4.8	0.09768	20.3	0.05947	14.8	0.02391	20.5
76a	16	1.855	2.4	1.349	1.2	398.2	3.8	562.2	1.5	22.20	2.3	0.09987	23.7	0.1160	8.4	0.02243	24.5
Ref 1		0.5558	4.6	0.4202	5.6	508.9	6.3	104.2	3.5	25.40	6.5	0.1267	65.2	0.04280	22.6	0.02416	22.1
Ref 2		0.5589	4.8	0.4237	5.9	488.3	6.2	99.32	1.6	25.39	2.8	0.07401	68.1	0.03365	22.2	0.02415	10.5
Ref 3		0.5754	2.8	0.4088	2.9	518.1	4	110.2	3.5	26.67	1.1	0.09044	58.4	0.03033	18.1	0.04298	3.3
Ref 4		0.5548	1.0	0.3923	7.1	500.1	3.2	109.0	5.8	25.42	6.7	0.06921	56.2	0.04165	16.1	0.04711	8.1

[a] HR, MR and LR refer to high, medium and low range scanning

Table 10. Continued

Sample number	Area	Cd111 (LR)		Sn118 (LR)		Sb121 (MR)		W182 (LR)		Tl205 (LR)		Pb208 (LR)		Bi209 (LR)	
		μg/g	%RSD	μg/g	%RSD	μg/g	%RSD	μg/g	%RSD	μg/g	%RSD	μg/g	%RSD	μg/g	%RSD
19 a	4	0.2108	2.2	0.07956	1.8	0.02217	11.1	0.01245	3.6	0.01976	4.1	1.339	5.0	0.01449	1.6
20a	4	0.4599	3.6	0.07182	2.2	0.02807	18.0	0.01459	6.3	0.01961	3.1	1.541	0.9	0.008874	2.4
21a	4	0.2085	3.0	0.2122	0.9	0.05859	7.7	0.005701	8.2	0.07381	3.9	5.268	3.1	0.04923	6.2
23a	4	0.2748	2.6	0.1391	1.1	0.01618	46.8	0.004303	6.4	0.09235	3.7	3.994	5.2	0.03227	6.3
24a	4	0.1280	2.8	0.1256	4.6	0.01332	44.5	0.003463	7.6	0.06721	1.7	3.919	2.8	0.02907	6.5
25a	5	0.1717	4.3	0.02238	3.4	0.01539	13.0	0.006106	12.5	0.005120	8.7	0.2199	1.4	0.002323	6.4
26a	5	0.1781	3.3	0.05938	5.7	0.01636	33.5	0.01756	7.3	0.01622	6.2	1.102	4.5	0.008582	8.0
27a	5	0.1917	4.0	0.09369	1.1	0.05332	4.7	0.01742	11.1	0.03507	3.1	1.519	2.7	0.01234	1.9
28a	5	0.1623	4.5	0.06034	1.8	0.02966	7.5	0.02135	0.7	0.01566	4.7	0.9839	2.5	0.005939	4.7
29a	5	0.1816	1.9	0.08346	1.4	0.03332	4.0	0.01791	0.6	0.02228	3.3	1.354	1.6	0.008129	6.5
30a	5	0.2397	3.6	0.07167	2.6	0.02265	11.0	0.01845	7.0	0.04625	8.0	1.420	7.3	0.005813	10.1
31a	6	0.08722	3.6	0.07242	5.1	0.05432	7.2	0.04406	3.8	0.06190	2.0	0.8767	1.6	0.006879	5.8
32a	6	0.06932	5.8	0.07966	7	0.04237	1.7	0.03011	2.4	0.05688	4.4	0.9872	1.0	0.005453	3.1
33a	6	0.07451	6.6	0.08335	2.1	0.05138	14.9	0.03252	6.5	0.05789	1.6	3.167	0.8	0.008102	6.5
41	8	0.1337	6.3	0.3466	4.1	0.1008	3.3	0.03512	3.8	0.1233	3.6	2.540	1.1	0.02459	3.4
42	8	0.1438	1.5	0.3729	2.4	0.1363	7.1	0.03823	4.0	0.08532	1.3	3.903	2.1	0.03018	4.1
44	10	0.1532	2.2	0.4048	1	0.1192	15.8	0.05727	2.0	0.06750	2.2	3.030	0.2	0.1912	3.4
46	10	0.2073	1.1	0.2361	1.5	0.1008	0.5	0.03039	7.7	0.02520	5.2	2.643	0.9	0.02153	1.8
47a	11	0.03161	7.4	0.1395	4.5	0.09299	18.9	0.05499	2.4	0.02588	1.9	0.8755	0.7	0.007106	2.4
48a	11	0.03460	9.9	0.1349	2.5	0.08546	13.4	0.06108	2.9	0.03919	3.5	1.129	1.2	0.007822	3.7
49a	11	0.03849	3.4	0.1330	4.7	0.1114	5.3	0.01892	1.2	0.01931	4.5	0.8023	0.9	0.01205	2.5
50a	11	0.03430	8.8	0.1244	6.6	0.04548	14.9	0.01072	8.6	0.02723	3.6	0.8201	1.7	0.006901	2.0
51a	11	0.05794	6.5	0.1466	3.4	0.08621	20.9	0.05172	4.6	0.01994	2.9	0.8541	2.2	0.008995	4.3
52a	12	0.02220	5.3	0.1015	2.3	0.04532	11.0	0.01845	6.2	0.006931	5.9	0.5715	3.7	0.01162	2.1
53a	12	0.02033	19.1	0.08412	3.7	0.06641	16.3	0.02383	3.3	0.008604	4.5	0.4584	1.5	0.002170	6.5
54a	12	0.02625	2.9	0.07415	6.1	0.04605	18.1	0.04199	5.4	0.005656	7.6	0.4759	6.0	0.002127	5.9
55a	12	0.01403	24.1	0.05950	3.7	0.03135	7.0	0.02288	6.7	0.004881	5.6	0.3306	3.9	0.002408	6.9

Sample number	Area	Cd111 (LR)		Sn118 (LR)		Sb121 (MR)		W182 (LR)		Tl205 (LR)		Pb208 (LR)		Bi209 (LR)	
		µg/g	%RSD	µg/g	%RSD	µg/g	%RSD	µg/g	%RSD	µg/g	%RSD	µg/g	%RSD	µg/g	%RSD
56a	12	0.01062	13.0	0.06854	4.2	0.04435	6.4	0.01672	0.5	0.005307	9.0	0.3349	2.7	0.006928	5.6
57a	13	0.03009	3.8	0.08562	3.7	0.05193	11.7	0.04166	6.2	0.04564	2.0	0.5035	1.5	0.006831	4.3
58a	13	0.03283	2.7	0.08787	3.9	0.06100	25.2	0.02969	6.0	0.01769	1.6	0.5077	2.1	0.01648	5.1
59a	13	0.03713	3.3	0.09788	4.2	0.06812	25.0	0.03759	6.1	0.07848	1.5	0.7424	5.2	0.006770	7.2
60a	13	0.03567	12.6	0.1013	1.2	0.06206	20.4	0.02982	10.2	0.05691	3.3	0.6378	2.9	0.007346	4.3
61a	13	0.02886	2.3	0.08929	0.8	0.05256	20.8	0.04140	4.5	0.05618	4.7	0.5834	0.7	0.004396	4.8
62a	14	0.03356	6.7	0.1124	2.1	0.09608	8.0	0.06741	7.6	0.05833	5.3	0.8712	5.1	0.01017	6.8
63a	14	0.01161	9.6	0.05099	4.6	0.04778	8.5	0.02726	3.6	0.03383	2.4	0.3857	4.5	0.001281	4.2
64a	14	0.02100	15.7	0.05409	6.4	0.03502	14.6	0.02007	10.5	0.02065	3.3	0.3478	3.7	0.008198	6.3
65a	14	0.02834	5.6	0.06429	4.7	0.04139	35.6	0.02009	7.6	0.01123	5.9	0.4777	5.3	0.001850	6.5
66a	14	0.02600	13.4	0.07518	3.9	0.06990	7.6	0.03093	11.3	0.04207	9.8	0.6706	9.2	0.002684	11.0
67a	15	0.02454	11.3	0.08667	6.9	0.05506	12.5	0.07040	4.1	0.02383	4.2	0.5852	3.7	0.006144	5.6
68a	15	0.02522	16.6	0.09044	4.8	0.06895	17.1	0.06322	2.6	0.01839	1.1	0.8307	1.6	0.02887	3.1
69a	15	0.03312	3.2	0.1091	1.4	0.05699	15.0	0.05863	2.0	0.01341	2.7	0.7620	0.9	0.002416	6.8
70a	15	0.01819	2.5	0.1960	2.8	0.05363	16.6	0.02829	1.3	0.00423	3.4	0.4956	6.9	0.007222	3.2
71a	15	0.02251	15.3	0.1518	2.8	0.09959	6.9	0.11659	3.5	0.01787	8.5	1.047	6.3	0.01186	6.2
72a	16	0.03942	4.0	0.1444	4.1	0.08480	8.8	0.09174	1.4	0.09395	2.0	0.9172	1.0	0.01900	0.8
73a	16	0.05667	3.4	0.07581	0.5	0.03697	4.7	0.04743	2.1	0.02287	8.4	0.5359	8.8	0.006958	10.0
74a	16	0.03789	10.8	0.07267	4.5	0.04175	23.6	0.07615	2.6	0.01564	3.3	0.3376	0.9	0.03112	0.4
75a	16	0.03713	6.5	0.08649	3.7	0.04599	18.4	0.06568	3.0	0.02860	1.7	0.4808	0.3	0.005093	2.4
76a	16	0.02980	13.7	0.1129	3	0.08094	16.6	0.06531	3.2	0.04765	4.5	0.8680	0.2	0.02181	2.9
Ref. 1		0.08102	8.1	0.08809	7.9	0.02051	30.4	0.009654	6.9	0.01594	0.7	2.532	1.1	0.005502	6.2
Ref. 2		0.07979	3.0	0.09746	0.5	0.02389	5.6	0.008718	6.0	0.01564	6.1	2.549	1.3	0.04388	5.4
Ref. 3		0.08460	7.0	0.1002	9.1	0.03292	44.1	0.008913	6.5	0.01550	0.4	2.518	0.9	0.007379	3.5
Ref. 4		0.07875	8.6	0.08260	1.6	0.02274	19.1	0.01291	7.0	0.01609	0.8	2.536	2.2	0.01542	2.2

[a] HR, MR and LR refer to high, medium and low range scanning

Table 11

This table contains averages and standard deviations (SD)of selected elements for each area. All values above LOQ values are included. Reference material (Ref.) is included as a base value in the final row.

Area	V51 (MR) [a]		Cr52 (MR)		Mn55 (MR)		Fe56 (MR)		Zn66 (MR)		As75 (HR)		Mo98 (MR)		Ag109 (MR)	
	µg/g	SD	µg/g	SD	µg/g	SD	µg/g	SD	µg/g	SD	µg/g	SD	µg/g	SD	µg/g	SD
4	6.599	4.358	5.558	3.855	127.9	72.13	2539	1555	38.13	16.73	0.4366	0.2310	0.09398	0.03573	0.3858	0.1363
5	2.057	1.554	1.378	0.7904	15.76	6.290	533.2	212.0	11.22	2.672	0.2317	0.08549	0.07543	0.01511	0.09984	0.06015
6	0.8096	0.3729	0.5076	0.1978	413.6	192.7	453.8	286.7	36.09	10.64	0.1273	0.02650	0.1023	0.02732	0.1152	0.06287
8	1.977	0.9297	1.300	0.5765	139.4	82.54	852.4	638.2	49.10	4.994	0.1790	0.02385	0.1916	0.02941	0.1161	0.03119
10	1.780	1.158	1.193	0.6561	323.7	13.57	923.9	836.6	42.91	14.90	0.1765	0.04017	0.1732	0.07545	0.09770	0.02095
11	6.543	1.9973	3.375	0.9128	246.2	20.93	1945	598.7	27.97	6.034	0.2167	0.02930	0.09976	0.03520	0.09159	0.02121
12	1.971	0.5062	1.121	0.2458	254.2	84.20	575.9	147.0	17.79	6.215	0.1040	0.03178	0.03000	0.007835	0.03396	0.007147
13	3.882	0.8729	1.947	0.3856	394.3	95.85	1143	251.2	27.66	2.016	0.1154	0.03442	0.04812	0.007454	0.02318	0.004193
14	1.685	0.8203	0.9982	0.3995	249.6	60.51	469.8	209.8	20.51	6.421	0.07622	0.02288	0.04334	0.01743	0.03070	0.01160
15	2.223	1.600	2.027	1.546	171.9	74.23	680.5	482.1	21.89	4.351	0.1222	0.06463	0.08639	0.02263	0.03313	0.008864
16	1.609	0.5330	1.307	0.4295	266.6	92.58	500.2	163.5	23.41	6.847	0.1062	0.04013	0.08786	0.04001	0.02760	0.006675
Ref.	0.5612	0.009650	0.4112	0.01416	503.8	12.74	105.7	4.958	25.72	0.6332	0.0901	0.02604	0.03711	0.006080	0.03460	0.01218

[a] HR, MR and LR refer to high, medium and low range scanning

Area	Cd111 (LR)		Sn118 (LR)		Sb121 (MR)		W182 (LR)		Tl205 (LR)		Pb208 (LR)		Bi209 (LR)	
	µg/g	SD	µg/g	SD	µg/g	SD	µg/g	SD	µg/g	SD	µg/g	SD	µg/g	SD
4	0.2564	0.1251	0.1257	0.05632	0.02767	0.01820	0.00810	0.005068	0.05455	0.03313	3.212	1.706	0.02679	0.01590
5	0.1875	0.02738	0.06515	0.02481	0.02845	0.01410	0.01647	0.005279	0.02343	0.01487	1.100	0.4756	0.007188	0.003362
6	0.07702	0.009210	0.07848	0.005560	0.04936	0.006223	0.03556	0.007460	0.05889	0.002651	1.677	1.291	0.006812	0.001326
8	0.1388	0.007146	0.3598	0.0186	0.1186	0.02510	0.03667	0.002201	0.1043	0.02685	3.221	0.9639	0.02738	0.003948
10	0.1802	0.03825	0.3205	0.1193	0.1100	0.01295	0.04383	0.01901	0.04635	0.02991	2.836	0.2739	0.1064	0.1200
11	0.03939	0.01066	0.1357	0.008203	0.08431	0.02410	0.03948	0.02295	0.02631	0.008007	0.8963	0.1334	0.008576	0.002110
12	0.01896	0.006307	0.0776	0.01609	0.04670	0.01257	0.02477	0.01007	0.006276	0.001510	0.4343	0.1022	0.005051	0.004199
13	0.03292	0.003529	0.09240	0.006809	0.05913	0.006857	0.03603	0.005949	0.05098	0.02211	0.5950	0.09958	0.008364	0.004677
14	0.02410	0.008318	0.07138	0.02480	0.05803	0.02500	0.03315	0.01971	0.03322	0.01838	0.5506	0.2184	0.004837	0.004060
15	0.02472	0.005442	0.1268	0.04653	0.06685	0.01928	0.06743	0.03183	0.01555	0.007328	0.7441	0.2160	0.01130	0.01038
16	0.04018	0.009934	0.09846	0.03017	0.05809	0.02289	0.06926	0.01626	0.04174	0.03151	0.6279	0.2528	0.01680	0.01083
Ref.	0.08104	0.002545	0.09208	0.008172	0.02502	0.005456	0.01005	0.001948	0.01579	0.0002710	2.534	0.01283	0.01805	0.01775

[a] HR, MR and LR refer to high, medium and low range scanning

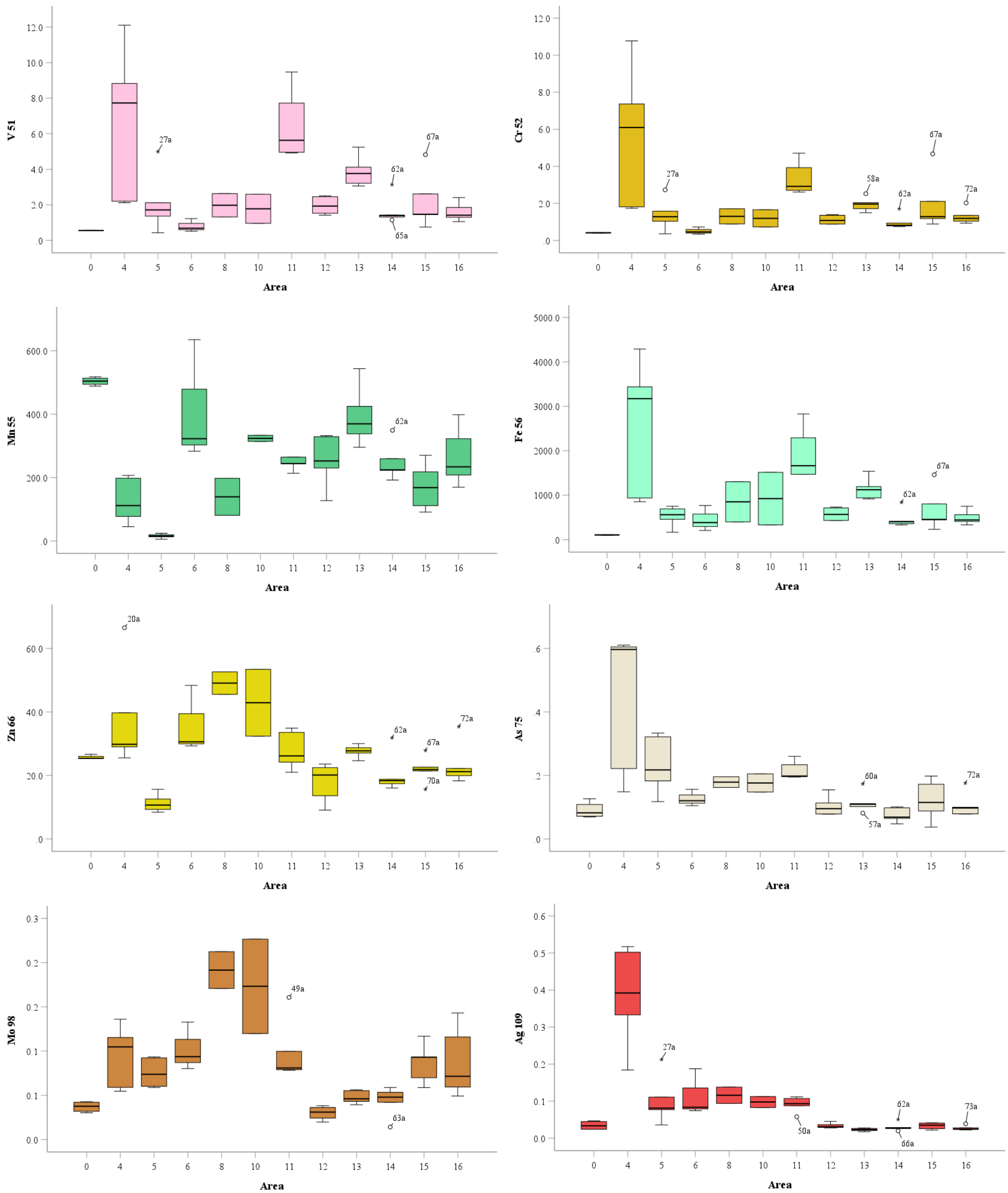

Figure 15. Box plots of V, Cr, Mn, Fe, Zn, As, Mo and Ag.

This figure contains box plots for V, Cr, Mn, Fe, Zn, As, Mo and Ag. The box is the first through third quartile rage of the data set, the band in the middle designates the median and whiskers display the maximum and minimum for each area excluding outliers. Potential outliers are labeled with the sample number and an empty circle. Extreme values are marked with a star and the sample label.

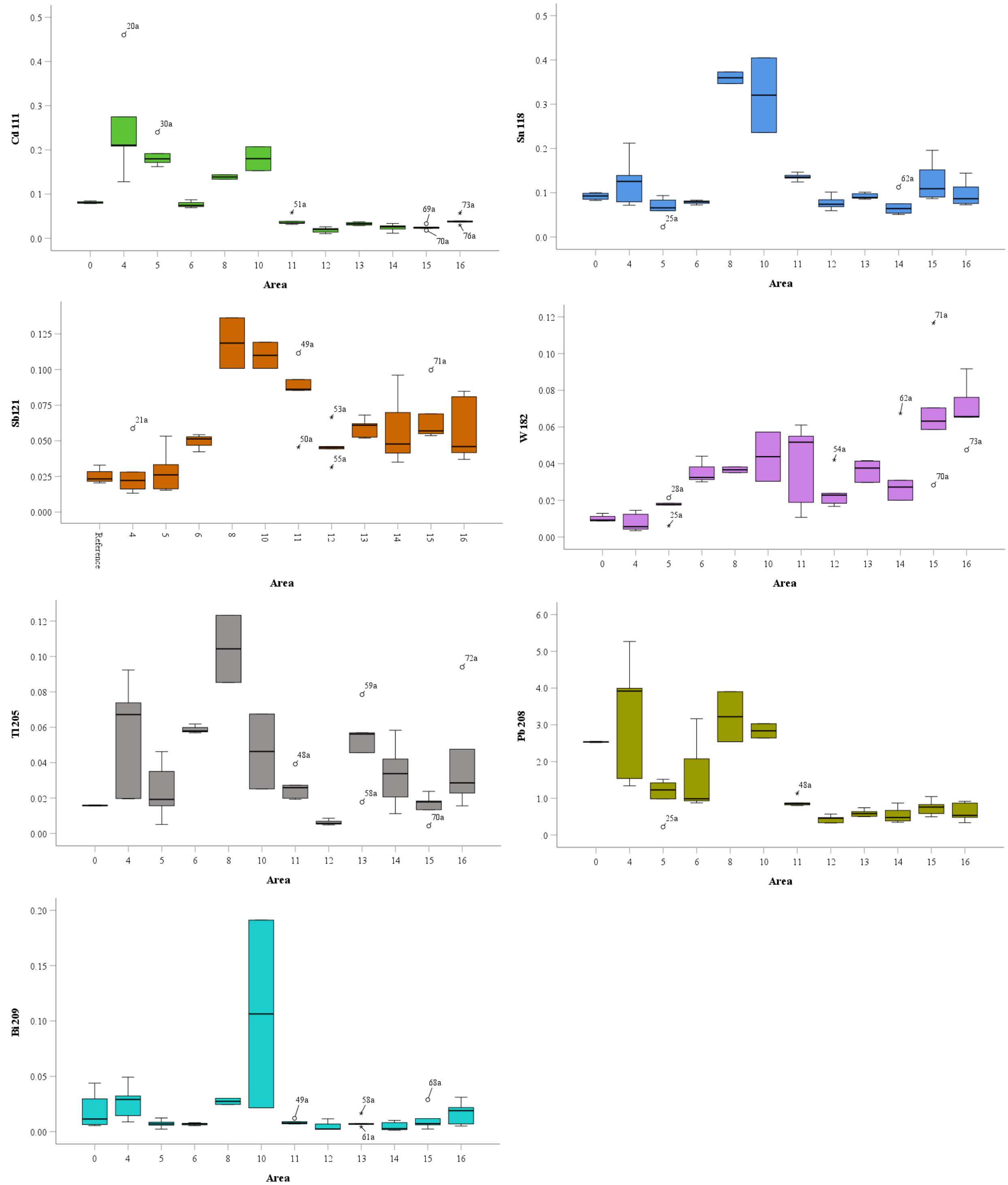

Figure 16. Boxplots of Cd, Sn, Sb, W, Tl, Pb and Bi.

This figure contains box plots for Cd, Sn, Sb, W, Tl, Pb, and Bi. The box is the first through third quartile rage of the data set, the band in the middle designates the median and whiskers display the maximum and minimum for each area excluding outliers. Potential outliers are labeled with the sample number and an empty circle. Extreme values are marked with a star and the sample label.

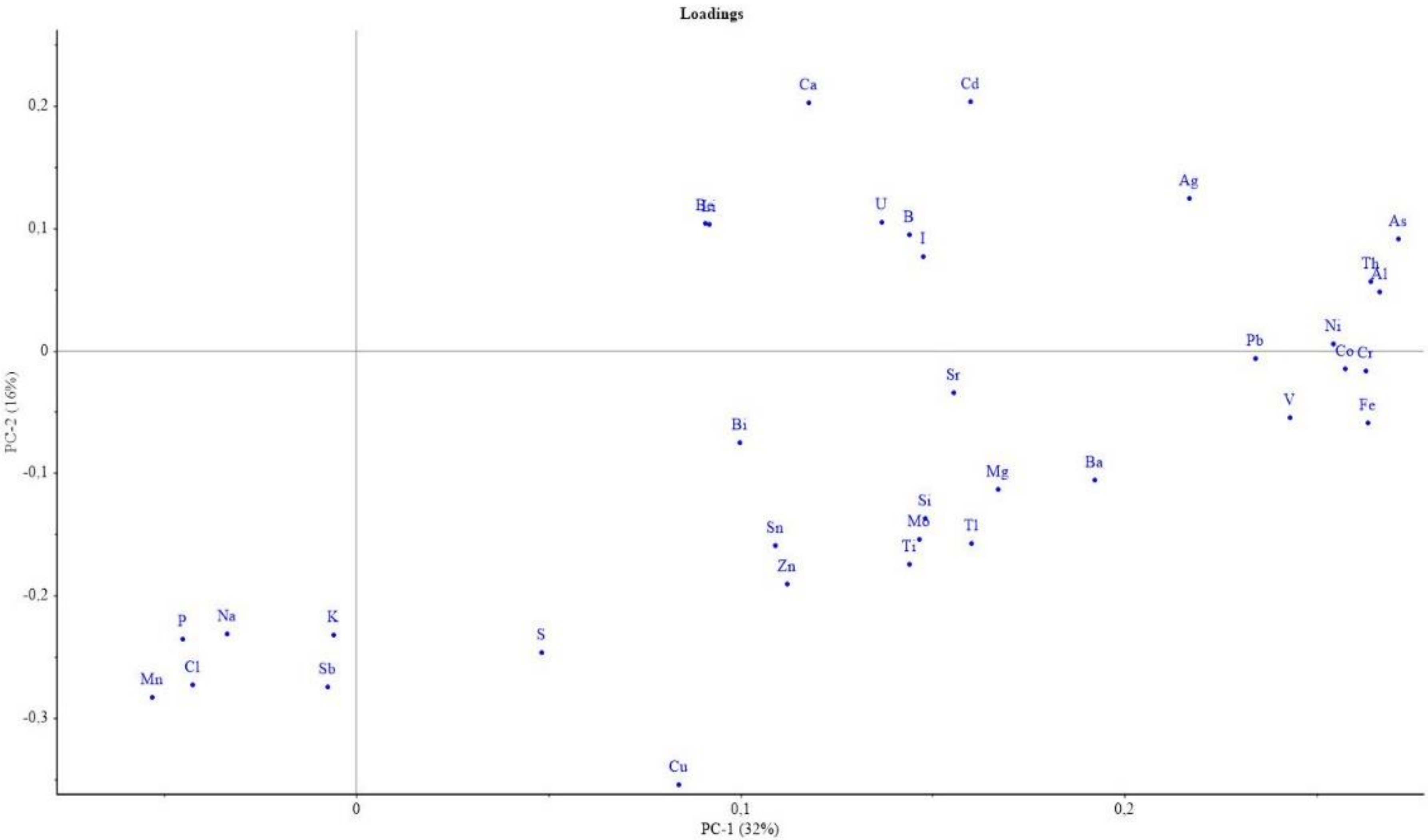

Figure 17. PC 1 & 2 for elements.

These figures show the loading and score plots for PC 1 (37%) and PC 2 (16%). Only values within the limit of quantification were included in the plot. Data was altered through mean scaling and centered by a standard deviation. Excessively noisy values were removed or scaled down to a value < |1|.

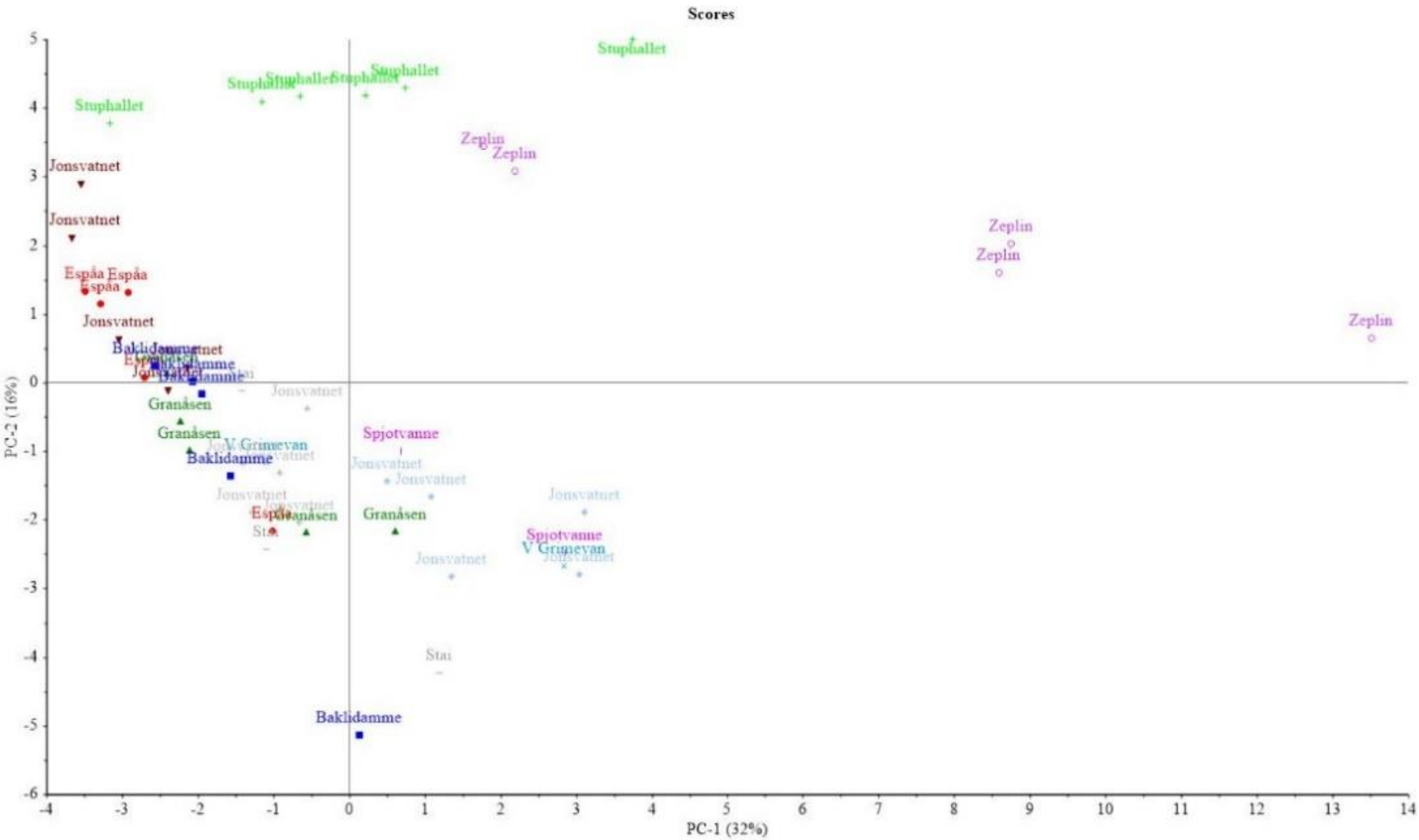

Figure 17. Continued

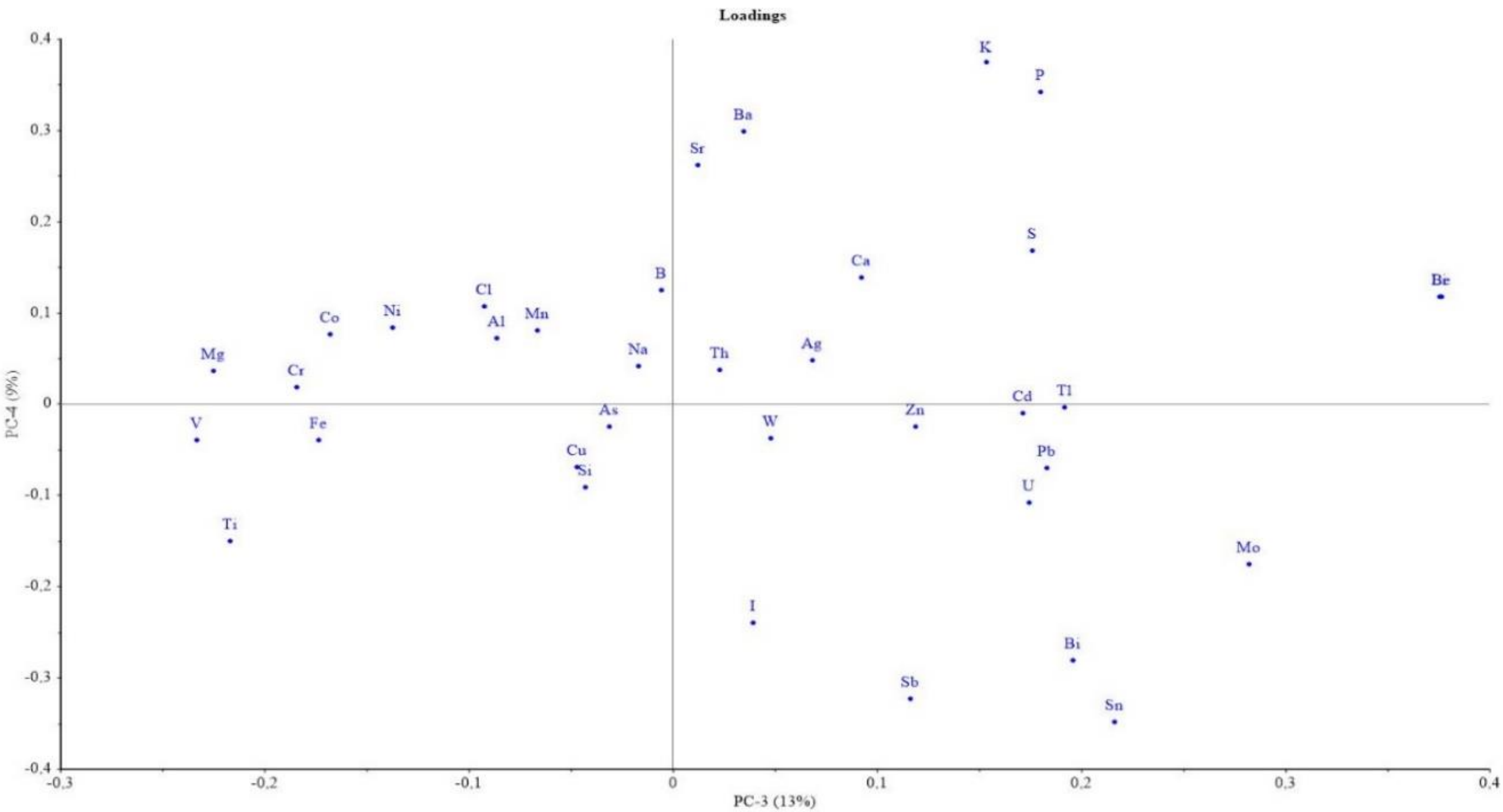

Figure 18. PC 3 & 4 for elements

The loading and score plots for PC 3 (13%) and PC 4 (9%) are shown in the figures. Only values within the limit of quantification were included in the plot. Data was altered through mean scaling and centered by a standard deviation. Excessively noisy values were removed or scaled down to a value < |1|.

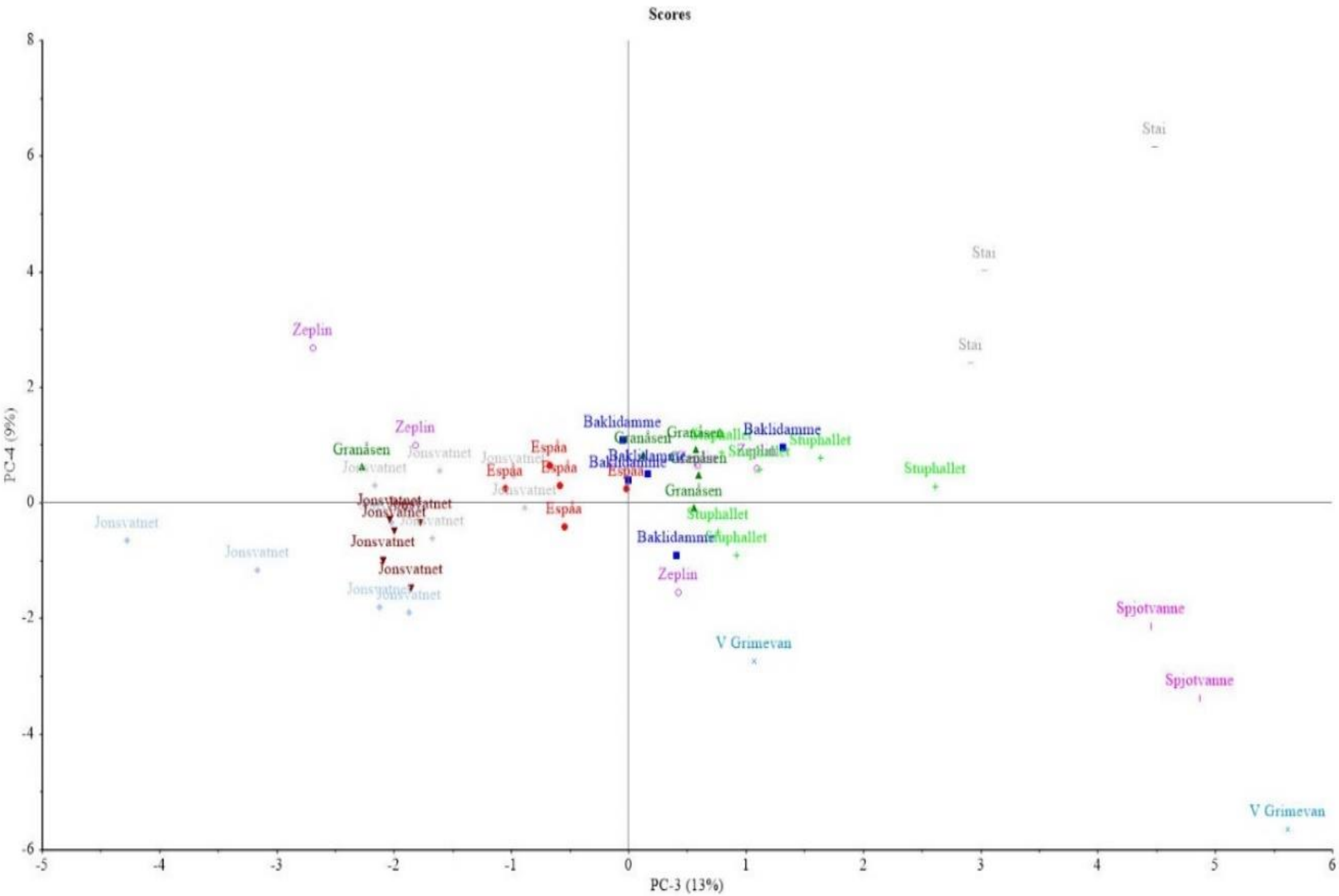

Figure 18. Continued

5 Discussion

5.1 PAHs in sampled areas

Upon examination of the PAH values, no clear northward depositional concentration trend was present, although the global distillation theory did appear to be supported as heavier compounds, such as the benzo- ene compounds, were not detected as frequently in Svalbard sampling sites when compared to other sampling areas. The general elevation of Area 4 readings including benzo[ghi]perylene, may be due to more local sources ,such as the Ny-Ålesund airport, or local vehicle transportation as the location is closer to developed areas than Area 5 and benzo[ghi]perylene has been correlated to petroleum sorces[83]. The elevated phenanthrene and pyrene values and presence of naphthalene, acenaphthylene and fluorene in Area 4, also suggests traffic emissions since the occurrence of these compounds together has been associated with traffic related PAH pollution[83]. Other elevated values in the Trondheim and Southern Norway regions, such as Area 15 and Area 16 compared to Areas 11- 13 and Area 10 compared to Area 6, roughly corresponds to their closeness to population centers.

The PAH values found reflected interesting relationships to those found in the literature as summarized in Table 12. In the Wang 2009[10], the average levels compiled from samples around the Ny-Ålesund Svalbard region reflected the concentration of lower ringed congers like naphthalene (2), fluorene (3) and phenanthrene (3), but the incomplete observation of the PAHs present in this study's samples prevents similar observation from being as definitively drawn. It was similarly notable that the Ny-Ålesund levels from the Wang 2009[10] study were higher than the levels observed in the unpolluted NILU 2015[83] survey areas. The relevant compound levels found in this study's Southern Norway and Trondheim sample districts were also elevated when compared to unpolluted sample areas of similar geographic coordinates, but they did not surpass the concentrations observed in more polluted areas for the compounds pyrene, benzo[b]fluoranthene, benzo[a] pyrene, and benzo[ghi]perylene.

Table 12

This summary table contains the average amount in ng/g of various PAHs from three different studies as well as a brief summary of the extraction and chemical analysis methods used. The NILU 2015 locations reflect non-polluted areas and were selected due to relative proximity to the sampled areas, with Laksely being the furthest north area, Mosvik closest to the Trondheim locations and Birkenes closest to the Grimevannet locations in the Southern Norway category. NILU Industries 2015[92] reflects more polluted areas due to specific industries, but also potentially due to their proximity to higher populations areas with the Orkanger location closet to Trondheim and Kvinesdal near by the Grimevannet locations for Southern Norway.

Study and Method	Wang 2009[10], Ultrasonic bath with activated copper clean up, column chromatography, GC/ MS	NILU 2015[83] Soxhlet, liquid-liquid partitioning, column chromatography, GC/LRMS			NILU Industries 2015[92] Hexane, liquid-liquid partitioning, column chromatography, GC/LRMS	
Area	Svalbard	Lakselv	Mosvik	Birkenes	Orkanger	Kvinesdal
# of Samples	12	5-10	5-10	5-10	10	10
Naphthalene [b]	41	< 2.8	< 2.9	< 2.9	5	2
Acenaphthylene [b]	7	< 0.10	< 0.10	< 0.10	0.7	0.8
Acenaphthene	9	< 0.34	< 0.34	< 0.34	18	1
Fluorene [b]	38	< 1.4	< 1.4	< 1.4	25	3
Phenanthrene [a, b]	72	< 21	< 21	< 21	137	17
Anthracene [b]	8	< 0.24	< 0.24	< 0.24	18	1
Fluoranthene [b]	7	3.58	1.97	2.09	372	33
Pyrene [a, b]	5	1.93	1.31	1.4	290	21
Benzo(a)anthracene	3	0.18	0.35	0.36	202	5
Chrysene	5	0.81	1.07	1.17	226	13
Benzo(b)fluoranthene [a]	6	0.71	1.31	1.45	259	17
Benzo(k)fluoranthene [a]	1.3	0.29	0.55	0.52	129	6
Benzo(a)pyrene [a]	6	0.4	0.72	0.68	247	8
Benzo(ghi)perylene [a]	4	0.39	0.86	0.85	183	10
Dibenzo(a,h)anthracene	0.4	0.04	0.08	0.13	45	2
Indeno(1,2,3-cd)pyrene	0.7	0.48	1.08	1.12	179	12
Total	213	34.69	35.18	35.65	2335	151

[a] These compounds were found in this study's HPLC FID-DAD analysis

[b] These compounds were found in this study's GC- MS analysis

5.2 Elemental analysis

Although all of the selected elements, V, Cr, Mn, Fe, Zn, As, Mo, Ag, Cd, Sn, Sb, W, Tl, and Pb, were significantly different by at least one area as determined by the Welsch ANOVA test, many were only dissimilar from the reference material, which was anticipated as it was a different moss species. In general, V, Mn, Fe, Zn, As, Mo, Ag, Cd, Sn, Sb, W, Tl, Pb and Bi were expected to show signs of LRT amplification at higher latitudes and Cr was projected to show local pollution trends. In actuality, the data showed the magnification of only three elements, As, Cd and Pb, in the Svalbard sample regions and due to the uncertainty, only the levels of Cd were significantly greater in Svalbard than in other areas. A converse trend was revealed for the element W and Mn, which yielded significantly different lower values in Svalbard than in other regions. Mn concentrations may be lower in Svalbard due sea aerosols, which have been shown to lower Mn values[40], as the sampling locations were closer that the other sampled areas to the ocean, but W may be explained by the bedrock contributions. Many of the other elements only revealed possible local contamination sources. For example, Sn concentrations Area 8 and Area 10 were significantly higher from most of the other samples. This may be explained by the geological influence in Area 8 as shown in Table 14, and it is possible that dust from Area 8 may have influenced Area 10, but that is less certain. The elements Ag and Sn have not been shown to specifically correlate between wet deposition collection and moss evaluation[40] and there is mixed evidence regarding Fe and Cr, which may additionally explain their concentrations.

Previous moss sampling surveys shown in Table 13 demonstrate a clear decrease in the LRT of metalloids and metals of concern over time. When comparing this study's element averages to the Svalbard, Trondheim and Southern Norway sampling regions (see Table 16 in Appendix B) to the averages in the Indre Troms - Vest Finnmark, Dovre rundt and Sørlandet areas, certain conclusions may be drawn. It is evident that the Svalbard elemental concentrations are often higher than the Indre Troms- Vest Finnmark values, which may reveal a greater effect of LRT to high Arctic areas. For the V, Cr, and As levels, the soil composition is most likely the cause, but the high Cd and Pb levels on Svaldbard may be due to LRT. The Cd levels may have also been influenced by sea bird guano, which is often high in Cd[25], as Area 5, Stuphallet, is a well-known marine bird nesting site. Trondheim metal and metalloid levels from the study data are also consistently higher than Dovre rundt levels, but this is probably due to Trondheim's greater population and urbanization adjacent to the sampled areas in contrast to the uninhabited Dovre rundt location. Sampled southern Norway concentrations for the elements listen in Table 13 were often similar to, or less than the 2015 levels, which possibly means that LRT of those elements is still decreasing.

Table 13

This table contains a summary of the average values of relevant elements in mg/kg from three different years. The three locations were selected from the Atmospheric Deposition of Heavy metals (ADHM) 2015[41] survey summary table and Berg 1997[2] study to relate roughly to the three different thesis sampling regions. ADHM and Berg both used data from Norwegian national moss monitoring surveys. Sørlandet and Birkenes were similar to the Grimevannet sampling areas, Dovre rundt and Kårvatn were similar to the Trondheim areas and Indre Troms- Vest Finnmark and Karpdalen were both the furthest North locations from their respective studies.

Element	ADHM 2015[41], microwave digestion, ICP- HRMS									Berg-1997[2] Nitric acid bomb digestion, ICP-MS		
Year	1977			1995			2015			1995		
Area	Sørlandet	Dovre rundt	Indre Troms-Vest Finnmark	Sørlandet	Dovre rundt	Indre Troms-Vest Finnmark	Sørlandet	Dovre rundt	Indre Troms-Vest Finnmark	Birkenes	Kårvatn	Karpdalen
V	11.8 ± 4.1	1.6 ± 0.7	1.6 ± 0.4	6.1 ± 1.3	1.57 ± 0.73	1.32 ± 0.53	2.2 ± 0.6	0.9 ± 0.53	0.3 ± 0.2	3.5 ±0.4	0.59 ± 0.14	2.7 ± 0.1
Cr	5.6 ± 1.9	1.2 ± 0.5	1.2 ± 0.5	1.7 ± 0.4	1.5 ± 0.8	0.8 ± 0.3	1.0 ± 0.3	0.7 ± 0.3	0.4 ± 0.2	1.1 ±0.1	0.43 ± 0.20	4.3 ± 0.3
Mn	-	-	-	-	-	-	-	-	-	110 ± 50	150 ± 50	210 ± 80
Fe	-	-	-	-	-	-	-	-	-	536 ±87	450 ± 30	3300 ±400
Zn	93 ±21	25.4 ± 3.6	30.5 ±17.5	61 ± 19	29 ± 12	27 ± 11	47.2 ± 0.26	20.6 ± 4.6	29.1 ± 5.5	40 ± 4	25 ± 6	42 ± 9.5
As	2.44 ± 0.86	0.25 ± 0.11	0.18 ± 0.07	0.90 ± 0.26	0.3 ± 0.2	< 0.15	0.20 ± 0.02	0.06 ± 0.02	0.07 ± 0.03	0.43	0.057 ±0.06	0.75 ±0.22
Mo	-	-	-	-	-	-	-	-	-	0.37 ± 0.03	0.051 ±0.026	0.010 ± 0.02
Cd	1.17 ± 0.15	0.06 ± 0.04	0.12 ± 0.08	0.41 ± 0.12	0.07 ± 0.03	0.07 ±0.03	0.22 ± 0.04	0.05 ± 0.02	0.04 ± 0.02	0.31 ± 0.07	0.062 ±0.023	0.15 ± 0.01
Sn	-	-	-	-	-	-	-	-	-	0.68 ± 0.08	0.052 ± 0.022	0.21 ± 0.03
Sb	1.40 ± 0.34	0.12 ±0.03	0.09 ± 0.02	0.32 ± 0.07	0.05 ± 0.02	0.04 ± 0.02	0.17 ± 0.05	0.04 ±0.02	0.018 ± 0.007	0.29 ± 0.02	0.034 ± 0.006	0.058 ± 0.015
W	-	-	-	-	-	-	-	-	-	0.084 ± 0.011	0.018 ± 0.012	0.044 ± 0.008
T	-	-	-	-	-	-	-	-	-	0.24 ±0.09	0.048 ± 0.033	0.060 ± 0.056
Pb	127 ± 30	8.9 ± 4.1	6.3 ± 3.0	23 ± 5	2.4 ± 0.7	2.1 ± 1.0	5.6 ± 1.0	0.56 ± 0.06	0.53 ± 0.09	24 ± 3.7	1.9 ± 0.71	4.3 ± 0.4

5.2.1 Principal component analysis

PCA revealed patterned groupings amongst the data. Figure 17 displayed the loadings and score plots from principal component (PC) 1, which described 32% of the variance, and PC 2, which explained 17% of the variance. Together these two PCs described almost half of the variance in the data set of, which mostly corresponds the variance in the Svalbard region samples. The Zeppelin area, or Area 4 as it was referred to in the tables, had three samples with particularly high values that correlated strongly to Co, Ni, Fe, and Al concentrations, all of which, except for nickel, do not participate as considerably in LRT. These in conjunction with the not quite as strong, but present correlations to As and Ag, closely resembled the expected elemental contributions from the parent soil materials listed in Table 13. In addition, Spearman's rho values linked these elements together at the 0.01 significance level (see Table 22 in Appendix B). Stuphallet, or Area 5, also appeared separate from the mainland Norway groups and was associated with high Cd levels. As mentioned previously, this sampling area was near the sea in a prominent marine bird nesting location and their guano may have produced the high Cd values[25]. This Svalbard sampling area hosted the most developed moss colonies of the sampling locations visited, possibly due to this input and the presence of a shielding cliff which may explain have influenced its metal values as well. The high correlation to Cd values may also be due to atmospheric deposition of dust. A small grouping of Zn and Sn on PC 1 may be correlated to Spjotevanne, Area 8, and Grimevannet, Area 10, as the parent soil in Area 8 contained these elements and Area 10 was possibly in range of dust from Area 8's parent soil material.

The results of PC 3, which corresponded to 13% of variance, and PC 4, which corresponded to 9% of the variance, could describe some of the interactions between the Trondheim and Southern Norway samples. PC 3 showed a grouping of Cd, Tl, Pb, and S linked to the Stai, or Area 6 locations. As none of these elements were particularly linked to the background soil material, they may have been due to LRT, or Area 6's proximity to E6, a major Norwegian highway. Area 6 of the Stai location from PC 4 also seemed associated with the elements P and K, which may be due for run off from fertilizers as those elements are commonly used in agriculture[25] and there are farms in the vicinity. Another grouping of PC 3 contained Mo, Sn, Bi and Pb and was connected to some of the Grimevannet and Spjotevannet samples. The elevated Sn and Pb may also be explained by the parent soil in Area 8, but the Mo and Bi levels may be due to LRT. Mg, V, Ti, Cr, Fe, and Co formed a lose grouping in PC 3 that may be explained by the potentially higher pollution levels in Trondheim Jonsvannet areas. These elements are commonly absorbed from the soil and parent soils with some of these elements are present in other areas of Trondheim, but that soil was not present in the Jonsvannet areas. It is possible that enrichment of these elements was due to the Statkraft waste incineration plant roughly 8-15 km from the sampling areas as wind generally travels toward Jonsvannet from the plant.

5.2.2 Elemental variation between sampling sites

In addition to LRT, elements can accumulate due to local pollution sources, natural sources and landscape features as well. The strong correlations presented in the Spearman's rho analysis of the elements with each other, suggests that they may have accumulated in conjunction with each other. Additionally, general patterns for essential elements may be explained by effect of moss on metal concentrations.

As it was recommended to avoid local pollution by sampling at least 300 meters from big roads, 100 meters from small roads, 4 km from industries, and 3 km from cites[1], most of the sampled areas should not reflect anthropogenic pollution, but not all. Area 4 nearby Zeppelin mountain was within 2 km of the Ny- Ålesund airport, which may explain the elevated levels of metals commonly found in tires, such as zinc[25], although levels of these metals were not statistically different from Area 5, a more remote area on Svalbard. Of the Trondheim locations, Area 15 was closest to a potential industrial source, the Statkraft waste incineration plant at roughly 8 km away with the next closest being Area 14 at approximately 12 km away from Statkraft. Neither of these locations showed distinct significant differences as defined by the Dunnetts T3 test from the other Trondheim locations, and as both locations were over 4 km away, any impact was most likely statistically insignificant. In the southern Norway areas, Area 6 was statistically different from many of the Trondheim locations for elements V, Cr, Cd, Sn, and Tl and sometimes statistically different from the Svalbard and other southern Norway areas (see Table 22 in Appendix B). This may possibly be related to the motorway number 3 that was located within a kilometer of the sampling area, or E6, a common through way from Oslo to

Trondheim, located on the other side of the sampled area. These roads may have contributed to dust deposition past the 400 meters that the sampling guidelines account for.

Natural propagation effects of dust, which can carry mineral particles like Li, AI, Sc, Ti, V, Cr, Fe, Co, Rb, Sr, Ta, Ga, and Th[40], and salt spray, which can reduce the ability of moss to uptake Cu and Zn [54] and increase overall Li, Mg, Cl, Ca, Br, Sr, and I levels[2], additionally may have altered the sampled areas although the Spearman's rho test did not find any negative correlations between typical salt spray elements and Cu and Zn. In the case of this study potential dust propagation, possibly more than sea spray effects, may explain some of the patterns observed in the descriptive statistics of all the sampled elements (see Table 16 in Appendix B), especially when the parent material of the sampled areas listed in Table 14 is considered.

Physical landscape characteristics such as elevation, also affect the element distribution of LRT[29, 93]. There is evidence that higher elevations reflect more LRT effects than low altitudes, which may be more influenced by local alluvial elemental contributions [29, 93]. As altitudinal effects were not considered in the selection of sampled locations, they may have affected the data. It has even been suggested that altitude may change the bioaccumulation factors of mosses[93], although in the case of gradual elevation changes, such as the differences between the sampled areas in this study, these findings may be more difficult to conclude.

Table 14

This table details the major rock types and the notable associated trace element distributions for each of the sampled areas. Notable association was determined by the comparison of element concentrations crustal values.

Area	Rock types	Elements
4	Sandstone, shale and coal	Ag, As, Ba, Cr, Cu, Mn, Ni, V, Zn
5	Carbonate rocks, evaporites and clastic sedimentary	
6	Sand grains, quartz and feldspar	Low Ti, Li, B
8	Herefoss granite	Ba, Pb, Sn, V, Zn
10	Banded gneiss	
11	Rhyolite and tough sandstone and layers of dark grey slate	Ag
12	Rhyolite and tough sandstone and layers of dark grey slate	Ag
13	Dark grey slate	
14	Sandstone and limestone	Ag
15	Greenstone and green slate	Co, Cr, Cu, Mn, Ni, V, Zn
16	Greenstone and green slate	Co, Cr, Cu, Mn, Ni, V, Zn

References: Contains data under the Norwegian license for public data (NLOD), Norwegian Geological Survey (NGU)[94], Norwegian Polar Institute [95], and Alloway[25].

5.3 Experimental limitations

The methodology employed for sampling, sample handling and extraction in this study could have been improved upon. Due to time and cost restraints presented by the nature of the thesis as well as inexperience, such improvements were neglected.

Currently the manual produced by the International Cooperative Program on the effects of air pollution on natural vegetation and crops (ICP vegetation), “Heavy Metals, Nitrogen and POPs in European Mosses: 2015 Survey”, is the recommended official method of heavy metal, POPs and nitrogen analysis for moss sampling[1]. This document outlines the methodology to collect moss samples and was used to craft this thesis’s methods, but as exact replication of these methods would have become cost prohibitive the thesis did not follow the protocol exactly and so may have accumulated potential errors due to this. Although, it should be noted that in a comprehensive review of the moss sampling techniques used by 369 papers, the authors found that not a single paper followed the exact ICP vegetation methodology with the vague wording being a contributing factor[1], in addition to lack of method revision despite the outdated aspects that result in less desirable outcomes and reduced conclusions that can be made from the research data[1]. This 2015 review’s[1] complied data specifically found that the number of samples should be not be 5-10 but 30 to ensure statistical certainty[1], whereas only six or less samples were taken from each area in this thesis. To further improve the statistical certainty of the data, especially in previously unsampled areas[52] like the Svalbard locations, a systematic sampling approach that ensures homogeneity in the sample density would have increased the reliability of results[96]. Although the statistical parameters intrinsically contain high variability that can overcome some sampling scheme errors to provide the spatial distribution of elements[96], reducing potential errors increases reliability.

Despite recommendations from the literature, some sampled locations were influenced by canopy overhang due to lack *H. splendens* within the sampling area. Although specifically canopy throughfall of precipitation has not been correlated to a significantly different element distribution, precipitation acquired through stem flow has [1]. The physiochemical properties of the plant matter effects the ion concentrations within precipitation that it comes into contact which results in decreased concentrations of Al, As, Co, Cr, Fe, Hg, S, and V in moss[1]. This possibly may have affected samples S47, S48, S49, S50; S57, S59; S62, S64, S66; S67, S71; S72, S73, S75 of areas 11, 13, 14, 15, 16, but there is no evidence visible in the data of a specific decrease.

A potential solution to the lack of the target species in desirable positions within the sample areas is to use moss bags, or transplanted moss. This technique has proven to be very effective for reducing the variability of contaminate uptake and has the advantage of exact temporal measurements[27, 48] along with serving as a good monitoring solution in highly urbanized areas[66]. The use of several species of moss, like *H. splendens*, *P. schreberi*, and *I. stoloniferum*, is another method that could be employed in future studies to improve the quality of the data from sampling areas, but the use of multiple species does require interspecies calibrations to be taken in each location[64].

There were two main concerns regarding the sample handling, the drying period and the parts of the moss structure used. Due to travel constraints from Ny-Ålesund back to NTNU in Trondheim as well as uncertainty concerning the level of dryness required, moss samples were left to dry for up to a month at room temperature. The majority of the literature regarding moss analysis agrees that drying should only occur for a maximum two weeks to prevent further temporal irrgulaites[1]. The lack of mercury levels detected in any of the samples may also suggest that this time period was long enough to allow the vaporization of volatiles, but as PAHs and PCBs have been shown to be stable up to eight and 17 months respectivly[97] this may not have affected the POPs levels in the samples. As *H. Splendis* growth is stunted in far north areas, the classic step-wise growth, as shown in Figure 6 previously, was non-distinguishable. Therefore, the entire sample was used as selecting specific years was not possible. Samples from other parts of Norway were sorted so that the only green and yellow sections were used. Due to the impossibility of year growth separation in the Svalbard group, no effort was made to do so in the other locations. Depending on the years contained in the Svalbard samples versus the mainland Norway samples, this may have resulted in a significant disparity in the time periods compared.

The methodologies for the extractions of POPs both produced less than optimal results. As this thesis was not focused on procedural optimization, the samples were only extracted by ASE and analyzed once with the given procedures designed for marine sediment and soil samples[49, 86-88]. When compared to soil, moss has considerably higher amounts of organic carbon (OC) and OM. Not only does OM strongly effect the adsorption of metals by the sample material[25], but higher OM levels also correlate to heightened organic pollutant levels and increased interferences from the matrix that can be unintentionally coextracted[97]. This may explain why the ASE extracts contained significant amounts of coextracted species. As these undesirable compounds could have potentially damaged the column, dilution of the samples was required before they were processed. The sample dilution of seven times may have resulted in pollutant levels below the detection limits and the dilution of ten times for A6 resulted in no readings above the LOQ values, but the more concentrated four times dilution of the pool samples from A4 and A5 caused significant contamination of the GC-MS column. An ASE methodology for a sample material with high organic matter may have resulted in a cleaner extract and increased detection recovery. Specifically for the PCB and PAH procedure, ASE extraction employed 100% dichloromethane, which may favor PAH extraction over PCB[97]. Low PCB levels in the sample areas, may also explain their absence as recent studies have also had limited success in detection[45, 98]. To contrast, the ASE extracts from the HPLC FID-DAD method did not require extra dilutions. This may have contributed to the larger range of detected compounds. In addition, the values detected from the less dilute GC-MS analyzed A4 and A5 samples contradicted the results from the more dilute samples of the same areas. For these reasons, the GC-MS data was considered more as an indicator of a certain compounds present than as exact amounts in the discussion.

The use of pooled samples each area also introduced error into the PAH procedure as sample 52 b from Area 12 was accidently added to the Area 11 pool sample, constituting 12.995% of the total. This may have significantly altered the data for As, Ag, Sn, and Pb for elemental analysis as Areas 11 and 12 were significantly different in these, but since PAHs mostly travel by a different transportation mechanism than metals and the sampling areas are relatively close compared to the other areas in the Trondheim region, the effect may not have been significant. The relatively similar values for these areas in Table 8 may support this.

6 Conclusion

This thesis set out to utilize moss in the measurement of PBT pollutants. Metal, metalloid, PAH, and PCB concentrations were the focal point to determine if there was significant accumulation of pollutants in high Arctic areas like Ny-Ålesund, Svalbard. Although the analysis methods for PAH and PCB determination were not as successful as anticipated, they did not seem to demonstrate a concentration pattern in high Arctic areas; instead, they seemed correlated to population centers and other possible pollutant sources. Of the 14 elements specifically evaluated for LRT, or local pollution, only Pb levels correlated to significant amplification in Svalbard. When compared to previous studies, the averaged concentrations of V, Cr, As, Cd, and Sn in the Svalbard sampled areas were greater than the most Northern reference area near West Finnmark sampled in 2015 by the National Moss monitoring protocol[41], which may suggest LRT. Further the monitoring of high Arctic areas should be considered as its concentrations may be dissimilar to mainland Norway LRT levels.

7 Future Work Recommendations

In continued evaluations of pollution in high Arctic areas, there are several improvements to this master thesis's research that could be implemented to yield better results. As mentioned previously in the discussion sections, the PAH and PCB determination methods produced less than optimal recovery results. It is recommended for the next moss survey to switch to the use of an analysis method that either accounts for high organic matter content[97], has been effective to extract PAHs and PCBs from moss specially[10, 11, 83, 99], or has been recommended by a moss air monitoring survey protocol such as the ICP vegiations[100]. It may also be advantageous to switch focus from PCB observation to more emergent pollutants as there has been some evidence that levels found in high Arctic areas are low[45, 98]. Among the various rising pollutants, there is some precedent for using moss to monitor organochlorine pesticides[101-104] and micro fibres[105].

For further metal and metalloid detection and comparisons within high Arctic areas, additional sampling locations near by Ny-Ålesund would decrease the influence of local pollution sources to the observation of overall trends in the area. The investigation of moss bag usage[48, 66, 67] over a summer period in Ny-Ålesund, may serve as a potential solution if *H. splendens* populations prove to be scarce. Additionally, sampling of remote comparisons sites in mainland Norway, such as those used for background locations in national moss monitoring surveys[83] may allow more robust comparisons and therefore reveal differences between sampling sites not seen in the present study.

Possible improvements to this thesis specifically include the amendment of sample locations, sample handling and procedural errors. The sampled areas displayed high variability within the sampling groups. To improve this, the use of a stricter sampling pattern, complete avoidance of any potential interferants such as tree or foliage cover and larger subsample sizes may be helpful[1]. Another confounder may have been that moss samples were left to dry past the optimum two-week drying period, possibly causing the loss of volatiles. The loss of certain PBT compounds such as mercury may have reduced their potential for detection. A mercury specific analysis method such as Hydride Generation of ASS, Cold vapor AAS[25] or another such protocol along with shorter drying periods may prove more effective in its future detection. The detection of PAHs and PCBs was severely limited by the improper use of internal standards by laboratory staff and non-effective clean-up routines. If there had been additional analysis time, a full method analysis to determine the optimum ASE settings may have improved detection rates among the respective GC-MS and HPLC FID-DAD procedures.

8 Citations

1. Fernández, J. A.; Boquete, M. T.; Carballeira, A.; Aboal, J. R., A critical review of protocols for moss biomonitoring of atmospheric deposition: Sampling and sample preparation. *Sci Total Environ* **2015,** *517*, 132-150.
2. Berg, T.; Steinnes, E., Recent trends in atmospheric deposition of trace elements in Norway as evident from the 1995 moss survey. *Sci Total Environ* **1997,** *208* (3), 197-206.
3. Halleraker, J. H.; Reimann, C.; de Caritat, P.; Finne, T. E.; Kashulina, G.; Niskaavaara, H.; Bogatyrev, I., Reliability of moss (Hylocomium splendens and Pleurozium schreberi) as a bioindicator of atmospheric chemistry in the Barents region: Interspecies and field duplicate variability. *The Science of the total environment* **1998,** *218* (2), 123-139.
4. Wojtuń, B.; Samecka-Cymerman, A.; Kolon, K.; Kempers, A. J.; Skrzypek, G., Metals in some dominant vascular plants, mosses, lichens, algae, and the biological soil crust in various types of terrestrial tundra, sw spitsbergen, norway. *Polar biology* **2013,** *36* (12), 1799-1809.
5. Kirk, J.; Gleason, A., Tracking Long-range Atmospheric Transport of Contaminants in Arctic Regions Using Lake Sediments. In *Environmental Contaminants: Using natural archives to track sources and long-term trends of pollution*, Blais, J. M.; Rosen, M. R.; Smol, J. P., Eds. Springer Netherlands: Dordrecht, 2015; pp 223-262.
6. Beitveit, G. M.; Jenssen, B. M.; Fossøy, F.; Maciej Ciesielski, T.; Gunnar Stokke, B. Contamination in an Arctic Environment: Abiotic and Biotic Impacts of Local Pollution. NTNU, 2016.
7. Jia, N.; Sun, L.; He, X.; You, K.; Zhou, X.; Long, N., Distributions and impact factors of antimony in topsoils and moss in Ny-Ålesund, Arctic. *Environ Pollut* **2012,** *171*, 72-77.
8. Bazzano, A.; Cappelletti, D.; Udisti, R.; Grotti, M., Long-range transport of atmospheric lead reaching Ny-Ålesund: Inter-annual and seasonal variations of potential source areas. *Atmospheric environment (1994)* **2016,** *139*, 11-19.
9. Halbach, K.; Mikkelsen, Ø.; Berg, T.; Steinnes, E., The presence of mercury and other trace metals in surface soils in the Norwegian Arctic. *Chemosphere* **2017,** *188*, 567-574.
10. Wang, Z.; Ma, X.; Na, G.; Lin, Z.; Ding, Q.; Yao, Z., Correlations between physicochemical properties of PAHs and their distribution in soil, moss and reindeer dung at Ny-Ålesund of the Arctic. *Environ Pollut* **2009,** *157* (11), 3132-3136.
11. Wang, Z.; Na, G.; Ma, X.; Ge, L.; Lin, Z.; Yao, Z., Characterizing the distribution of selected PBDEs in soil, moss and reindeer dung at Ny-Ålesund of the Arctic. *Chemosphere* **2015,** *137*, 9-13.
12. Mróz, T.; Mróz, T.; Szufa, K.; Szufa, K.; Frontasyeva, M. V.; Frontasyeva, M. V.; Tselmovich, V.; Tselmovich, V.; Ostrovnaya, T.; Ostrovnaya, T.; Kornaś, A.; Kornaś, A.; Olech, M. A.; Olech, M. A.; Mietelski, J. W.; Mietelski, J. W.; Brudecki, K.; Brudecki, K., Determination of element composition and extraterrestrial material occurrence in moss and lichen samples from King George Island (Antarctica) using reactor neutron activation analysis and SEM microscopy. *Environ Sci Pollut Res Int* **2018,** *25* (1), 436-446.
13. Eiliv Steinnes, H. U., Metal pollution around
Norwegian industries
studied by analysis of
naturally growing moss
samples 2015 survey. Norwegian Institute for Air Research: 2017; p 81.
14. Lead, W. A.; Steinnes, E.; Jones, K. C., Atmospheric Deposition of PCBs to Moss (Hylocomium splendens) in Norway between 1977 and 1990. *Environ. Sci. Technol* **1996,** *30* (2), 524-530.
15. Harmens, H.; Foan, L.; Simon, V.; Mills, G., Terrestrial mosses as biomonitors of atmospheric POPs pollution: A review. *Environ Pollut* **2013,** *173*, 245-254.
16. Harmens, H.; Norris, D. A.; Sharps, K.; Mills, G.; Alber, R.; Aleksiayenak, Y.; Blum, O.; Cucu-Man, S. M.; Dam, M.; De Temmerman, L.; Ene, A.; Fernández, J. A.; Martinez-Abaigar, J.; Frontasyeva, M.; Godzik, B.; Jeran, Z.; Lazo, P.; Leblond, S.; Liiv, S.; Magnússon, S. H.; Maňkovská, B.; Karlsson, G. P.; Piispanen, J.; Poikolainen, J.; Santamaria, J. M.; Skudnik, M.; Spiric, Z.; Stafilov, T.; Steinnes, E.; Stihi, C.; Suchara, I.; Thöni, L.; Todoran, R.; Yurukova, L.; Zechmeister, H. G., Heavy metal and nitrogen concentrations in mosses are declining across Europe whilst some "hotspots" remain in 2010. *Environ Pollut* **2015,** *200*, 93-104.
17. Brune, W. H., The ozone story: A model for addressing climate change? *Bulletin of the Atomic Scientists* **2015,** *71* (1), 75-84.

18. Gouin, T.; Mackay, D.; Jones, K. C.; Harner, T.; Meijer, S. N., Evidence for the “grasshopper” effect and fractionation during long-range atmospheric transport of organic contaminants. *Environ Pollut* **2004,** *128* (1), 139-148.
19. Wayne, R. P., *Chemistry of Atmospheres*. 3 ed.; Oxford University Press: New York, United States, 2000.
20. The Editors of Encyclopaedia Britannica, G. L.; Rafferty, J. P.; Tikkanen, A. Hadley cell. https://www.britannica.com/science/Hadley-cell.
21. The Editors of Encyclopaedia Britannica, D. D.; Lotha, G.; Pallardy, R.; Promeet, D.; Rodriguez, E.; Sampaolo, M.; Tikkanen, A.; Young, G. Wind. https://www.britannica.com/science/wind (accessed 5, April 2021).
22. Dunbar, B. Earth's Atmospheric Layers. https://www.nasa.gov/mission_pages/sunearth/science/atmosphere-layers2.html (accessed 26/3/2021).
23. Wania, F.; Mackay, D., Tracking the distribution of persistent organic pollutants. *Environmental science & technology* **1996,** *30* (9), 390A-396A.
24. Blais, J. M.; Rosen, M. R.; Smol, J. P., Environmental Contaminants : Using natural archives to track sources and long-term trends of pollution. 1st ed. 2015. ed.; Springer Netherlands : Imprint: Springer: Dordrecht, 2015.
25. Alloway, B. J., Heavy Metals in Soils : Trace Metals and Metalloids in Soils and their Bioavailability. 3rd ed. 2013. ed.; Springer Netherlands : Imprint: Springer: Dordrecht, 2013.
26. Ross, H., On the use of mosses (Hylocomium splendens and Pleurozium schreberi) for estimating atmospheric trace metal deposition. *Water, Air, and Soil Pollution* **1990,** *50* (1-2).
27. Augusto, S.; Máguas, C.; Branquinho, C., Guidelines for biomonitoring persistent organic pollutants (POPs), using lichens and aquatic mosses – A review. *Environ Pollut* **2013,** *180*, 330-338.
28. Klaassen, C. D.; Casarett, L. J., *Casarett and Doull's Toxicology: The Basic Science of Poisons*. Ninth edition. ed.; McGraw-Hill Medical: New York, 2019.
29. Catalan, J., Tracking Long-Range Atmospheric Transport of Trace Metals, Polycyclic Aromatic Hydrocarbons, and Organohalogen Compounds Using Lake Sediments of Mountain Regions. In *Environmental Contaminants: Using natural archives to track sources and long-term trends of pollution*, Blais, J. M.; Rosen, M. R.; Smol, J. P., Eds. Springer Netherlands: Dordrecht, 2015; pp 263-322.
30. Hasselbach, L.; Ver Hoef, J. M.; Ford, J.; Neitlich, P.; Crecelius, E.; Berryman, S.; Wolk, B.; Bohle, T., Spatial patterns of cadmium and lead deposition on and adjacent to National Park Service lands in the vicinity of Red Dog Mine, Alaska. *Sci Total Environ* **2005,** *348* (1), 211-230.
31. Chaligava, O.; Shetekauri, S.; Badawy, W. M.; Frontasyeva, M. V.; Zinicovscaia, I.; Shetekauri, T.; Kvlividze, A.; Vergel, K.; Yushin, N., Characterization of Trace Elements in Atmospheric Deposition Studied by Moss Biomonitoring in Georgia. *Arch Environ Contam Toxicol* **2021,** *80* (2), 350-367.
32. González, A. G.; Pokrovsky, O. S., Metal adsorption on mosses: Toward a universal adsorption model. *J Colloid Interface Sci* **2014,** *415*, 169-178.
33. González, A. G.; Jimenez-Villacorta, F.; Beike, A. K.; Reski, R.; Adamo, P.; Pokrovsky, O. S., Chemical and structural characterization of copper adsorbed on mosses (Bryophyta). *J Hazard Mater* **2016,** *308*, 343-354.
34. Czikkely, M.; Neubauer, E.; Fekete, I.; Ymeri, P.; Fogarassy, C., Review of Heavy Metal Adsorption Processes by Several Organic Matters from Wastewaters. *Water* **2018,** *10* (10), 1377.
35. Christensen, E. R.; Steinnes, E.; Eggen, O. A., Anthropogenic and geogenic mass input of trace elements to moss and natural surface soil in Norway. *Science of The Total Environment* **2018,** *613-614*, 371-378.
36. Blais, J. M.; Rosen, M. R.; Smol, J. P., Using Natural Archives to Track Sources and Long-Term Trends of Pollution: Some Final Thoughts and Suggestions for Future Directions. In *Environmental Contaminants: Using natural archives to track sources and long-term trends of pollution*, Blais, J. M.; Rosen, M. R.; Smol, J. P., Eds. Springer Netherlands: Dordrecht, 2015; pp 499-506.
37. Torunn, B.; Katrine, A.; Eiliv, S., Transport of Hg from Atmospheric mercury depletion events to the mainland of Norway and its possible influence on Hg deposition. *Geophysical research letters* **2008,** *35* (9), L09802-n/a.
38. Steinnes, E.; Friedland, A. J., Metal contamination of natural surface soils from long-range atmospheric transport: Existing and missing knowledge. *Dossiers environnement* **2006,** *14* (3), 169-186.
39. Steinnes, E.; Sjøbakk, T. E.; Berg, T., *Temporal trends in long-range atmospheric transport of heavy metals to Norway*. EDP Sciences: Les Ulis, 2003.
40. Berg, T.; Steinnes, E., Use of mosses (Hylocomium splendens and Pleurozium schreberi) as biomonitors of heavy metal deposition: From relative to absolute deposition values. *Environmental Pollution* **1997,** *98* (1), 61-71.
41. Eilliv Steinnes, H. T. U., Katrine Aspmo Pfaffhuber, Torunn Berg *Atmospheric deposition of heavy metals in Norway*; Norwegian Institute for Air Research: 2015; p 57.

42. Halbach, K.; Mikkelsen, Ø.; Steinnes, E., Study of mercury and selected trace elements in soil in the Norwegian Arctic, Svalbard. NTNU: 2016.
43. Steffen, A.; Douglas, T.; Amyot, M.; Ariya, P.; Aspmo, K.; Berg, T.; Bottenheim, J.; Brooks, S.; Cobbett, F.; Dastoor, A.; Dommergue, A.; Ebinghaus, R.; Ferrari, C.; Gardfeldt, K.; Goodsite, M. E.; Lean, D.; Poulain, A. J.; Scherz, C.; Skov, H.; Sommar, J.; Temme, C., A synthesis of atmospheric mercury depletion event chemistry in the atmosphere and snow. *Atmospheric chemistry and physics* **2008,** *8* (6), 1445-1482.
44. Callén, M. S.; Callén, M. S.; de la Cruz, M. T.; de la Cruz, M. T.; López, J. M.; López, J. M.; Murillo, R.; Murillo, R.; Navarro, M. V.; Navarro, M. V.; Mastral, A. M.; Mastral, A. M., Long-Range Atmospheric Transport and Local Pollution Sources on PAH Concentrations in a South European Urban Area. Fulfilling of the European Directive. *Water, air, and soil pollution* **2008,** *190* (1), 271-285.
45. Dreyer, A.; Nickel, S.; Schröder, W., (Persistent) Organic pollutants in Germany: results from a pilot study within the 2015 moss survey. *Environ Sci Eur* **2018,** *30* (1), 1-14.
46. Mackay, D.; Celsie, A. K. D.; Parnis, J. M., The evolution and future of environmental partition coefficients. *Environmental Reviews* **2016,** *24* (1), 101-113.
47. Wenche Aas, S. P., Sverre Solberg, Karl Espen Yttri, Monitoring of long-range
transported air pollutants in
Norway. In *Annual report 2014*, Norwegian Institute for Air Research: 2015; p 109.
48. Ares, A.; Aboal, J. R.; Carballeira, A.; Giordano, S.; Adamo, P.; Fernández, J. A., Moss bag biomonitoring: A methodological review. *Sci Total Environ* **2012,** *432*, 143-158.
49. Pintado-Herrera, M. G.; González-Mazo, E.; Lara-Martín, P. A., In-cell clean-up pressurized liquid extraction and gas chromatography–tandem mass spectrometry determination of hydrophobic persistent and emerging organic pollutants in coastal sediments. *Journal of Chromatography A* **2016,** *1429*, 107-118.
50. Henderson Jr, J. W.; Biazzo, W.; Long, W., Polycyclic Aromatic Hydrocarbon (PAH) Separations Using ZORBAX Eclipse PAH Columns–Analyses from Six to 24 PAHs. *Agilent Technologies. May* **2008,** *29*.
51. Carter, M. R.; Gregorich, E. G.; Canadian Society of Soil, S., *Soil sampling and methods of analysis*. 2nd ed. ed.; CRC Press: Boca Raton, Fla, 2008.
52. Fifield, F. W.; Haines, P. J., *Environmental analytical chemistry*. 2nd ed. ed.; Blackwell Science: Oxford, 2000.
53. Äyräs, M.; Pavlov, V.; Reimann, C., Comparison of sulphur and heavy metal contents and their regional distribution in humus and moss samples from the vicinity of Nikel and Zapoljarnij, Kola Peninsula, Russia. *Water, air, and soil pollution* **1997,** *98* (3), 361-380.
54. Berg, T.; Røyset, O.; Steinnes, E., Moss (Hylocomium splendens) used as biomonitor of atmospheric trace element deposition: Estimation of uptake efficiencies. *Atmospheric environment (1994)* **1995,** *29* (3), 353-360.
55. Kasiuliene, A.; Paulauskas, V.; Marozas, V.; Waara, S., Accumulation of heavy metals in forest dwarf shrubs and dominant mosses as bioindicators of atmospheric pollution. 2019; Vol. 24, p 1079.
56. Peters, K., Floor moss Hylocomium splendens , Rostock. 2006.
57. Barandovski, L.; Barandovski, L.; Cekova, M.; Cekova, M.; Frontasyeva, M. V.; Frontasyeva, M. V.; Pavlov, S. S.; Pavlov, S. S.; Stafilov, T.; Stafilov, T.; Steinnes, E.; Steinnes, E.; Urumov, V.; Urumov, V., Atmospheric deposition of trace element pollutants in Macedonia studied by the moss biomonitoring technique. *Environ Monit Assess* **2008,** *138* (1), 107-118.
58. Steinnes, E.; Berg, T.; Uggerud, H. T., Three decades of atmospheric metal deposition in Norway as evident from analysis of moss samples. *Science of The Total Environment* **2011,** *412-413*, 351-358.
59. Abdusamadzoda, D.; Abdushukurov, D. A.; Duliu, O. G.; Zinicovscaia, I.; Yushin, N. S.; Frontasyeva, M. V., Investigations of the Atmospheric Deposition of Major and Trace Elements in Western Tajikistan by Using the Hylocomium splendens Moss as Bioindicators. *Arch Environ Contam Toxicol* **2020,** *78* (1), 60-67.
60. Brumbaugh, W. G.; Morman, S. A.; May, T. W., Concentrations and bioaccessibility of metals in vegetation and dust near a mining haul road, Cape Krusenstern National Monument, Alaska. *Environ Monit Assess* **2011,** *182* (1), 325-340.
61. Allajbeu, S.; Qarri, F.; Marku, E.; Bekteshi, L.; Ibro, V.; Frontasyeva, M. V.; Stafilov, T.; Lazo, P., Contamination scale of atmospheric deposition for assessing air quality in Albania evaluated from most toxic heavy metal and moss biomonitoring. *Air quality, atmosphere and health* **2017,** *10* (5), 587-599.
62. Shirato, S.; Iizuka, A.; Mizukoshi, A.; Noguchi, M.; Yamasaki, A.; Yanagisawa, Y., Optimized arrangement of constant ambient air monitoring stations in the Kanto region of Japan. *Int J Environ Res Public Health* **2015,** *12* (3), 2950-2966.
63. Trends in Atmospheric Carbon Dioxide. https://www.esrl.noaa.gov/gmd/ccgg/trends/ (accessed 30/03/2021).

64. Cowden, P.; Aherne, J., Interspecies comparison of three moss species (Hylocomium splendens, Pleurozium schreberi, and Isothecium stoloniferum) as biomonitors of trace element deposition. *Environ Monit Assess* **2019,** *191* (4), 1-13.
65. Dragovic, S.; Mihailovic, N., Analysis of mosses and topsoils for detecting sources of heavy metal pollution: multivariate and enrichment factor analysis. *Environ Monit Assess* **2009,** *157* (1-4), 383-390.
66. Capozzi, F.; Giordano, S.; Di Palma, A.; Spagnuolo, V.; De Nicola, F.; Adamo, P., Biomonitoring of atmospheric pollution by moss bags: Discriminating urban-rural structure in a fragmented landscape. *Chemosphere* **2016,** *149*, 211-218.
67. Giordano, S.; Adamo, P.; Spagnuolo, V.; Tretiach, M.; Bargagli, R., Accumulation of airborne trace elements in mosses, lichens and synthetic materials exposed at urban monitoring stations: Towards a harmonisation of the moss-bag technique. *Chemosphere* **2013,** *90* (2), 292-299.
68. Winkler, J.; Ghosh, S., Therapeutic Potential of Fulvic Acid in Chronic Inflammatory Diseases and Diabetes. *Journal of Diabetes Research* **2018,** *2018*, 5391014.
69. Turull, M.; Elias, G.; Fontàs, C.; Díez, S., Exploring new DGT samplers containing a polymer inclusion membrane for mercury monitoring. *Environmental Science and Pollution Research* **2017,** *24* (12), 10919-10928.
70. Operating Instructions for Oscillating Mill MM400. Retsch: Retsch GmbH, 42781 Haan, Retsch-Allee 1-5, Germany 2016.
71. Harris, D. C., *Exploring Chemical Analysis*. 4th ed.; Clancy Marshall: 41 Madison Avenue, New York, NY 10010, 2009.
72. Manahan, S. E., *Environmental chemistry*. 9th ed. ed.; CRC Press: Boca Raton, Fla, 2010.
73. Veggi, P. C.; Martinez, J.; Meireles, M. A. A., Fundamentals of Microwave Extraction. Springer US: 2012; pp 15-52.
74. Otson, R.; Williams, D. T., Evaluation of a liquid-liquid extraction tecnique for water pollutants. *Journal of Chromatography A* **1981,** *212* (2), 187-197.
75. Richter, B. E.; Jones, B. A.; Ezzell, J. L.; Porter, N. L.; Avdalovic, N.; Pohl, C., Accelerated Solvent Extraction: A Technique for Sample Preparation. *Analytical Chemistry* **1996,** *68* (6), 1033-1039.
76. Giergielewicz-Możajska, H.; Dąbrowski, Ł.; Namieśnik, J., Accelerated Solvent Extraction (ASE) in the Analysis of Environmental Solid Samples — Some Aspects of Theory and Practice. *Critical Reviews in Analytical Chemistry* **2001,** *31* (3), 149-165.
77. Holger Franz, V. J., Fluorescence Method Development
Handbook In *Application Handbook 70302*, Thermo Fisher Scientific: Germering, Germany, 2015.
78. Bisutti, I.; Hilke, I.; Raessler, M., Determination of total organic carbon – an overview of current methods. *TrAC Trends in Analytical Chemistry* **2004,** *23* (10-11), 716-726.
79. Maximilian O Besenhard, A. T., Luca Mazzei,Eva Sorensen, Recent advances in modelling and control of liquid chromatography. *Current Opinion in Chemical Engineering* **2021,** *32*.
80. Kitson, F. G., *What Is GC/MS?* San Diego :, 1996; p 3-23.
81. *Friendship Among Equals*. ISO Central Secretariat: Geneve 20 Switzerland.
82. *Heavy Metals, Nitrogen and POPs in European Mosses: 2015 Survey*; ICP Vegetation Programme Coordination Centre, Centre for Ecology and Hydrology, Environment Centre Wales, Bangor, Gwynedd, UK, 2015; p 14.
83. Anne Karine Halse, H. U., Eiliv Steinnes, Martin Schlabach, PAH measurements in air and moss around selected industrial sites in
Norway 2015. Norwegian Institute for Air Research: 2017; p 49.
84. Yakovleva, E. V.; Gabov, D. N.; Beznosikov, V. A.; Kondratenok, B. M.; Dubrovskiy, Y. A., Accumulation of PAHs in Tundra Plants and Soils under the Influence of Coal Mining. *Polycyclic aromatic compounds* **2017,** *37* (2-3), 203-218.
85. *Test report: Botanical samples, leaves, radix, soil*; p 1.
86. Brett Murphy, S. L., Bruce Richter, Richard Carlson, Simultaneous Extraction of PAHs and PCBs from Environmental Samples Using
Accelerated Solvent Extraction. *Thermo Fisher Scientific* **2012**, 5.
87. Birhanu, M. Z.; Schmid, R.; Mikklesen, O., Determination of Poly Chlorinated biphenyls in sediment of Trondheim fjord (Norway) and Lake Tana (Ethiopia) using pressurized liquid extraction (PLE) and Gas Chromatography - Mass Spectrometry (GC-MS). NTNU: 2017.
88. Dionex, Extraction of PAHs from Environmental
Samples by Accelerated Solvent Extraction (ASE). *Dionex Cooperation* **2011**, 4.

89. Rietveld, T.; Hout, R. v., Statistics in language research : analysis of variance. Reprint 2010. ed.; Mouton de Gruyter: Berlin ;,New York, 2005.

90. Liu, H. Comparing W Comparing Welch's ANOVA, a Kruskal-W A, a Kruskal-Wallis test and tr allis test and traditional aditional
ANOVA in case of Heterogeneity of Variance. Virginia Commonwealth University, Graduate School at VCU Scholars Compass, 2015.

91. Mital C. Shingala, D. A. R., Comparison of Post Hoc Tests for Unequal
Variance. *International Journal of New Technologies in Science and Engineering 2* (5).

92. Martin Schlabach, E. S., Hilde Thelle Uggerud, Atmospheric deposition of organic contaminants in Norway. In *National moss survey 2015*, Norwegian Institute for Air Research: 2016; p 37.

93. Xiao, J.; Han, X.; Sun, S.; Wang, L.; Rinklebe, J., Heavy metals in different moss species in alpine ecosystems of Mountain Gongga, China: Geochemical characteristics and controlling factors. *Environ Pollut* **2021,** *272*, 115991-115991.

94. BERGGRUNN. Norges Geologiske Undersøkelse: 2015; pp Map viewer- Bedrock.

95. Polarinstitutt, N., Geologi on Svalbardkartet. Norwegian Polar Institute Norsk Polarinstitutt, Sysselmannen på Svalbard

96. Qarri, F.; Qarri, F.; Lazo, P.; Lazo, P.; Bekteshi, L.; Bekteshi, L.; Stafilov, T.; Stafilov, T.; Frontasyeva, M.; Frontasyeva, M.; Harmens, H.; Harmens, H., The effect of sampling scheme in the survey of atmospheric deposition of heavy metals in Albania by using moss biomonitoring. *Environ Sci Pollut Res Int* **2015,** *22* (3), 2258-2271.

97. Brändli, R. C.; Bucheli, T. D.; Kupper, T.; Stadelmann, F. X.; Tarradellas, J., Optimised accelerated solvent extraction of PCBs and PAHs from compost. *International Journal of Environmental Analytical Chemistry* **2006,** *86* (7), 505-525.

98. Huber, C. E.; Mikkelsen, Ø.; Steinnes, E. Study of Long Range Transported Pollutants in Arctic Soil. NTNU, 2017.

99. Martinez-Swatson, K.; Mihály, E.; Lange, C.; Ernst, M.; Dela Cruz, M.; Price, M. J.; Mikkelsen, T. N.; Christensen, J. H.; Lundholm, N.; Rønsted, N., Biomonitoring of Polycyclic Aromatic Hydrocarbon Deposition in Greenland Using Historical Moss Herbarium Specimens Shows a Decrease in Pollution During the 20th Century. *Frontiers in plant science* **2020,** *11*, 1085-1085.

100. *Heavy Metals, Nitrogen and POPs in European Mosses: 2020 Survey*; ICP Vegetation Programme Coordination Centre, Centre for Ecology and Hydrology, Environment Centre Wales, Bangor, Gwynedd, UK, 2020; p 27.

101. Shen, L.; Wania, F.; Lei, Y. D.; Teixeira, C.; Muir, D. C. G.; Bidleman, T. F., Atmospheric Distribution and Long-Range Transport Behavior of Organochlorine Pesticides in North America. *Environ. Sci. Technol* **2005,** *39* (2), 409-420.

102. Lim, T. B.; Xu, R.; Tan, B.; Obbard, J. P., Persistent organic pollutants in moss as bioindicators of atmospheric pollution in Singapore. *Chemosphere* **2006,** *64* (4), 596-602.

103. Tarcau, D.; Cucu-Man, S.; Boruvkova, J.; Klanova, J.; Covaci, A., Organochlorine pesticides in soil, moss and tree-bark from North-Eastern Romania. *Sci Total Environ* **2013,** *456-457*, 317-324.

104. Simonich, S. L.; Hites, R. A., Global distribution of persistent organochlorine compounds. *Science* **1995,** *269* (5232), 1851-1854.

105. Roblin, B.; Aherne, J., Moss as a biomonitor for the atmospheric deposition of anthropogenic microfibres. *Sci Total Environ* **2020,** *715*, 136973-136973.

106. Weging, S., Study of trace elements, natural organic matter and selected environmental toxicants in soil, overbank deposit and riverwater at Mitrahalvøya, to establish bias correction for studies of long range transported pollutants in Ny-Ålesund. NTNU: Trondhiem, Norway, 2021.

1 Appendix A

1.1 Percent TOC, TIC and ROC data

Table 15

This table contains the percent Total Organic Carbon (TOC), Total Inorganic Carbon (TIC) and Residual Organic Carbon of selected samples from each of the sampling areas. The detection limit was ± |0.002| mg.

Samples number	Area	TOC %	TIC %	ROC %
20a	4	37.52	0.85	0.04
21a	4	35.38	1.05	0.05
24a	4	34.48	0.90	0.05
25a	5	38.39	0.62	0.06
27a	5	35.63	0.88	0.16
30a	5	37.75	0.74	0.07
31a	6	37.76	0.65	0.07
32a	6	37.62	0.54	0.06
41	8	38.16	0.69	0.05
42	8	39.46	0.85	0.06
44	10	38.00	0.64	0.06
46	10	39.11	0.67	0.06
47a	11	38.69	0.73	0.06
49a	11	38.73	0.70	0.06
50a	11	37.71	0.68	0.06
52a	12	38.92	0.58	0.07
54a	12	39.88	0.59	0.06
55a	12	39.53	0.82	0.07
58a	13	37.94	0.62	0.06
59a	13	38.84	0.57	0.06
61a	13	38.73	0.78	0.06
63a	14	39.21	0.84	0.10
64a	14	38.53	0.73	0.11
66a	14	38.96	0.58	0.09
67a	15	38.63	0.65	0.07
69a	15	38.74	0.63	0.08
71a	15	38.91	0.69	0.08
72a	16	38.74	0.71	0.06
74a	16	38.71	0.55	0.11
75a	16	37.36	0.74	0.07

2 Appendix B

2.1 HR ICP-MS

Table 16

Descriptive statistics for 60 elements measured. LOQ values are not incorporated in the table.

Element	Area	Mean µg/g	Median µg/g	Min µg/g	Max µg/g	SD µg/g	RSD %
Li 7	Svalbard	2.19	0.80	0.16	6.641	2.312	105.61
	Trondheim	0.206	0.176	0.0738	0.5826	0.1235	60.04
	S. Norway	0.36	0.20	0.1091	1.121	0.3571	100.3
Be9	Svalbard	0.13	0.05	0.01	0.4738	0.1498	117.2
	Trondheim	0.014	0.012	0.00705	0.03591	0.006452	46.00
	S. Norway	0.04	0.03	0.01384	0.08415	0.02520	69.81
B11	Svalbard	8.171	5.877	1.925	21.84	5.875	71.90
	Trondheim	4.245	3.723	1.397	10.32	2.258	53.19
	S. Norway	2.197	1.902	1.067	4.762	1.257	57.22
Na23	Svalbard	248.5	209.5	124.6	554.0	122.8	49.43
	Trondheim	383.8	388.5	157.3	869.7	138.8	36.17
	S. Norway	284.3	315.5	170.1	391.6	78.47	27.60
Mg25	Svalbard	1745	1673	1072	2607	486.9	27.90
	Trondheim	1707	1741	1004	2612	409.4	23.98
	S. Norway	1212	1237	883.6	1368	158.2	13.06
Al27	Svalbard	2867	1293	274.2	10307	3332	116.2
	Trondheim	677.7	630.6	278.8	1680	336.9	49.72
	S. Norway	775.6	605.9	324.6	1258	422.7	54.51
Si30	Svalbard	1680	1666	572.6	2387	499.3	29.72
	Trondheim	1577	1580	574.6	3152	700.9	44.46
	S. Norway	1786	1409	1022	2764	708.0	39.64
P31	Svalbard	830.6	812.8	628.2	1032	137.3	16.53
	Trondheim	1143	1079	516.4	1839	331.3	28.98
	S. Norway	1651	1695	808.7	2707	752.5	45.58
S34	Svalbard	734.7	716.0	618.5	899.3	87.22	11.87
	Trondheim	767.5	759.5	421.0	1194	147.8	19.26
	S. Norway	935.0	868.4	771.7	1442	229.8	24.57
K39	Svalbard	3703	3666	2258	5871	1073	28.97
	Trondheim	5124	5017	2624	7177	1172	22.88
	S. Norway	7786	5823	4020	16245	4362	56.02
Ca44	Svalbard	6257	4630	3880	16947	3784	60.48
	Trondheim	2316	2162	1451	4068	623.6	26.92
	S. Norway	2701	2253	1504	4849	1395	51.64
Sc45	Svalbard	0.4925	0.2525	0.04775	1.639	0.5273	107.1

	Trondheim	0.3135	0.2753	0.07773	0.9945	0.2228	71.08
	S. Norway	0.1738	0.09912	0.04855	0.3743	0.1371	78.85
Ti49	Svalbard	55.32	42.12	13.40	129.3	35.51	64.19
	Trondheim	74.81	53.17	16.28	210.3	53.68	71.75
	S. Norway	52.08	31.64	15.37	113.7	39.16	75.20
V51	Svalbard	4.122	2.123	0.4306	12.11	3.799	92.17
	Trondheim	2.985	2.434	0.7528	9.475	2.096	70.20
	S. Norway	1.420	1.229	0.5145	2.634	0.8641	60.84
Cr52	Svalbard	3.278	1.732	0.3577	10.78	3.320	101.3
	Trondheim	1.796	1.376	0.7488	4.709	1.092	60.83
	S. Norway	0.9296	0.7288	0.3375	1.707	0.5458	58.72
Mn55	Svalbard	66.73	24.53	5.781	206.82	74.36	111.4
	Trondheim	263.8	248.3	91.12	543.6	96.18	36.46
	S. Norway	309.6	314.1	81.07	635.0	169.3	54.70
Fe56	Svalbard	1445	753	167.6	4291	1445	100.0
	Trondheim	885.8	724.5	232.8	2829	622.2	70.24
	S. Norway	702.0	401.1	207.8	1516	516.4	73.56
Co59	Svalbard	0.9616	0.3423	0.08541	3.838	1.172	121.9
	Trondheim	0.4408	0.3631	0.1270	1.229	0.2923	66.31
	S. Norway	0.2493	0.1929	0.1421	0.3737	0.1032	41.39
Ni60	Svalbard	2.946	2.151	0.3768	10.71	3.035	103.0
	Trondheim	1.406	1.302	0.5090	3.395	0.7070	50.27
	S. Norway	0.9609	0.9581	0.5578	1.342	0.2912	30.30
Cu63	Svalbard	2.939	2.258	0.6713	7.111	2.003	68.17
	Trondheim	5.074	4.714	3.194	7.225	1.039	20.47
	S. Norway	6.053	5.843	4.474	7.355	0.9318	15.39
Zn66	Svalbard	23.46	15.66	8.439	66.54	17.69	75.43
	Trondheim	23.21	22.34	9.086	35.38	6.294	27.12
	S. Norway	41.75	45.57	29.32	53.44	10.65	25.50
Ga69	Svalbard	0.8595	0.3944	0.08221	3.064	0.9965	115.9
	Trondheim	0.2058	0.1832	0.06784	0.6008	0.1249	60.72
	S. Norway	0.2597	0.1729	0.08817	0.5413	0.1760	67.77
As75	Svalbard	0.3248	0.2516	0.1175	0.6106	0.1909	58.76
	Trondheim	0.1235	0.1015	0.03738	0.2604	0.05749	46.57
	S. Norway	0.1561	0.1565	0.1048	0.2049	0.03641	23.32
Br81	Svalbard	2.824	2.915	0.2893	6.842	1.809	64.05
	Trondheim	0.8583	1.0114	0.04227	1.756	0.4437	51.70
	S. Norway	2.908	2.918	2.343	3.512	0.4403	15.14
Rb85	Svalbard	6.164	3.976	1.344	17.46	4.900	79.49
	Trondheim	11.50	9.141	3.499	33.86	6.705	58.33
	S. Norway	19.82	20.59	11.13	26.44	6.107	30.82
Sr88	Svalbard	19.37	19.01	10.39	29.69	5.256	27.13
	Trondheim	14.78	13.74	5.898	28.88	5.668	38.36
	S. Norway	16.06	12.51	7.573	34.57	9.512	59.22

Y89	Svalbard	1.227	0.7914	0.2299	3.771	1.094	89.20
	Trondheim	0.3293	0.2703	0.0759	1.079	0.2357	71.56
	S. Norway	0.7589	0.4400	0.1559	1.755	0.6501	85.66
Zr90	Svalbard	0.6522	0.3854	0.1064	1.701	0.5542	84.99
	Trondheim	0.2917	0.2641	0.1044	0.6968	0.1350	46.28
	S. Norway	0.6430	0.5303	0.2337	1.454	0.4406	68.51
Nb93	Svalbard	0.07457	0.08380	0.02814	0.1193	0.03303	44.29
	Trondheim	0.04408	0.04174	0.01938	0.08304	0.01605	36.40
	S. Norway	0.1977	0.1059	0.04687	0.5065	0.1822	92.17
Mo98	Svalbard	0.08386	0.07711	0.05469	0.1360	0.02681	31.97
	Trondheim	0.06591	0.05760	0.01419	0.1607	0.03519	53.39
	S. Norway	0.1481	0.1328	0.08022	0.2266	0.05687	38.41
Ag109	Svalbard	0.2298	0.1842	0.03595	0.5172	0.1776	77.27
	Trondheim	0.04003	0.02855	0.01747	0.1117	0.02590	64.69
	S. Norway	0.1105	0.09402	0.07433	0.1876	0.04036	36.54
Cd111	Svalbard	0.2016	0.1838	0.09572	0.4543	0.08864	43.96
	Trondheim	0.01914	0.01228	0.0008353	0.05457	0.01599	83.57
	S. Norway	0.08377	0.06816	0.01184	0.2232	0.07079	84.50
Sn118	Svalbard	0.09265	0.07956	0.02238	0.2122	0.05075	54.77
	Trondheim	0.1004	0.08986	0.05099	0.1960	0.03380	33.67
	S. Norway	0.2280	0.2361	0.07242	0.4048	0.1492	65.44
Sb121	Svalbard	0.02809	0.02265	0.01332	0.05859	0.01523	54.22
	Trondheim	0.06219	0.05603	0.03135	0.1114	0.02133	34.30
	S. Norway	0.08646	0.10084	0.04237	0.1363	0.03692	42.70
I127	Svalbard	3.670	3.520	1.874	5.410	1.147	31.24
	Trondheim	2.479	2.146	1.117	5.000	0.8753	35.31
	S. Norway	2.719	3.292	1.399	3.685	0.9502	34.94
Cs133	Svalbard	0.2871	0.1949	0.03864	0.7160	0.2332	81.25
	Trondheim	0.1450	0.1322	0.04575	0.3753	0.09537	65.77
	S. Norway	0.3536	0.1783	0.04093	1.322	0.4464	126.2
Ba137	Svalbard	3.319	1.373	0.3457	11.41	3.503	105.5
	Trondheim	2.063	1.830	0.8898	5.149	1.000	48.45
	S. Norway	4.309	3.447	1.126	9.535	3.404	79.01
La139	Svalbard	1.959	1.008	0.2036	6.004	2.056	104.9
	Trondheim	0.1958	0.1689	0.06086	0.4603	0.09848	50.31
	S. Norway	0.9418	0.5785	0.2569	2.257	0.7777	82.57
Ce140	Svalbard	4.289	1.983	0.4520	13.42	4.569	106.5
	Trondheim	0.4341	0.3767	0.1471	1.067	0.2200	50.68
	S. Norway	2.064	1.287	0.5032	4.980	1.702	82.46
Pr141	Svalbard	0.5111	0.2531	0.05263	1.637	0.5456	106.7
	Trondheim	0.05306	0.04705	0.01794	0.1357	0.02754	51.90
	S. Norway	0.2289	0.1287	0.05646	0.5889	0.1987	86.80
Nd146	Svalbard	1.947	0.9572	0.2043	6.431	2.081	106.9
	Trondheim	0.2182	0.1927	0.07134	0.5808	0.1173	53.76

	S. Norway	0.8442	0.4816	0.2149	2.152	0.7182	85.08
Sm147	Svalbard	0.3813	0.1924	0.03786	1.310	0.4126	108.2
	Trondheim	0.05341	0.05067	0.01460	0.1539	0.03206	60.02
	S. Norway	0.1663	0.08894	0.04295	0.4163	0.1394	83.82
Eu153	Svalbard	0.07714	0.03821	0.007245	0.2796	0.08611	111.6
	Trondheim	0.01618	0.01474	0.004823	0.04699	0.01004	62.08
	S. Norway	0.02791	0.02065	0.01100	0.05683	0.01820	65.20
Gd155	Svalbard	0.6030	0.3250	0.07752	1.916	0.6119	101.5
	Trondheim	0.1403	0.1197	0.04720	0.3476	0.0792	56.44
	S. Norway	0.3800	0.2901	0.1527	0.6893	0.2227	58.62
Tb159	Svalbard	0.05341	0.03154	0.007119	0.1789	0.05415	101.4
	Trondheim	0.01100	0.009920	0.002695	0.03392	0.007279	66.17
	S. Norway	0.02778	0.01538	0.006283	0.06051	0.02337	84.15
Dy163	Svalbard	0.2648	0.1767	0.04517	0.8326	0.2488	93.97
	Trondheim	0.06733	0.05847	0.01518	0.2089	0.04608	68.43
	S. Norway	0.1533	0.08763	0.03378	0.3450	0.1324	86.37
Ho165	Svalbard	0.04813	0.03215	0.009461	0.1435	0.04282	88.97
	Trondheim	0.01398	0.01153	0.003269	0.04426	0.009695	69.35
	S. Norway	0.03003	0.01712	0.006403	0.06920	0.02608	86.85
Er166	Svalbard	0.1339	0.09336	0.02825	0.3780	0.1130	84.40
	Trondheim	0.04212	0.03461	0.009044	0.1326	0.02931	69.60
	S. Norway	0.08936	0.05199	0.01904	0.2027	0.07636	85.45
Tm169	Svalbard	0.01640	0.01209	0.004146	0.04240	0.01282	78.14
	Trondheim	0.005848	0.004638	0.001302	0.01855	0.004076	69.70
	S. Norway	0.01204	0.007283	0.002307	0.02720	0.01041	86.50
Yb172	Svalbard	0.09650	0.07346	0.02604	0.2418	0.07236	74.98
	Trondheim	0.03765	0.03063	0.008352	0.1224	0.02677	71.10
	S. Norway	0.07586	0.04603	0.01579	0.1661	0.06325	83.37
Lu175	Svalbard	0.01396	0.01051	0.004020	0.03409	0.01033	73.96
	Trondheim	0.005303	0.004368	0.001183	0.01624	0.003515	66.29
	S. Norway	0.01118	0.006216	0.002084	0.02415	0.009645	86.30
Hf178	Svalbard	0.01304	0.007992	0.000736	0.03680	0.01175	90.09
	Trondheim	0.006114	0.005367	0.001641	0.01552	0.003465	56.67
	S. Norway	0.01516	0.01267	0.004773	0.04054	0.01239	81.71
Ta181	Svalbard	0.001103	0.0009552	0.0002892	0.002206	0.0006805	61.68
	Trondheim	0.001176	0.001166	0.0004132	0.002103	0.0004320	36.74
	S. Norway	0.002390	0.002018	0.001197	0.004526	0.001146	47.93
W182	Svalbard	0.01266	0.01459	0.003463	0.02135	0.006579	51.95
	Trondheim	0.04502	0.04153	0.01072	0.1166	0.02497	55.46
	S. Norway	0.03824	0.03512	0.03011	0.05727	0.009716	25.41
Tl205	Svalbard	0.03758	0.02228	0.005120	0.09235	0.02853	75.91
	Trondheim	0.02901	0.02176	0.0042283	0.09395	0.02244	77.33
	S. Norway	0.06828	0.06190	0.02520	0.1233	0.03015	44.15
Pb208	Svalbard	2.060	1.420	0.2199	5.268	1.579	76.66

	Trondheim	0.6414	0.5843	0.3306	1.129	0.2221	34.63
	S. Norway	2.449	2.643	0.8767	3.903	1.127	46.01
Bi209	Svalbard	0.01610	0.008874	0.002323	0.04923	0.01454	90.35
	Trondheim	0.009154	0.007032	0.001281	0.03112	0.007517	82.12
	S. Norway	0.04113	0.02153	0.005453	0.1912	0.06687	162.6
Th232	Svalbard	0.5135	0.2219	0.05530	1.673	0.5678	110.6
	Trondheim	0.04338	0.03745	0.01450	0.09592	0.02207	50.87
	S. Norway	0.2503	0.1052	0.04897	0.7920	0.2700	107.9
U238	Svalbard	0.1879	0.08822	0.02007	0.9842	0.2741	145.8
	Trondheim	0.01728	0.01518	0.005355	0.03837	0.008270	47.86
	S. Norway	0.1302	0.04311	0.01525	0.5623	0.1962	150.7

2.2 Detection limits

Table 17

The LOQ values for the elements measured by HR ICP-MS are listen in the table. Two elements Au and Nb were tested for , but as there was no concentration in the blanks or samples, LOQ values are set to the lowest calibration standards avlible at 0,004 µg/L and 0,04 µg/L respectively.

Li7(LR)[a]	Be9(LR)	B11(MR)	Na23(MR)	Mg25(MR)	Al27(MR)	Si30(MR)	P31(MR)
µg/L	µg/L	µg/L	µg/L	µg/L	µg/L	µg/L	µg/L
0.08334	0.01328	0.5995	4.086	0.2374	0.3531	33.82	10.82

S34(MR)	Cl35(MR)	K39(HR)	Ca44(MR)	Sc45(MR)	Ti49(MR)	V51(MR)	Cr52(MR)
µg/L	µg/L	µg/L	µg/L	µg/L	µg/L	µg/L	µg/L
8.796	301.9	6.857	3.243	0.005468	0.2102	0.008848	0.03198

Cr53(MR)	Mn55(MR)	Fe56(MR)	Co59(MR)	Ni60(MR)	Cu63(MR)	Zn66(MR)	Ga69(MR)
µg/L	µg/L	µg/L	µg/L	µg/L	µg/L	µg/L	µg/L
0.1021	0.03146	0.1627	0.007320	0.05378	0.04357	0.1254	0.002514

As75(HR)	Se78(HR)	Br81(MR)	Rb85(MR)	Sr88(MR)	Y89(LR)	Zr90(LR)	Mo98(MR)
µg/L	µg/L	µg/L	µg/L	µg/L	µg/L	µg/L	µg/L
0.05530	0.3126	20.80	0.02205	0.01726	0.0003033	0.002380	0.01817

Ru101(MR)	Pd105(HR)	Ag109(MR)	Cd111(LR)	Cd111(MR)	Sn118(LR)	Sb121(MR)	I127(MR)
µg/L	µg/L	µg/L	µg/L	µg/L	µg/L	µg/L	µg/L
0.009169	0.03442	0.02807	0.005150	0.007912	0.01161	0.007722	0.6427

Cs133(LR)	Ba137(MR)	La139(MR)	Ce140(LR)	Pr141(LR)	Nd146(LR)	Sm147(LR)	Eu153(MR)
µg/L	µg/L	µg/L	µg/L	µg/L	µg/L	µg/L	µg/L
0.002313	0.01482	0.001276	0.0002762	0.0002980	0.0004849	0.0008626	0.004408

Gd155(MR)	Tb159(LR)	Dy163(LR)	Ho165(LR)	Er166(LR)	Tm169(LR)	Yb172(LR)	Lu175(LR)
µg/L	µg/L	µg/L	µg/L	µg/L	µg/L	µg/L	µg/L
0.01056	0.0002766	0.0009762	0.0001160	0.0001558	0.0001775	0.0003706	0.0001686

Hf178(LR)	Ta181(LR)	W182(LR)	Pt195(LR)	Hg202(LR)	Tl205(LR)	Pb208(LR)	Bi209(LR)
µg/L	µg/L	µg/L	µg/L	µg/L	µg/L	µg/L	µg/L
0.001534	0.0003230	0.001531	0.001481	0.02168	0.0003372	0.003706	0.0007272

Th232(LR)	U238(LR)
µg/L	µg/L
0.001886	0.0002136

[a] LR, MR, HR denote low, medium and high range scanning.

2.3 Statistics

Table 18

The results of the Levene variance test for the selected element group are shown in this table. The significance (Sig.) is designated when values are <0.05 and the null hypothesis violated.

Element	Sig.
V51	0.000*
Cr52	0.000*
Mn55	0.000*
Fe56	0.000*
Zn66	0.004
As75	0.000*
Mo98	0.000*
Ag109	0.000*
Cd111	0.000*
Sn118	0.000*
Sb121	0.151
W182	0.019*
Tl205	0.000*
Pb208	0.000*
Bi209	0.000*

*These results are of unequal variance.

Table 19

This table shows categories that are deemed non- normal by the Shapiro-Wilk's normality test. The test was conducted for each of the sampling areas individually and combined. The data set rejects the normality assumption when the significance (Sig.) values are < 0.05. Areas where there were less than three samples, eight and ten, were excluded. Of the selected elements Mn55 had no cases of non-normality and is not presented.

Element	Area	Sig.
V51	14	0.006
	All	0.000
Cr52	14	0.010
	All	0.000
Fe56	All	0.000
Zn66	Ref.	0.003
	14	0.012
	16	0.032
	All	0.001
As75	4	0.029
	16	0.032
	All	0.000
Mo98	11	0.015
	All	0.000
Ag109	All	0.000
Cd111	11	0.033
	All	0.000
Sn118	All	0.000
Sb121	15	0.048
	All	0.017
W182	5	0.014
	14	0.028
	All	0.001
Tl205	All	0.000
Pb208	11	0.029
	All	0.000
Bi209	All	0.000

Table 20

The results of the ANOVA and Welch test or, Robust Tests of Equality of Means for the selected elements is listed in this table. Significance (Sig.) is designated when values are < 0.05, suggesting that the element is significantly different from at least one of the other areas.

	ANOVA	Welch
Element	Sig.	Sig.
V51	0.000*	0.000*
Cr52	0.000*	0.000*
Mn55	0.000*	0.000*
Fe56	0.000*	0.000*
Zn66	0.000*	0.000*
As75	0.000*	0.002*
Mo98	0.000*	0.000*
Ag109	0.000*	0.001*
Cd111	0.000*	0.000*
Sn118	0.000*	0.000*
Sb121	0.000*	0.000*
W182	0.000*	0.000*
Tl205	0.000*	0.000*
Pb208	0.000*	0.000*
Bi209	0.000*	0.013*

* Significantly different

Table 21

The significant results, as designated by values < 0.05, of the Dunnett's T3 test are summarized for the selected element grouping. If a group relationship was completely demonstrated by a previous area, the later area was not repeated.

Element	Comparison Area	Areas with Corresponding Significant difference
V51	Reference	11, 12, 13
	6	11, 13
	13	Reference, 6, 16
Cr52	Reference	11, 12, 13
	6	11, 13
	11	Reference, 6, 14
Mn55	Reference	4, 5, 10, 11, 12, 14, 15
	4	Reference, 10, 13
	5	Reference, 10, 11, 12, 13, 14
Fe56	Reference	11, 12, 13
Zn66	Reference	5
	5	Reference, 11, 13
As75	Reference	11
	11	Reference, 12, 13, 14, 16
Mo98	Reference	5
	5	Reference, 12, 11
Ag109	Reference	11
	11	Reference, 12, 13, 14, 15, 16
Cd111	Reference	5, 11, 12, 13, 14, 15, 16
	5	Reference, 6, 11, 12, 13, 14, 15,16
	6	5, 8, 12, 14, 15
	8	6, 11, 12, 14, 15, 16
Sn118	Reference	11
	4	8
	5	8, 11
	6	11
	8	4, 5, 12, 14, 15, 16
	11	Reference, 5, 6, 12, 13
Sb121	Reference	13
	5	13
W182	Reference	8, 13, 16
	4	8, 13, 16
	5	8, 13, 16
	12	16

Element	Comparison Area	Areas with Corresponding Significant difference
Tl205	Reference	6, 12
	5	6
	6	Reference, 5, 11, 12, 15
Pb208	Reference	5, 11, 12, 13, 14, 15, 16
	11	Reference, 12

Table 22

This is a summary of the Spearman's rho test results that were correlated at the 0.01 level for all 60 elements. The full chart is available in the supplementary material.

Element	Positive correlation	Negative correlation
Li7	Be, B, Mg, Al, Si, Ca, Sc, Ti, V, Cr, Fe, Co, Ni, Zn*, Ga, As, Br, Sr, Y, Zr, Nb, Mo, Ag, Cd, Sn*, I, Ba*, La, Ce, Pr, Nd, Sm, Eu, Gd, Tb, Dy, Ho, Er, Tm, Yb, Lu, Hf, Tl, Pb,Bi, Th, U	K*, Ta*, W*
Be9	Li, Mg*, Al, Si, S*, Ca, Sc, Ti, V, Cr, Fe, Co, Ni*, Ga, As, Br, Sr, Y, Zr, Nb, Mo, Ag, Cd, I, Cs*, Ba, La, Ce, Pr, Nb, Sm, Eu, Gd, Tb, Dy, Ho, Er, Tm, Yb, Lu, Hf, Tl, Pb, Bi*, Th, U	Cl*, Mn, W*
B11	Li, Mg, Ca, Cr*, Ni, Cd*, Pb	Ta*
Na23	Mg, P, S, Cl*, K, Sc*, Ti*, Cr*, Co*, Cu, Mo, Sn*, Sb, W	Ag, Cd*, Pb*
Mg25	Li, Be*, B, Na, Al, Si, Ca, Sc, Ti, V, Cr, Fe, Co, Ni, Cu, Ga, As, Sr, Y, Zr, Mo*, Sn, I, Ba, La*, Ce*, Pr, Nd, Sm, Eu, Gd, Tb, Dy, Ho, Er, Tm, Yb, Lu, Hf, W*, Tl*, Th*, U*	Ta
Al27	Li, Be, Mg, Si, S*, Ca, Sc, Ti, V, Cr, Fe, Co, Ni, Cu*, Zn*, Ga, As, Br, Sr, Y, Zr, Nb, Mo, Ag, Cd, Sn, I, Cs*, Ba, La, Ce, Pr, Nd, Sm, Eu, Gd, Tb, Dy, Ho, Er, Tm, Yb, Lu, Hf, Tl, Pb, Bi*, Th, U	Mn, Ta
Si30	Li, Be, Mg, Al, S, Ca, Sc, Ti, V, Cr, Fe, Co, Ni, Cu, Zn, Ga, As, Sr, Y, Zr, Nb, Mo, Ag, Sn, Sb, I, Ba, La, Ce, Pr, Nd, Sm, Eu, Gd, Tb, Dy, Ho, Er, Tm, Yb, Lu, Hf, Tl, Th, U	Ta*
P31	Na, S, K, Mn*, Zn*, W	Ag*
S34	Be*, Na, Al*, Si, P, Cl*, K*, Ca*, Ti*, Cr*, Fe*, Co*, Ni*, Cu, Zn, Ga*, As*, Sr, Y, Zr, Nb, Mo, Sn,Sb, I*, Ba, La*, Ce, Pr, Nd, Sm, Eu, Gd, Tb, Dy, Ho, Er, Tm, Yb, Lu, Hf, W, Tl, Th*, U*	
Cl35	Na*, S*, Mn, Cu	Be*, Cl, Ag*, Cd, Cs
K39	Na, P, S*, Mn*, Cu, Zn, Rb, Ba, W, Tl	Li*, Cd*, I, U
Ca44	Li, Be, B, Mg, Al, Si, S*, Sc*, Ti*, V*, Cr, Fe, Co, Ni*, Ga, As, Br*, Sr, Y, Zr, Nb*, Mo*, Ag, Cd, I, Ba, La, Ce, Pr, Nd, Mo, Ag, Cd, I, Ba, La, Ce, Pr, Nd, Sm, Eu, Gd, Tb, Dy, Ho, Er, Tm, Yb, Lu, Hf, Th, U	Mn, Rb, Ta*
Sc45	Li, Be, Na, Mg, Al, Si, Ca*, Ti, V, Cr, Fe, Co, Ni, Cu, Zn*, Ga, As, Sr, Y, Zr, Nb*, Mo*, Sn, Sb*, I, Ba, La, Ce, Pr, Nd, Sm, Eu, Gd, Tb, Dy, Ho, Er, Tm, Yb, Lu, Hf, Tl, Th, U	Ta
Ti49	Li, Be, Na*, Mg, Al, Si, S*, Ca*, Sc, V, Cr, Fe, Co, Ni, Cu, Zn*, Ga, As, Sr, Y, Zr, Nb, Sn, Sb, I, Ba, La, Ce, Pr, Nd, Sm, Eu,Gd, Tb, Dy, Ho, Er, Tm, Yb, Lu, Hf, Tl, Th, U	Ta
V51	Li, Be, Mg, Al, Si, Ca*, Sc, Ti, Cr, Fe, Co, Ni, Cu, Ga, As, Sr, Y, Zr, Nb*, Sn, Sb*, I, Ba, La, Ce, Pr, Nd, Sm, Eu, Gd, Tb, Dy, Ho, Er, Tm, Yb, Lu, Hf, Tl, Th, U	Ta
Cr52	Li, Be, B*, Na*, Mg, Al, Si, S*, Ca, Sc, Ti, V, Fe, Co, Ni, Cu, Ga, As, Sr, Y, Zr, Nb*, Mo, Sn, Sb, I, Ba, La, Ce, Pr, Nd, Sm, Eu, Gd, Tb, Dy, Ho, Er, Tm, Yb, Lu, Hf, Tl, Bi*, Th, U	Ta
Mn55	P*, K*, Zn, Rb	Be, Al*, Ca, As*, Y*, Zr*, Mo*, Ag, I, La*, Ce*, Pr, Nd*, Sm*, Tb*, Dy*, Ho*, Tm*, Hf*, Th, U
Fe56	Li, Be, Mg, Al, Si, S*, Ca, Sc, Ti, V, Cr, Co, Ni, Cu, Zn, Ga, As, Sr, Y, Zr, Nb, Mo, Ag*, Sn, Sb*, I, Ba, La, Ce, Pr, Nd, Sm, Eu, Gd, Tb, Dy, Ho, Er, Tm, Yb, Lu, Hf, Tl, Bi*, Th, U	Ta
Co59	Li, Be, Na*, Mg, Al, Si, S*, Ca, Sc, Ti, V, Cr, Fe, Ni, Cu, Zn, Ga, As, Sr, Y, Zr, Nb*, Mo, Sn, Sb*, I, Ba, La, Ce, Pr, Nd, Sm, Eu, Gd, Tb, Dy, Ho, Er, Tm, Yb, Lu, Hf, Tl, Pb, Bi,Th, U	Ta
Ni60	Li, Be*, B, Mg, Al, Si, S*, Ca*, Sc, Ti, V, Cr, Fe, Co, Cu, Zn, Ga, As, Sr, Y, Zr, Mo, Cd*, Sn, I, Cs*, Ba, La, Ce, Pr, Nd, Sm, Eu, Gd, Tb, Dy, Ho, Er, Tm, Yb, Lu, Hf, Tl, Pb, Bi, Th*, U	Ta

Cu63	Na, Mg, Al*, Si, S, Cl, K, Sc, Ti, V, Cr, Mn*, Fe, Co, Ni, Zn, Ga*, Rb*, Zr, Mo, Sn, Sb, Ba, Gd*, Hf, W, Tl, Bi*	
Zn66	Li*, Al*, Si, P*, S, K, Sc*, Ti*, Mn, Fe, Co, Ni, Cu, Ga*, As*, Rb, Y, Zr, Nb*, Mo*, Ag*, Cd*, Sn, Sb, Ba, La, Ce, Pr, Nd, Sm, Eu, Gd, Tb, Dy, Ho*, Er, Tm*, Yb, Lu, Hf, Tl, Pb, Bi, Th*	
Ga69	Li, Be, Mg, Al, Si, S*, Ca, Sc, Ti, V, Cr, Fe, Co, Ni, Cu*, Zn*, As, Br, Sr, Y, Zr, Nb, Mo, Ag, Cd, Sn, I, Cs*, Ba, La, Ce, Pr, Nd, Sm, Eu, Gd, Tb, Dy, Ho, Er, Tm, Yb, Yu, Hf, Tl, Pb, Bi*, Th, U	Ta
As75	Li, Be, Mg, Al, Si, S*, Ca, Sc, Ti, V, Cr, Fe, Fe, Co, Ni, Zn*, Ga, Br, Sr, Y, Zr, Nb, Mo, Ag, Cd, Sn, I, Ba, La, Ce, Pr, Nd, Sm, Eu, Gd, Tb, Dy, Ho, Er, Tm, Yb, Lu, Hf, Tl, Pb, Bi*, Th, U	K*, Mn*, Rb*
Br81	Br, Be, Al, Ca*, Ga, As, Y, Zr, Nb, Mo, Ag, Cd, I, La, Ce, Pr, Nd, Sm, Eu, Gd, Tb, Dy, Ho, Er, Tm, Yb, Lu, Hf, Tl*, Pb, Th, U	
Rb85	P, K, Mn, Cu*, Zn, Cs, Tl	Ca, As*, Sr*, I*
Sr88	Li, Be, Mg, Al, Si, S, Ca, Sc, Ti, V, Cr, Fe, Co, Ni, Ga, As, Y, Zr, Nb, Mo, Ag, Cd*, I, Ba, La, Ce, Pr, Nd, Sm, Eu, Gd, Tb, Dy, Tb, Dy, Ho, Er, Tm, Yb, Lu, Hf, Tl, Th, U	Rb*, Ta
Y89	Li, Be, Mg, Al, Si, S, Ca, Sc, Ti, V, Cr, Fe, Co, Ni, Zn, Ga, As, Br, Sr, Zr, Nb, Mo, Ag, Cd, Sn, I, Cs*, Ba, La, Ce, Pr, Nd, Sm, Eu, Gd, Tb, Dy, Ho, Er, Tm, Yb, Lu, Hf, Tl, Pb, Bi*, Th, U	Mn*, Ta*
Zr90	Li, Be, Mg, Al, Si, S, Ca, Sc, Ti, V, Cr, Fe, Co, Ni, Cu, Zn, Ga, As, Br, Sr, Y, Nb, Mo, Ag, Cd*, Sn, Sb*, I, Ba, La, Ce, Pr, Nd, Sm, Eu, Gd, Tb, Dy, Ho, Er, Tm, Yb, Lu, Hf, Tl, Pb, Bi, Th, U	
Nb93	Li, Be, Al, Si, S, Ca*, Sc*, Ti, V*, Cr*, Fe, Co*, Zn*, Ga, As, Br, Sr, Y, Zr, Mo, Ag, Cd, I, La, Ce, Pr, Nd, Sm, Eu, Gd, Tb, Dy, Ho, Er, Tm, Yb, Lu, Hf, Ta*, Tl, Pb, Th, U	
Mo98	Li, Be, Na*, Mg*, Al, Si, S, Ca*, Sc*, Cr, Fe, Co, Ni, Cu, Zn*, Ga, As, Br, Sr, Y, Zr, Nb, Ag, Cd, Sn, Sb, I, Cs*, Ba, La, Ce, Pr, Nd, Sm, Eu, Gd, Tb, Dy, Ho, Er, Tm, Yb, Lu, Hf, Tl, Pb, Bi, Th, U	Mn*
Ag109	Li, Be, Al, Si, Ca, Fe*, Zn*, Ga, As, Br, Sr, Y, Zr, Nb, Mo, Cd,I, Ba, La, Ce, Pr, Nd, Sm, Eu, Gd, Tb, Dy, Ho, Er, m, Yb, Lu, Hf, Pb, Bi*, Th, U	Na, P*, Cl*, K*, Mn, W*
Cd111	Li, Be, B*, Al, Ca, Ni*, Zn*, Ga, As, Br, Sr*, Y, Zr*, Nb, Mo, Ag, I, Cs*, La, Ce, Pr, Nd, Sm, Eu, Gd, Tb, Dy, Ho, Er, Tm, Yb, Lu, Hf*, Tl*, Pb, Bi, Th, U	Na*, Cl, K*, W
Sn118	Sn*, Na*, Mg, Al, Si, S, Sc, Ti, V, Cr, Fe, Co, Ni, Cu, Zn, Ga, As, Y, Zr, Mo, Sb, I, Ba, La*, Ce*, Pr*, Nd*, Sm*, Eu*, Gd, Tb*, Dy*, Ho*, Er*, Tm*, Yb, Lu*,Hf, Tl, Pb, Bi, U*	
Sb121	Na, Si, S, Cl, Sc*, Ti, V*, Cr*, Fe*, Co*, Cu, Zn, Zr*, Mo, Sn, I*, Ba*, Hf, W, Tl	
I127	Li, Be, Mg, Al, Si, S*, Ca, Sc, Ti, V, Cr, Fe, Co, Ni, Ga, As, Br, Sr, Y, Zr, Nb, Mo, Ag, Cd, Sn, Sb*, Cs*, La, Ce, Pr, Nd, Sm, Eu, Gd, Tb, Dy, Ho, Er, Tm, Yb, Lu, Hf, Tl, Pb*, Bi*, Th, U	K, Mn, Rb*
Cs133	Be*, Al*, Ni*, Ga*,Rb, Y*, Mo*, Cd*, I*, Tb*, Dy*, Ho*, Er*, Tm*, Yb*, Lu*, Tl, Bi	Cl
Ba137	Li*, Be, Mg, Al, Si, S, K, Ca, Sc, Ti, V, Cr, Fe, Co, Ni, Cu, Zn, Ga, As, Sr, Y, Zr, Mo, Ag, Sn, Sb*, La, Ce, Pr, Nd, Sm, Eu, Gd, Tb, Dy, Ho, Er, Tm, Yb, Lu, Hf, Tl*, Th, U	Ta
La139	Li, Be, Mg*, Al, Si, S*, Ca, Sc, Ti, V, Cr, Fe, Co, Ni, Zn, Ga, As, Br, Sr, Y, Zr, Nb, Mo, Ag, Cd, Sn*, I, Ba, Ce, Pr, Nd, Sm, Eu, Gd, Tb, Dy, Ho, Er, Tm, Yb, Lu, Hf, Tl, Pb, Bi, Th, U	Mn*
Ce140	Li, Be, Mg*, Al, Si, S, Ca, Sc, Ti, V, Cr, Fe, Co, Ni, Zn, Ga, As, Br, Sr, Y, Zr, Nb, Mo, Ag, Cd, Sn*, I, Ba, La, Pr, Nd, Sm, Eu, Gd, Tb, Dy, Ho, Er, Tm, Yb, Lu, Hf, Tl, Pb, Bi, Th, U	Mn*

Pr141	Li, Be, Mg, Al, Si, S, Ca, Sc, Ti, V, Cr, Fe, Co, Ni, Zn, Ga, As, Br, Sr, Y, Zr, Nb, Mo, Ag, Cd, Sn*, I, Ba, La, Ce, Pr, Nd, Sm, Eu, Gd, Tb, Dy, Ho, Er, Tm, Yb, Lu, Hf, Tl, Pb, Bi, Th, U	Mn*
Nd146	Li, Be, Mg, Al, Si, S, Ca, Sc, Ti, V, Cr, Fe, Co, Ni, Zn, Ga, As, Br, Sr, Y, Zr, Nb, Mo, Ag, Cd, Sn*, I, Ba, La, Ce, Pr, Sm, Eu, Gd, Tb, Dy, Ho, Er, Tm, Yb, Lu, Hf, Tl, Pb, Bi, Th, U	Mn*
Sm147	Li, Be, Mg, Al, Si, S, Ca, Sc, Ti, V, Cr, Fe, Co, Ni, Zn, Ga, As, Br, Sr, Y, Zr, Nb, Mo, Ag, Cd, Sn*, I, Cs*, Ba, La, Ce, Pr, Nd, Eu, Gd, Tb, Dy, Ho, Er, Tm, Yb, Lu, Hf, Tl, Pb, Bi, Th, U	Mn*
Eu153	Li, Be, Mg, Al, Si, S, Ca, Sc, Ti, V, Cr, Fe, Co, Ni, Zn, Ga, As, Br, Sr, Y, Zr, Nb, Mo, Ag, Cd, Sn*, I, Ba, La, Ce, Pr, Nd, Sm, Gd, Tb, Dy, Ho, Er, Tm, Yb, Lu, Hf, Tl, Pb, Bi,	Ta*
Gd155	Li, Be, Mg, Al, Si, S, Ca, Sc, Ti, V, Cr, Fe, Co, Ni, Cu*,Zn, Ga, As, Br, Sr, Y, Zr, Nb, Mo, Ag, Cd, Sn I, Ba, La, Ce, Pr, Nd, Sm, Eu, Tb, Dy, Ho, Er, Tm, Yb, Lu, Hf, Tl, Pb, Bi, Th, U	
Tb159	Li, Be, Mg, Al, Si, S, Ca, Sc, Ti, V, Cr, Fe, Co, Ni, Cu*,Zn, Ga, As, Br, Sr, Y, Zr, Nb, Mo, Ag, Cd, Sn*,I, Cs*, Ba, La, Ce, Pr, Nd, Sm, Eu, Gd, Dy, Ho, Er, Tm, Yb, Lu, Hf, Tl, Pb, Bi*, Th, U	Mn*, Ta*
Dy163	Li, Be, Mg, Al, Si, S, Ca, Sc, Ti, V, Cr, Fe, Co, Ni, Cu*,Zn, Ga, As, Br, Sr, Y, Zr, Nb, Mo, Ag, Cd, Sn*, I,Cs*, Ba, La, Ce, Pr, Nd, Sm, Eu, Gd, Tb, Ho, Er, Tm, Yb, Lu, Hf, Tl, Pb, Bi*, Th, U	Ta*
Ho165	Li, Be, Mg, Al, Si, S, Ca, Sc, Ti, V, Cr, Fe, Co, Ni, Zn*, Ga, As, Br, Sr, Y, Zr, Nb, Mo, Ag, Cd, Sn*, I, Cs*, Ba, La, Ce, Pr, Nd, Sm, Eu, Gd, Tb, Dy, Er, Tm, Yb, Lu, Hf, Tl, Pb, Bi*, Th, U	Mn*,Ta*
Er166	Li, Be, Mg, Al, Si, S, Ca, Sc, Ti, V, Cr, Fe, Co, Ni, Zn, Ga, As, Br, Sr, Y, Zr, Nb, Mo, Ag, Cd, Sn*, I, Cs*, Ba, La, Ce, Pr, Nd, Sm, Eu, Gd, Tb, Dy, Ho, Tm, Yb, Lu, Hf, Tl, Pb, Bi*, Th, U	Ta*
Tm169	Li, Be, Mg, Al, Si, S, Ca, Sc, Ti, V, Cr, Fe, Co, Ni, Zn*, Ga, As, Br, Sr, Y, Zr, Nb, Mo, Ag, Cd, Sn*, I, Cs*, Ba, La, Ce, Pr, Nd, Sm, Eu, Gd, Tb, Dy, Ho, Er, Yb, Lu, Hf, Tl, Pb, Ni*, Th, U	Mn*, Ta*
Yb172	Li, Be, Mg, Al, Si, S, Ca, Sc, Ti, V, Cr, Fe, Co, Ni, Zn, Ga, As, Br, Sr, Y, Zr, Nb, Mo, Ag, Cd, Sn, I, Cs*, Ba, La, Ce, Pr, Nd, Sm, Eu, Gd, Tb, Dy, Ho, Er, Tm, Lu, Hf, Tl, Pb, Bi*, Th, U	Ta
Lu175	Li, Be, Mg, Al, Si, S, Ca, Sc, Ti, V, Cr, Fe, Co, Ni, Zn*, Ga, As, Br, Sr, Y, Zr, Nb, Mo, Ag, Cd, Sn*, I, Cs*. Ba, La, Ce, Pr, Nd, Sm, Eu, Gd, Tb, Dy,Ho, Er, Tm, Yb, Hf, Tl, Pb, Bi,Th, U	Ta*
Hf178	Li, Be, Mg, Al, Si, S, Ca, Sc, Ti, V, Cr, Fe, Co, Ni, Zn*, Ga, As, Br, Sr, Y, Zr, Nb, Mo, Ag, Cd*, Sn, Sb, I, Ba, La, Ce, Pr, Nd, Sm, Eu, Gd, Tb, Dy, Ho, Er, Tm, Yb, Lu, Tl, Pb, Bi,Th, U	Mn*
Ta181	Nb*, W*	Li*,B*, Mg, Al, Si*, Ca*, Sc, Ti, V, Cr, Fe, Co, Ni, Ga, Sr, Y*, Ba, Eu*, Tb*, Dy*, Ho*, Er*, Tm*, Yb*, Lu*,
W182	Na, Mg*, P, S, Cl, K, Cu, Sb, Ta*	Li*, Be*, Ag*, Cd
Tl205	Li, Be, Mg*, Al, Si, S, K*, Sc, Ti, V, Cr, Fe, Co, Ni, Cu, Zn, Ga, As, Br*, Rb, Sr, Y, Zr, Nb, Mo, Cd*, Sn, Sb, I,Cs, Ba*, La, Ce, Pr, Nd, Sm, Eu, Gd, Tb, Dy, Ho, Er, Tm, Yb, Lu, Hf, Pb, Bi*, Th, U	
Pb208	Li, Be, B, Al, Ni, Zn, Ga*, As, Br, Y, Zr, Nb, Mo, Ag, Cd, Sn, I*, La, Ce, Pr, Nd, Sm, Eu, Gd, Tb, Dy, Ho, Er, Tm, Yb, Lu, Hf, Tl, Bi, Th, U	Na*, Cl, K*, W
Bi209	Li, Be*, Al*, Cr*, Fe*, Ni, Cu*, Zn, Ga*, As*, Y*, Zr, Mo, Ag*, Cd, Sn, I*, Cs, La, Ce, Pr, Nd, Sm, Eu*, Gd, Tb*, Dy*, Ho*, Er*, Tm*, Yb*, Lu*, Hf, Tl*, Pb, Th, U	
Th232	Li, Be, Mg*, Al, Si, S*, Ca, Sc, Ti, V, Cr, Fe, Co, Ni*, Zn*, Ga, As, Br, Sr, Y, Zr, Nb, Mo, Ag, Cd, I, Ba, La, Ce, Pr, Nd, Sm, Eu, Gd, Tb, Dy, Ho, Er, Tm, Yb, Lu, Hf, Tl, Pb, Bi, U*	Mn

U238	Li, Be, Mg*, Al, Si, S*, Ca, Sc, Ti, V, Cr, Fe, Co, Ni, Ga, As, Br, Sr, Y, Zr, Nb, Mo, Ag, Cd, Sn*, I, Ba, La, Ce, Pr, Nd, Sm, Eu, Gd, Tb, Dy, Ho, Er, Tm, Yb, Lu, Hf, Tl, Pb, Bi, Th	K*, Mn

* Correlation is significant at the 0.05 level (2-tailed).

Appendix C

2.4 PAH

Table 23

Certified reference material 1941b Organic in Marine Sediment from the National Institute of Standards & Technology values. This material was used in the HPLC- FID- DAD PAH detection method.

Compound	Concentration in reference material (ug/kg)	Uncertainty ± (ug/kg)
Phenanthrene	406.00	44.00
Anthracene	184.00	18.00
Pyrene	581.00	39.00
Chrysene	291.00	31.00
Benzo[b]fluoranthene	453.00	21.00
Benzo[k]fluoranthene	225.00	18.00
Benzo[a]pyrene	358.00	17.00
Dibenz[a,c]anthracene	36.70	5.20
Benzo[ghi]perylene	307.00	45.00

2.5 Detection limits

Table 24

These detection limits of the GC-MS method was determined during procedural analysis in an unpublished master thesis[106].

Name	LOD	LOQ
	ppb	ppb
Naphthalene	0.8354	6.122
Acenaphthylene	3.473	14.72
Acenaphthene	1.283	14.55
Fluorene	1.578	7.261
Phenanthrene	4.562	13.62
Anthracene	4.129	15.09
Fluoranthene	4.436	16.27
Pyrene	5.144	17.51
Benzo[a]anthracene	5.434	16.11
Chrysene	5.660	16.03
Benzo[b]fluoranthene	9.339	32.38
Benzo[k]fluoranthene	9.808	31.91
Benzo[a]pyrene	11.99	42.96
Indeno[1.2.3-cd]pyrene	19.77	72.33
Dibenzo[a,h]anthracene	18.14	66.32
Benzo[ghi]perylene	19.83	78.85
PCB28	4.387	15.79
PCB52	5.223	14.56
PCB101	8.087	30.42
PCB118	5.923	13.78
PCB138	6.232	17.28
PCB153	7.390	19.66
PCB180	8.156	26.08

3 Appendix D

3.1 Sample locations

Table 25

The table below records the latitude and longitude of each sample. Sample locations where only plastics were sampled are designated with a P and locations were only metals a M.

Sample number	Area	Latitude	Longitude
S19	4	78°54.843'	11°51.049'
S20	4	78°54.851'	11°51.037'
S21	4	78°54.773'	11°51.264'
S23	4	78°54.845'	11°50.964'
S24	4	78°54.852'	11°51.011'
S25	5	78°57.599'	11°38.667'
S26	5	78°57.589'	11°38.007'
S27	5	78°57.591'	11°37.968'
S28	5	78°57.578'	11°38.037'
S29	5	78°57.570'	11°38.061'
S30	5	78°57.575'	11°38.007'
S31	6 P	61°28.025'	11°01.554'
S32	6 P	61°27.955'	10°59.979'
S33	6 P	61°27.954'	10°59.986'
S34	6 M	61°27.950'	10°59.991'
S35	6 M	61°27.958'	11°00.014'
S41	8	58°23.164'	8°14.893'
S42	8	58°23.164'	8°14.892'
S44	10	58°18.122'	8°19.913'
S45	10 M	58°18.122'	8°19.913'
S46	10	58°18.122'	8°19.913'
S47	11	63°22.899'	10°36.651'
S48	11	63°22.887'	10°36.655'
S49	11	63°22.987'	10°36.652'
S50	11	63°22.901'	10°36.645'
S51	11	63°22.894'	10°36.669'
S52	12	63°22.851'	10°37.356'
S53	12	63°22.849'	10°37.358'
S54	12	63°22.839'	10°37.364'
S55	12	63°22.835'	10°37.351'
S56	12	63°22.836'	10°37.349'
S57	13	63°20.190'	10°38.253'
S58	13	63°20.177'	10°38.290'
S59	13	63°20.163'	10°38.283'

S60	13	63°20.158'	10°38.288'
S61	13	63°20.152'	10°38.291'
S62	14	63°20.721'	10°32.001'
S63	14	63°20.722'	10°31.933'
S64	14	63°20.721'	10°31.935'
S65	14	63°20.705'	10°31.920'
S66	14	63°20.709'	10°31.916'
S67	15	63°22.795'	10°18.555'
S68	15	63°22.955'	10°18.132'
S69	15	63°22.779'	10°18.467'
S70	15	63°22.913'	10°18.222'
S71	15	63°22.947'	10°18.171'
S72	16	63°25.124'	10°18.967'
S73	16	63°25.168'	10°19.012'
S74	16	63°25.142'	10°19.048'
S75	16	63°25.141'	10°19.045'
S76	16	63°25.162'	10°19.087'

3.1.1 Pictures

Figure 19. Image of the Zeppelin Mountain sampling location.

This is a picture of sampling Area 4 at the base of Zeppelin Mountain near by Ny-Ålesund.

Figure 20. Image of the Stuphallet sampling location.

This picture shows sampling Area 5 in an area referred to as Stuphallet.

Figure 21. Image of the Stai sampling location.

This picture shows the sampling location for Area 6 near the town of Stai.

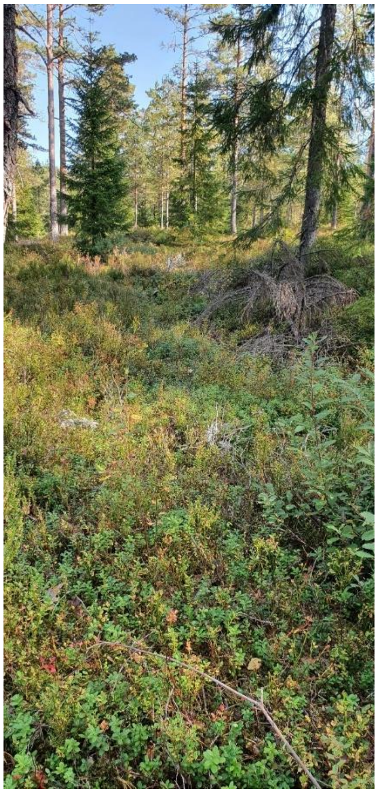

Figure 22. Image of the Spjotevannet sampling location.

This picture shows the sampling location of Area 8 nearby Spjotevannet and Grimevannet.

Figure 23. Image of the V. Grimevannet sampling location.

The picture was taken near west Grimevannet labeled as Area 10.

Figure 24. Image of the moss found near Jonsvannet Area 11.

This picture shows the moss found at Area 11.

Figure 25. Image of the moss found near Jonsvannet Area 12.

The picture shows the moss found at Area 12.

Figure 26. Image of Jonsvannet Area 13.

This picture shows Area 13.

Figure 27. Image of Espåa sampling area.

This picture shows Area 14

Figure 28. Image of Granåsen sampling area.

This picture shows Area 15.

Figure 29. Image of Baklidammen

This picture depicts Area 16.

Astrid Ellinor Schick

Long Range Transport of Pollutants to Arctic Environments

NTNU

Norwegian University of
Science and Technology